GalvaScience LLC

PO Box 501, Springville, AL 35146

Current Knowledge of the Cracking of Steels During Galvanizing

A Synthesis of the Available Technical Literature and Collective Experience for the American Institute of Steel Construction

Thomas J. Kinstler
GalvaScience LLC

Introduction, Background, and Research Approach

For almost a century, the application of hot-dipped zinc coatings has been a standard method of protection of steel from corrosion. The use of such galvanized steel has resulted in long-term value in safety, resource preservation, and economy of the use of iron and steel. As a "dip and drain" methodology utilizing molten zinc, certain limitations on sizes, and required design accommodations have been well known, and routinely applied. For example, ASTM Standards for galvanized coatings[1], materials selection and treatment for galvanizing[2], and design of products to be galvanized[3] were published in the United States in 1928, 1932, and 1955 respectively, and no doubt similar Standards and Practices were published in other locations at similar times.

For the most part, these Standard, Practices, and Guides have served well in avoiding significant problems, and the Standards and Guides have grown in scope, detail and application as the use of galvanized coatings has grown with the modern development of the uses and properties of steel. Indeed it can be reasonably said that almost all cases of problems related to the properties of steels after galvanizing can be traced back to the lack of use, misapplication, or misinterpretation of the Standards and Practices which had otherwise guided the successful use of galvanized coatings for decades.

The growing full documentation of corrosion performance, coupled with the slow cleansing of the atmospheric environment, and known, simple and practical application parameters lead to the almost ubiquitous use of hot dip galvanizing in infrastructure applications such as highway barriers, and electrical transmission structures, to the point where galvanized steel became almost "invisible" in North America because it was virtually everywhere. On other continents, the use of galvanized steel was even more widespread. Numerous industrial process applications came to pass as testing and adoption became more widely known.[4, 5] The steels and galvanizing practices were mutually compatible within the aforementioned guidelines. A major world-wide study on the mechanical properties of then-current construction steels demonstrated the retention of mechanical and dynamic properties after hot dip galvanizing for the almost all of the common structural steels.[6]

Within the past decade, sporadic reports of cracks in steel after hot dip galvanizing have occurred when oxy-fuel cut, welded, or sharply cold formed.[7] These reports were usually anecdotal, with a wide range of test and processing data, and documentation. Early attempts to catalog, characterize, or find relationships among the disparate reports were unsuccessful. In the United States, the primary known occurrences were on oxy-fuel cut "copes" in industrial frame structures. No geographical or other correlation could be seen including fabricator shop, methods, or galvanizing shop. The small number of occurrences made any statistical investigation problematic. Notwithstanding the absence of a database of occurrences, the frequency does not seem to be changing over recent time, however, heightened awareness and information flow has made the phenomenon more prominent in steel, fabrication and galvanizing circles. A number of investigations of specific cracks have been completed[8] and are included in the synthesis following, however it is possible and probable that other investigations have been withheld from this collaborative effort to more closely explore the cause of this phenomenon.

An example of a typical cope crack is shown below.

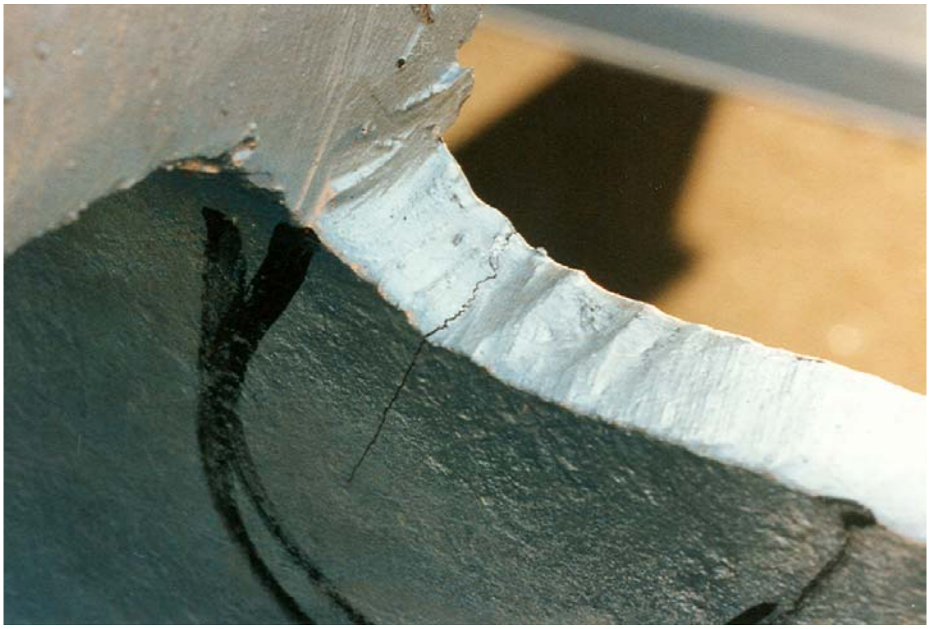

Figure 1 - Typical Crack on Flame-Cut Cope

In addition to the problem occurring on flame-cut edges, some cracks have been found at the termination, heat affected zone (HAZ) of, or occasionally within the body of a weld.

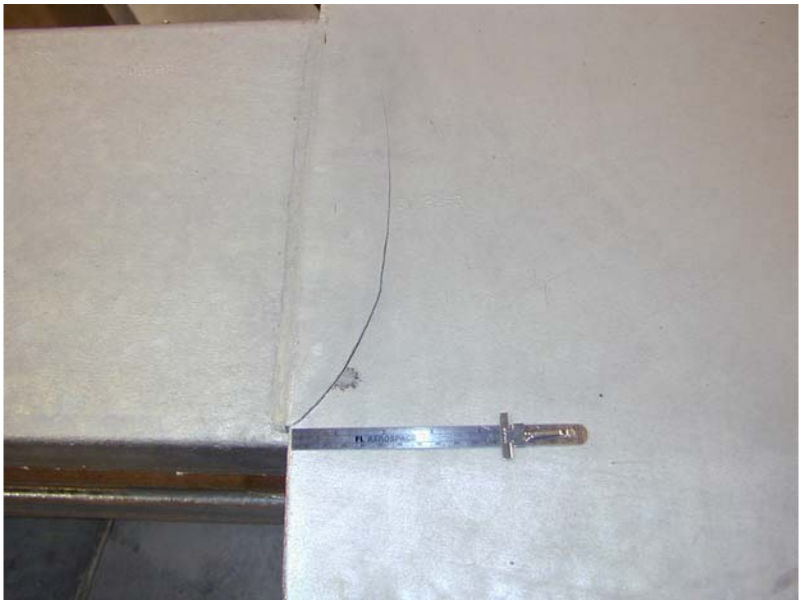

Figure 2 - Crack at Weld Termination

A corollary occurrence, which has been well documented in the past, is cracks occurring on sharply cold-formed bends – a phenomenon for which guidelines for avoidance have been available for decades[2]. In virtually every case examined in detail, three consistent factors stand out:

1. The fractures are almost always intergranular

2. The fractures are the result of, or at the location of some thermal or cold-forming process

3. The fracture surface is coated with zinc or zinc reaction products

The constancy of the above factors strongly suggest that the mechanism of the fractures is liquid metal embrittlement (LME), also known as liquid metal assisted cracking (LMAC) or liquid metal induced cracking (LMIC). The application of the various names for the phenomenon could be the source of endless discussion as each description partially correctly, but perhaps incompletely describes the phenomenon. For the purpose of this synthesis, LMAC will be the adopted terminology, with the full knowledge that one of the other terms may be more familiar to the reader.

The LMAC phenomenon is generally known but perhaps not as well researched as other brittle fracture phenomena. As a general rule, it is a mechanism one in which the ductility of a solid metal is reduced by surface contact with a liquid metal[9]. More directly, Joseph, Picat and Barbier describe the phenomenon as the brittle fracture, or loss in ductility, of a usually ductile metal in the presence of liquid metal. Some authors add to this definition the necessary influence of some external load or internal residual stress[10]. To this day the underlying mechanics are still not completely described, but it is generally considered that the phenomenon requires:

1. An "embrittleing metal, usually but not necessarily a liquid,

2. A normally ductile "embrittled" metal, and

3. Some force field acting at the place and time of the embrittling metal contact

The occurrence of LMAC is usually specific, in that only certain metal couples interact, and require adequate wetting of the solid metal by the liquid metal. Surprisingly for the steel-zinc couple is that couples which form intermetallic compounds normally do not experience LMAC. Since intermetallics formation is the very basis for hot dip galvanizing, the occurrence of LMAC in galvanizing is an anomaly which further indicates the lack of fundamental knowledge, and probably helps explain the few number of events, and low number of published technical investigations.

While the elementary mechanism (it is not necessary that there be only one mechanism applicable to all couples and occurrences) remains unsubstantiated, the phenomenon for fabricated and galvanized steel remains one where the above mentioned conditions of intergranular fracture initiated at points of thermal or mechanical processing are necessary for the problem to occur.

The galvanizing process has been practiced for a century, generally with little change in the components or practices, other than improvements in efficiency, although new zinc bath compositions have appeared within the past decade. However the new zinc alloys have not been universally adopted. The steel fabricating process has developed at a measured pace with the predominant practices today of thermal cutting, and subassembly by welding. The production and strength of steels has changed as a result of the adoption of newer methods and compositions. Table 1 lists world and major steel producing nations and percent production by process[11]. It has been noted that in 2002, 40% of all steel crossed an international border, up from just over 22% in 1975.[12] Thus steel manufacture is becoming more "international," with the result that fabricators and galvanizers are more likely to see steels from a wide variety of sources and processes, and produced from a wide variety of feed materials. To date, notwithstanding the lack of any comprehensive database, no correlation has been made between source of steel material or method of steel production. Further, the dynamics of the steel marketplace suggests that segregation or specification of selected steels which are less sensitive to LMAC as a result of their origin or process history, should that be found to be the case, is unlikely to be an adequate strategy to ameliorate the problem.

Table 1 – Crude Steel Production by Process 2003

Country	Million Tonnes	% Oxygen	% Electric
France	19.8	60.7	39.3
FR Germany	44.8	70.0	30.0
Italy	26.7	37.0	63.0
Spain	16.5	22.7	77.3
United Kingdom	13.3	80.1	19.9
Russia	62.7	61.4	14.9
Ukraine	36.9	48.6	5.4
Other European	51.6	59.9	40.1
Former USSR	108.0	56.8	13.1
Canada	15.9	59.7	40.3
Mexico	15.2	30.2	69.8
United States	90.4	51.1	50.4
Brazil	31.1	78.8	21.2
China	220.1	83.2	16.7
Japan	110.5	73.6	26.4
India	31.8	48.7	45.6
South Korea	46.3	55.2	44.8
World	963.1	63.3	33.1

The change in production method over the past 100 years in the United States is diagrammed in Figure 2.

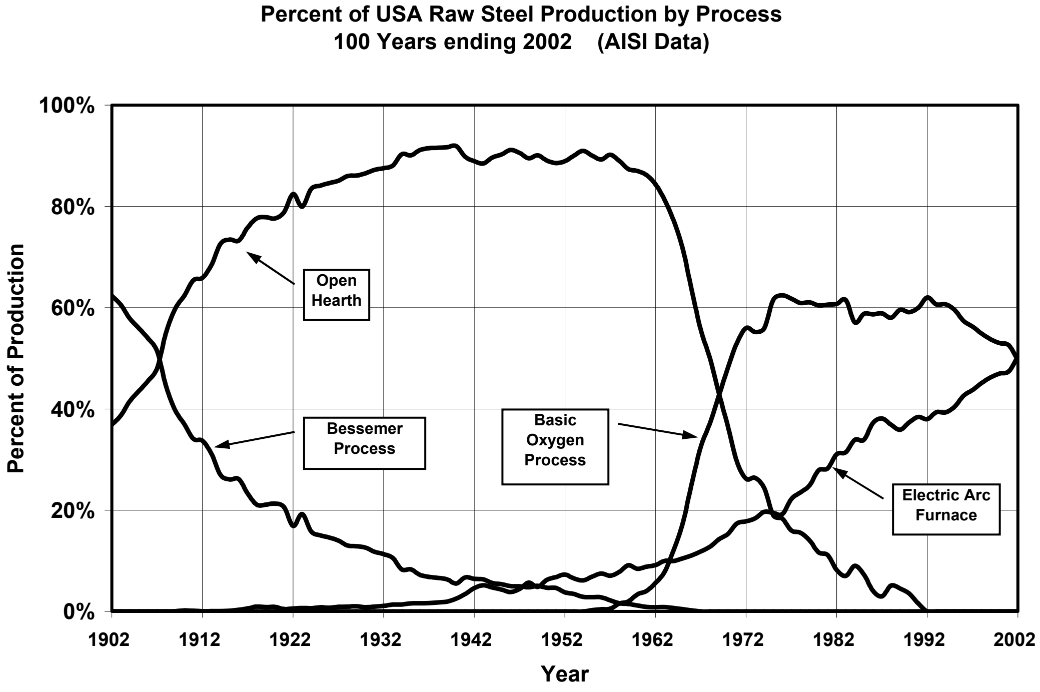

Figure 3 - US Raw Steel Production Processes through 2002

From the standpoint of structural shapes, the roughly 50/50 split between Oxygen and Electric Arc (EAF) processing is misleading in that virtually all US production of structural shapes is by the EAF process, using primarily scrap steel as a feed source.

The hot dip galvanizing process is a “dip and drain” sequence in which steel is prepared, usually by acid pickling and fluxing, and immersed in molten zinc for a period ranging from one to ten minutes (depending on original temperature, and mass of steel), withdrawn, cooled, and finished for shipment. The process flow[13] for Structural Steel is shown in Figure 3.

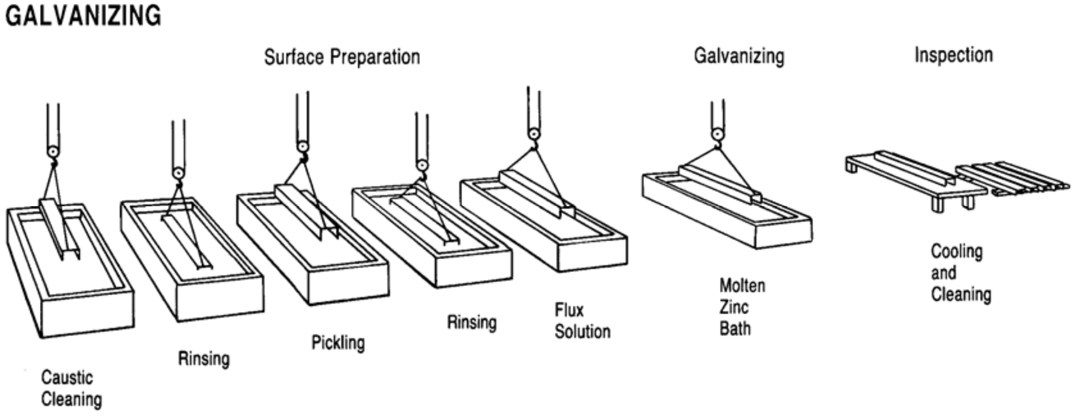

Figure 4 - Typical Galvanizing Process Flow (from American Galvanizers Association)

The result of the interaction between the molten zinc and the properly prepared steel is a layered coating consisting of zinc-iron intermetallic phases (reaction products), covered by a layer of solid zinc, as shown in Figure 4.

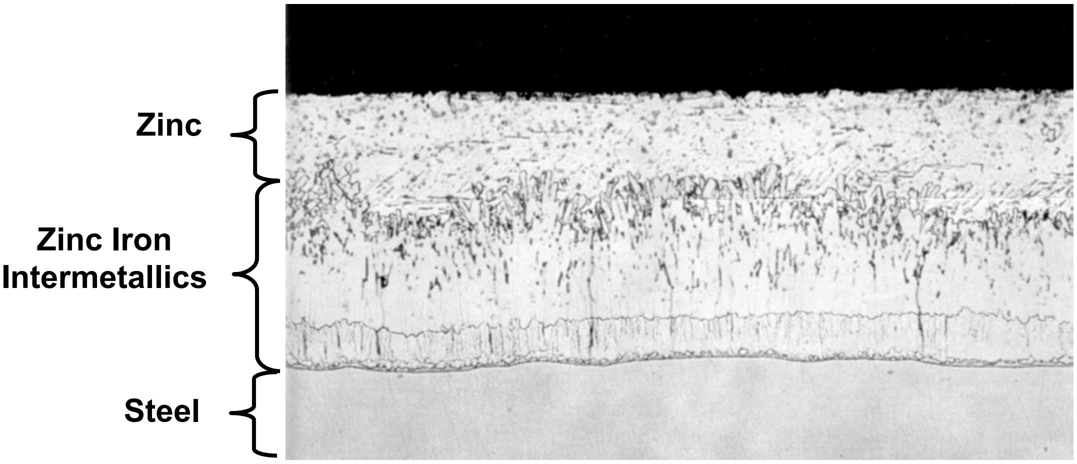

Figure 5 - Typical Galvanizing Microstructure (Nominally 100μm in thickness)

In relation to forces, temperature ranges, and reactions having a bearing on the cracking phenomenon, the relevant factors in the process flow in Figure 3 are the acid pickling step, the thermal transient from the steel temperature after fluxing (ranging from ambient to ≥100°C depending on process) through the ~ 450°C (~840°F) molten zinc bath and the natural or induced cooling back to ambient temperature afterward. While in molten zinc, the buoyant force generated is a function of the density ratio of molten zinc to steel, which is approximately 0.9. Therefore, the "weight" of the steel being galvanized, and therefore the "dead load" on the steel is about 10% of its weight in air.

The microstructure shown in Figure 4 is typical of the coating formed on steels whose compositions and processing history do not promote enhanced reactivity between zinc and steel. Certain levels of elements in steel, such as silicon, manganese, and phosphorus can accelerate the zinc-iron reaction resulting in non-uniform coatings, in the most benign form, to brittle and non-adherent coatings in the most aggressive cases. High reactivity in steels being galvanized has been recognized for well over 50 years, but now appears to be occurring more frequently., and in the mid 1990s was associated with changes in steel making practice, and particularly the more widespread use of continuous casting.[14] In addition, easily diffusible elements such free nitrogen can, under the thermal transient of the galvanizing process, accelerate "aging" of the steel and potentially degrade the mechanical properties of the steel after galvanizing. Therefore, galvanizers have the option of including certain controlled and beneficial additives in the molten zinc to reduce zinc-iron reactivity, enhance zinc drainage, and/or exercise some control over the structure of the outer zinc surface, and therefore somewhat affect the aesthetics and uniformity of the galvanized coating.

Lead is often found with zinc as an ore, and depending on the refining process, and the intended use of the zinc, may be found at up to about 1.4% in zinc, although a more typical concentration in a galvanizing bath is about 1% (Prime Western Grade, or "PW" zinc). Lead has been known to enhance the drainage of molten zinc spelter on removal of the steel from the galvanizing bath, and therefore the thickness and uniformity of the resultant galvanized coating. Bismuth can be substituted for lead in zinc with a similar enhancement in drainage characteristics. Nickel has been used in zinc to retard the reaction rate between zinc, and steels, which because of their composition, tend to form thick and unsightly galvanized coatings. In recent years, tin has been found to have a similar retarding effect on the reaction rate as well as enhancing drainage[15]. Aluminum is often controlled within a certain range to enhance the "brightness" of the outer zinc layer. Vanadium and Titanium have also been seen to have beneficial effects in counteracting enhanced-reactivity when such sensitive steels are galvanized[16]. With the exception of Lead and Aluminum, the use of additives to the zinc has been developed over the past twenty years, with more widespread, although by no means universal, adoption during the past decade in North America. Lead, Tin, and Bismuth have lower melting points than zinc, while Aluminum and Nickel are higher. The zinc used in batch hot dip galvanizing in North America is often in accordance with ASTM B6,[17] which allows for the use of such additives.

In early 2000, about 25% of the responders to a processing survey by the American Galvanizers Association reported that they used no Prime Western zinc.[18] In 2003, the trend towards the switch from Prime Western zinc to High Grade, or Special High Grade zinc, which is lower in Lead, was definitely established.[19]

It must be noted that although the use of zinc alloy spelters has been growing over the past decade, the problem of cope cracking found after galvanizing well predated the adoption of such alloys. In addition, notwithstanding the lack of any comprehensive database, no correlation has been made between source of lead in zinc and cracking. Indeed, Prime Western zinc was the predominant material used throughout the previous century of commercial batch hot dip galvanizing when such cracking was unreported.

The perceived increase in the occurrence of cracks found after galvanizing has led to a number of research programs and experiments, the earliest modern substantial body of work being undertaken in Japan in the early 1980s, and was primarily focused on welding. Following cracks occurring on framing cutouts or "copes" on structural shapes in the early 1990s, this author conducted a number or literature searches, experiments, and technical dialogues to illuminate if possible, the causes of those cracks. In the middle 1990s, a comprehensive research investigation was undertaken by the International Lead Zinc Research Organization. Various unpublished investigations were also undertaken.

In 2004, The American Institute of Steel Construction (AISC) instituted a project to the extent possible collect all of the direct and ancillary technical publications, any unpublished research which might become available, and anecdotes which may be related to the cope cracking and similar phenomenon to synthesize a document, which would provide a current-knowledge base, and more closely define those areas where further technical investigation might prove fruitful.

Literature and Knowledge Survey

Over 150 technical documents ranging from test and anecdotal reports to books and comprehensive published papers were collected, assembled, and reviewed for this synthesis of the current related work, and no attempt is made here to list or comment on all of the contributions or literature reviewed. This document is not a "literature list," catalog, or database, and brevity of explanation of any particular issue herein does not imply a sparse degree of technical support. Most of the results, experiences, and published conclusions are at least compatible, often complementary and confirmatory, and align with a general explanation and mechanism for the phenomenon. Occasionally, contradictory results remain unexplained. For the purpose of "synthesizing" a disparate collection of technical work, it is important to consider the "Degree of Certainty" found in either the works themselves, or the way in which they are related to form a cohesive theory or explanation:

- *Direct Observation or Experimentation*
- *Interpolation*
- *Extrapolation*
- *Parallelism*
- *Convergence of Probabilities*
- *Exhaustion of Other Possibilities*

The highest confidence can be given to those methodologies at the top of the list, while a growing degree of uncertainty can be prudently expected as the list is traversed downward.

A number of relevant searches of the technical literature have been completed in the past including those by McDonald,[20] Weigand,[21] Zervoudis and Anderson,[22] and Kinstler.[23] Comprehensive experimental programs include those sponsored by the International Lead Zinc Research Organization[6, 24]

Beginning in 1991, early experiments and reports were completed by Kinstler.[25, 26, 27] In that experimental program, tensile tests were completed at the galvanizing temperature of 840°F in the presence of, and absence of zinc. The actual traces are shown in Figure 6. The two curves are offset for clarity, but it is clear that the elastic portion of the curve is not affected by the presence of zinc, but beyond some point, there is a dramatic and sudden loss of ductility, and brittle fracture results. These curves are in complete agreement (with adjustment for scale) with other similar experiments[28], such as that shown in Figure 7, where the effect of acid pickling versus abrasive cleaning to determine the possibility of hydrogen embrittlement effects is explored. In Figure 7, the upper curve defined by white whole circles is for the basic steel at room temperature, while the curve defined by black whole circles is for the basic steel after galvanizing and stripping of the zinc coating in 10% H_2SO_4, again at room temperature. The middle curves defined by horizontal half circles are for the steel at 460°, either pickled in 10% H_2SO_4 or ground clean prior to galvanizing, while the remaining curves defined by vertical half circles, is for the same two cleaning conditions, but immersed in liquid zinc.

In both the Kinstler and the Kikuchi Results, the sudden drop in ductility in the presence of zinc is evident, and is consistent with the general theory of LMAC.

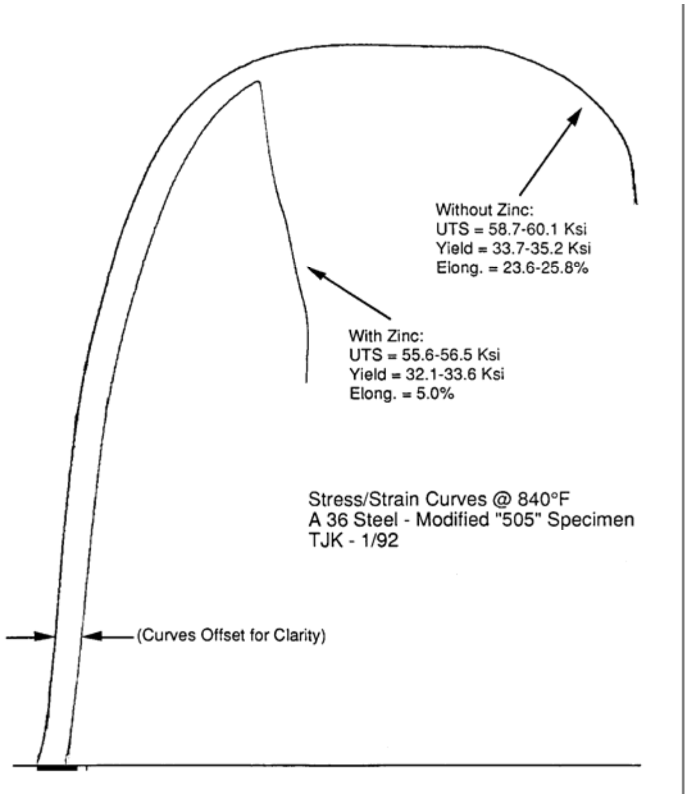

Figure 6 - Stress/Strain Curve with and without Zinc at 840 Degrees F (Kinstler)

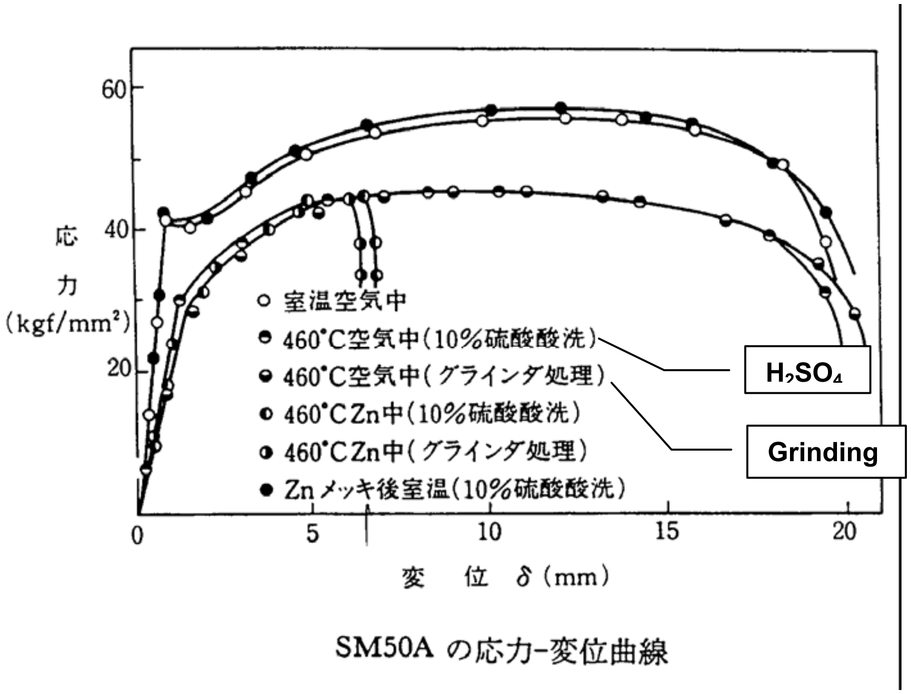

Figure 7 - Stress/Strain Curve at RT, ~ 460 Degrees C, and with Acid Pickling or Abrasive Cleaning (Grinding), with and without Zinc (from Kikuchi)

The point at which the drop in ductility occurs is further modified by the stress-concentration factor, and has been studied by Kikuchi and Iezawa.[29] Figure 8 shows the large drop in ductility as the stress-concentration factor (K_t) increases.

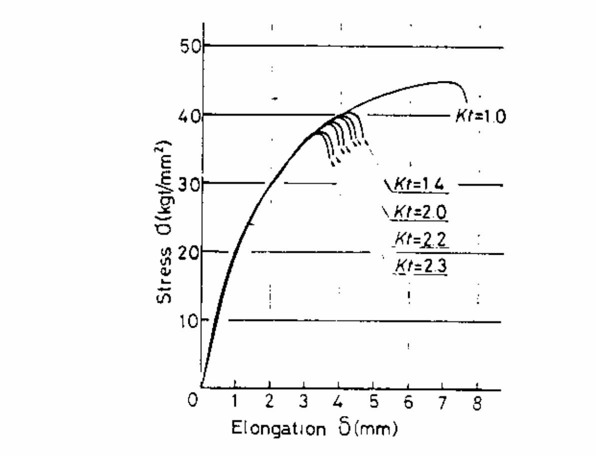

Figure 8 - Effect of Stress-Concentration Factor on Ductility of Steel in Molten Zinc (Kikuchi et al)

Laboratory examination of cracks occurring in copes of structural beams after galvanizing were completed by many with usually similar results. Many of these examinations have been contributed to this synthesis in confidence, and are proprietary in nature, however the exposition by Kinstler[30] (Metallography courtesy of John Zervoudis, Teck Cominco) of such an examination is typical and expansive.

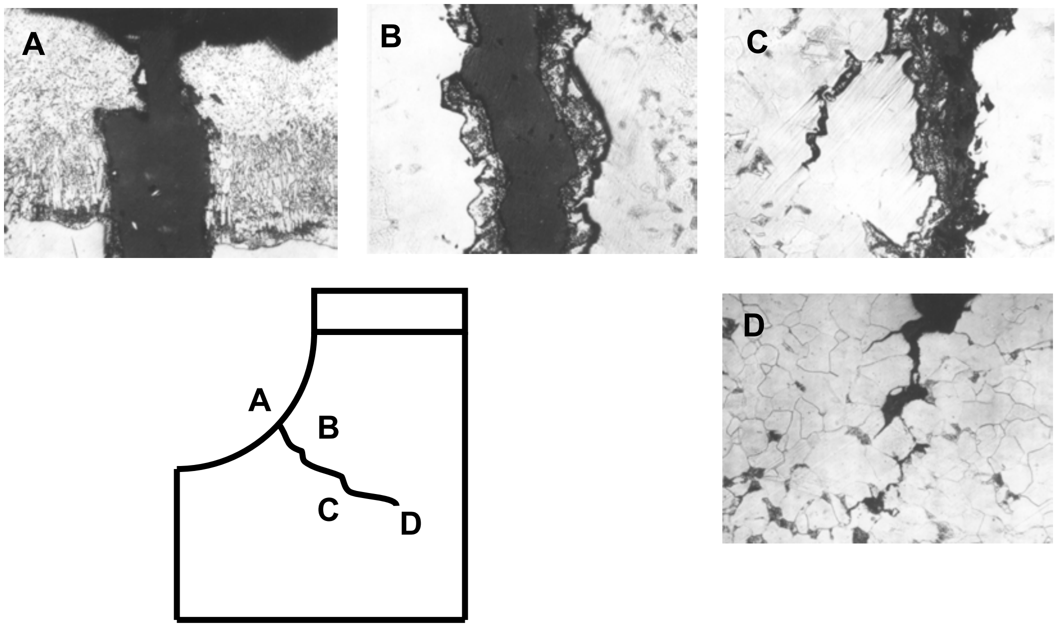

Figure 9 - Profile View of Crack in Flame-cut Cope found after Galvanizing

A crack found in a coped beam after galvanizing was sectioned midway along the plane of the web into "left and right hand" samples, one section was viewed in profile, and shown in Figure 9. The galvanized coating is typical, with ductile zinc η phase outer layer atop the zinc-iron ζ and δ intermetallic phases, as shown in view A. Views B, C, and D show zinc-iron intermetallics on the fracture surface, with small branching. The orientation of the crack essentially perpendicular to the flame-cut surface suggests the tensile force field driving the crack was parallel with the flame-cut edge.

The “opposite hand” sample crack was forced open to reveal both the original crack fracture surface as well as the newly fractured formerly un-cracked surface, and shown in Figure 10.

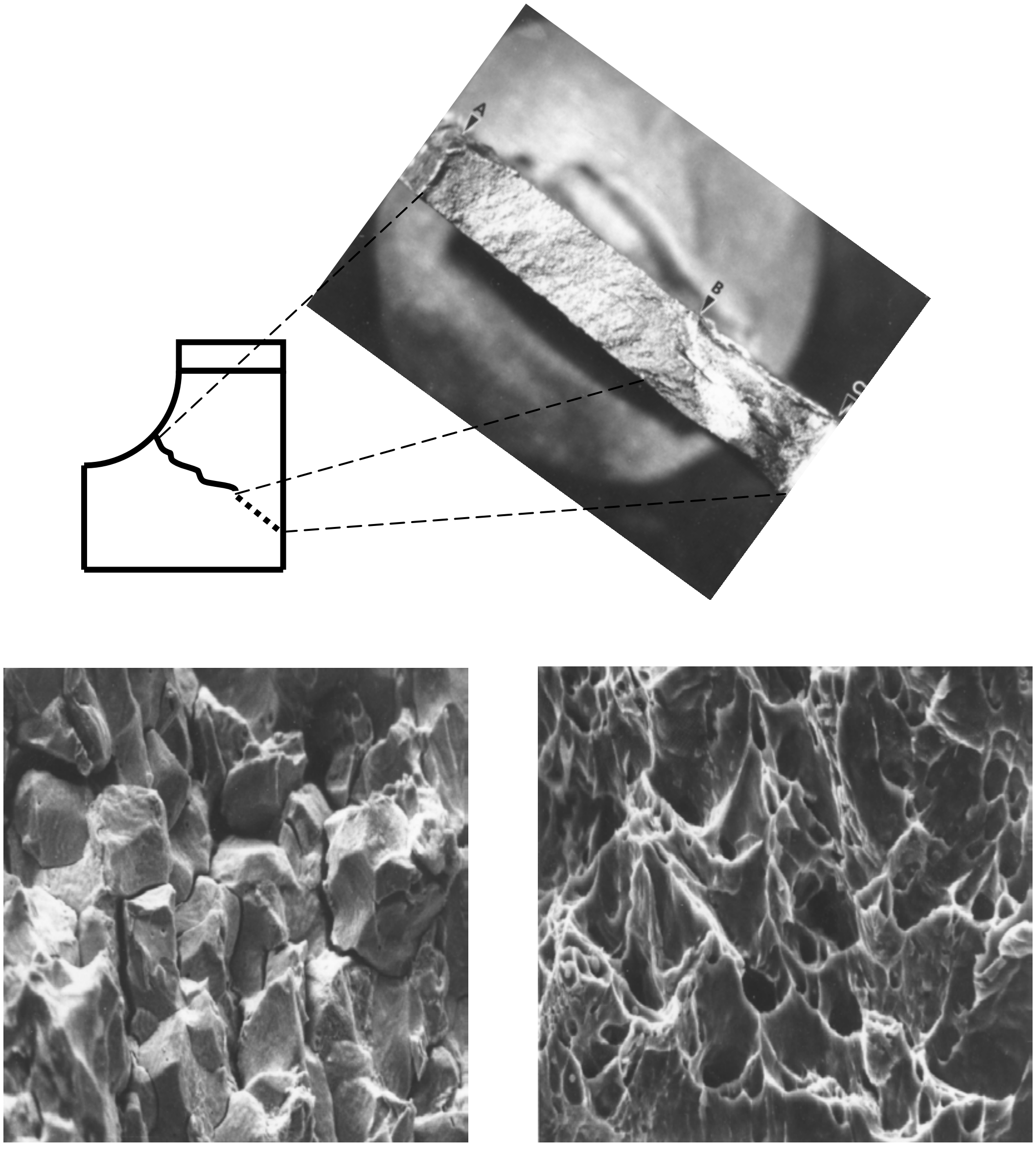

Figure 10 - Original and "Forced" Fracture Surfaces of Partial Crack Shown in Figure 9, with Morphology of Each Surface (Old on Left, New on Right)

The brittle-looking, intergranular surface on the left is in contrast to the ductile appearance on the right, indicating clearly that the bulk steel was not “embrittled” in the classic sense, but rather that some confluence of conditions caused or allowed grain boundary penetration of the zinc, with resulting de-cohesion of the structure. The crack ended when either the supply of liquid zinc was exhausted, the crack entered an area where the driving tensile force field was below some critical value, and/or the toughness properties of the newly-entered steel structure was sufficient to arrest the crack growth and would not sustain crack propagation.

The response of steel to stress in molten zinc as outlined above is an intrinsic effect which has clearly been operative during the almost century-long period of successful hot dip galvanizing, within which almost all reported cracking occurrences could not be related to the non-compliance, for whatever the reason, to well known and published design and fabrication Standards, criteria and guidelines. The appearance of what can arguably be called the "new" crack phenomenon must be related to some change or changes along the continuum of steel manufacture, structure design, steel fabrication, and galvanizing practice.

It is well established that the phenomenon of LMAC is related to the confluence of three factors, 1) a tensile force field, 2) a specific liquid metal, and (given that the cracking does not appear randomly along a steel surface, but is restricted to areas subjected to cold work or thermal transients such as a HAZ from cutting or welding), 3) a material condition or processing-induced sensitivity.

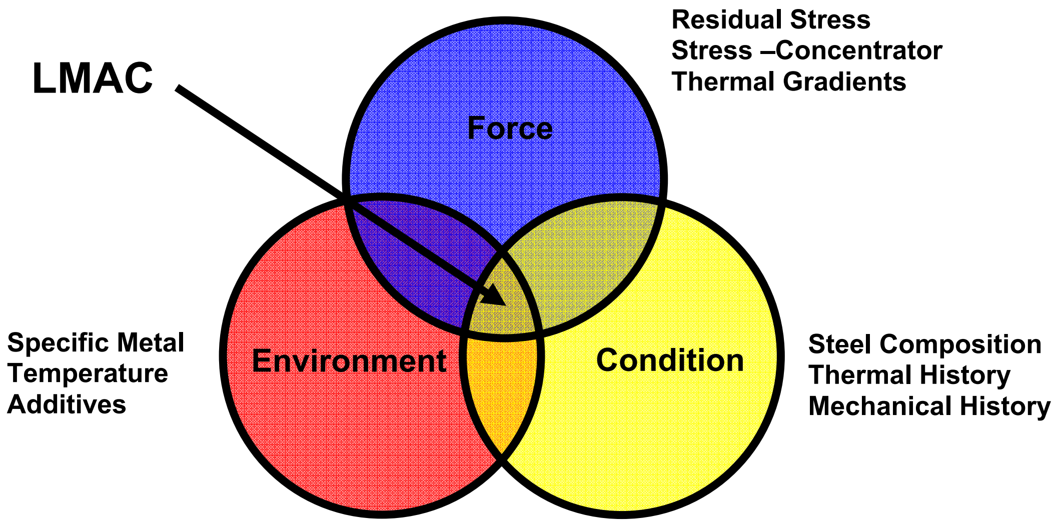

Figure 11 - Liquid Metal Assisted Cracking

The factors shown in Figure 11 are not always isolated from one another as implied in the diagram. For example, residual stress is related to thermal history, and other factors could have partial, or interdependent relationships. However the Venn diagram does show that it is the contemporaneous confluence of all three factors, Force, Environment and Condition which brings about the potential for LMAC in the fabricated steel / galvanizing context. Notwithstanding the partial interrelationships of some of the necessary factors, various contributions to the technical literature have served to illuminate specific sectors of the phenomenon.

Forces – Residual and Induced

It is reasonable to expect that tensile forces are necessary for the cracks to occur. There are two divisions of forces (stresses) which can be operative in the galvanizing context, residual stresses, and induced stresses. Either one of these forces can be macro, mini, or micro in magnitude and spacial range. For example, residual stresses as a result of the mechanical and thermal transients of rolling exist in balance form in a wide flange section. But the overall "macro" balance is composed of locations where the "mini" areas and magnitude of the local forces are compressive, and are algebraically balanced by tensile stresses in other "mini" portions of the section. An example of the location and direction of those stresses for a welded girder is shown below:[31] Note that the tensile stress at the web/flange intersection equals the yield point σ_Y

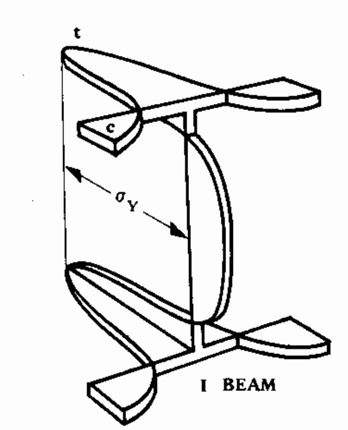

Figure 12 - Balanced Residual Stresses in an I Beam (from Lay)

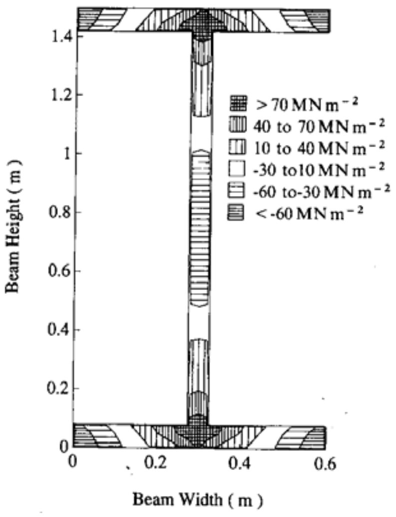

Figure 13 - Typical Residual Stresses in Beam Cross-Section (from Cresdee et al)

The magnitude of such stresses has been characterized by Cresdee, et al[32] who explored the induced as well as residual stresses as affecting dimensional stability during galvanizing. Heat flows across boundary surfaces and therefore internal thermal gradients are sensitive to the value of the convective heat transfer coefficient.[32] They found by experimentation that the heat transfer coefficient "best fit" was 1350 $Wm^{-2} K^{-1}$ for zinc, and 2700 $Wm^{-2} K^{-1}$ for water in quenching.

The concentration of tensile residual stress in the region of the web/flange intersection is assumed to be parallel to the axis of the beam. However Sedlack[33] et al recently published an interesting article about a cracking experience in Europe, where a Teilkopfplatten (half end-plate) detail is often used in framing, and cracks have been found in the web at the end of the weld, and projecting into the web parallel to the long axis of the beam .

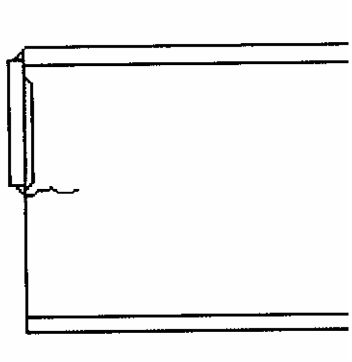

Figure 14 - Crack Location at End of Half-Plate Weld (Sedlacek et al)

For a crack to propagate parallel to the beam axis, the tensile force field must necessarily be perpendicular to the beam axis at the point of cracking. Sedlacek et al have found that while the residual stress field axis is parallel to the beam and in the web/flange region in most of the beam, there is an "end effect," as diagrammed below, where the parallel stress field begins to turn towards the center of the beam beginning at about one beam-height from the end. Thus, at the end edge of the web, the stress field is perpendicular to the long axis, and thus if of sufficient magnitude, is able to drive the crack growth.

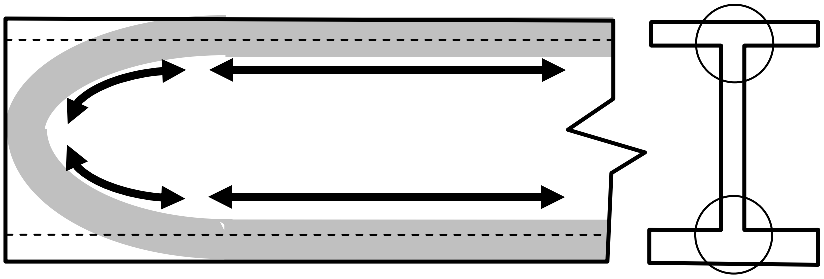

Figure 15 - End Effect for Residual Tensile Stress Field

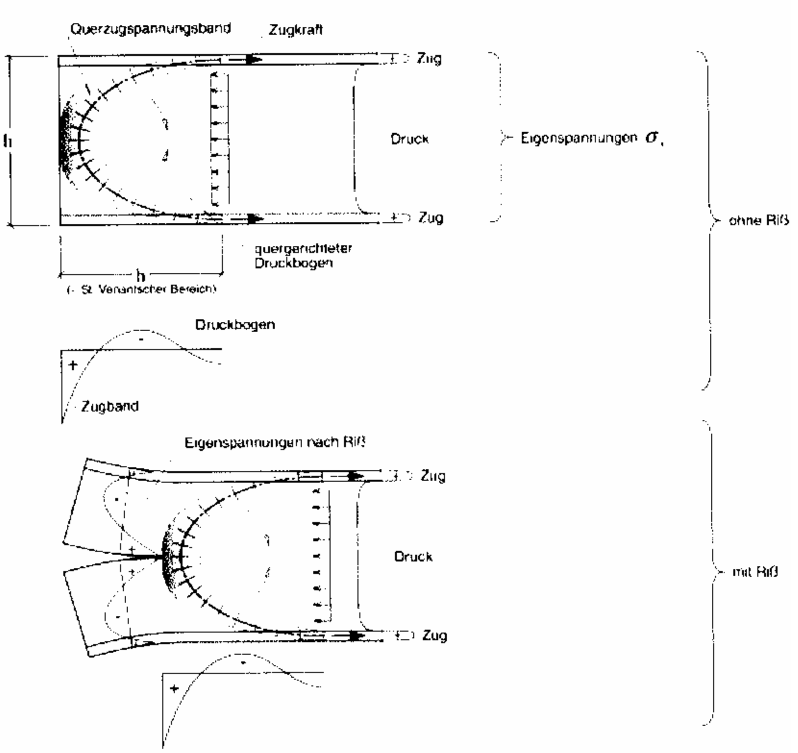

Figure 16 - Stress Pattern and Crack Development at Beam End (Sedlacek et al)

Induced stresses as a result of galvanizing have been studied by numerous researchers. As a general rule, the first stress developed by the surface heating should be compressive. Surface heating should attempt to expand the surface of the steel, however the surrounding colder mass acts as a restraint on the expansion, and therefore the surface undergoes compression until the inner core begins to expand. Once the inner core heats to the surface (galvanizing) temperature, the differential expansion stress is reduced until the galvanizing reaction is complete, and upon withdrawal from the molten zinc, the surface begins to cool with its contraction restrained by the higher temperature inner core. The result is a tensile surface stress. The instantaneous heating differential effect has been reported in the work of St. Beyer et al.[34] Although dealing with high temperature galvanizing (~560°C), higher than galvanizing temperature for structural steel, they showed heating rates, and stress development in the earlier phases was compressive at the steel surface.

The data in Figure 17 (Temperature difference above, and stress generated below) shows significant stresses compressive stresses developed as a result of higher surface temperatures (“Rand” = surface, “Kern” = center) with a few seconds of immersion in the zinc bath. The compressive stresses are unlikely to facilitate cracking during the time that the compressive stress is operative, however, a quick reversal of stresses back to tensile results from further galvanizing exposure. This reversal of stresses brings to light the “Bauschinger Effect,” in which plastic deformation increases yield strength in the direction of plastic flow, but decreases it in other directions.[35] The phenomenon is described as:

> "*Bauschinger Effect* – The other loading condition occurs when the test piece is initially loaded in compression beyond the elastic limit and then unloaded. The unload path is parallel to the initial load path but offset by the set: on reloading in tension the elastic limit is much lower, and the shape of the stress strain curve is significantly different. The same phenomenon occurs if the initial loading is in tension, and the subsequent loading is in compression."[36]

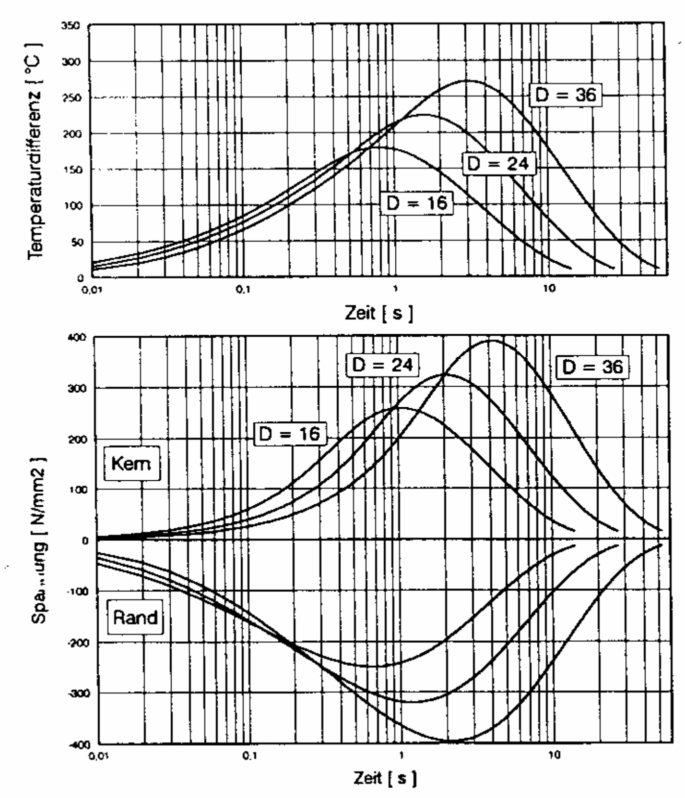

Figure 17 - Temperature Differential and Stress Values for Fasteners of Three Diameters in High Temperature Galvanizing (from Beyer et al)

Figure 18 shows the effect of the stress direction reversal, in that the compression loading beyond the elastic limit results in compression strains, and when the stress is reversed as reloading in tension, the yield point is lower, and thus the second tension loading results in tension yielding, and thus tension straining at lower loads than would be the case if the piece had not been loaded beyond the yield point in compression initially. The relevance of this to the possible facilitator of LMAC is two fold:

1. Most descriptions of the LMAC mechanism include the requirement for strains beyond the elastic limit, at which point, grain boundary penetration takes place.

2. The yield points, and additionally the elastic modulus of steel changes with temperature. In the initial (few seconds, perhaps) phases of hot dip galvanizing, the constrained expansion of the surface results in compression while the elastic modulus and the yield point is lowering with rising temperature. Subsequent

temperature equilibration releases the constrained expansion, reverses the stress direction, and on removal from the molten zinc, the tensile stresses generated by constrained contraction due to the hotter inner core, combined with a lower elastic modulus and lower (temperature related) yield point plus the lowering of the yield point related to the Bauschinger Effect can result in plastic tension strains, while in the presence of the draining molten zinc.

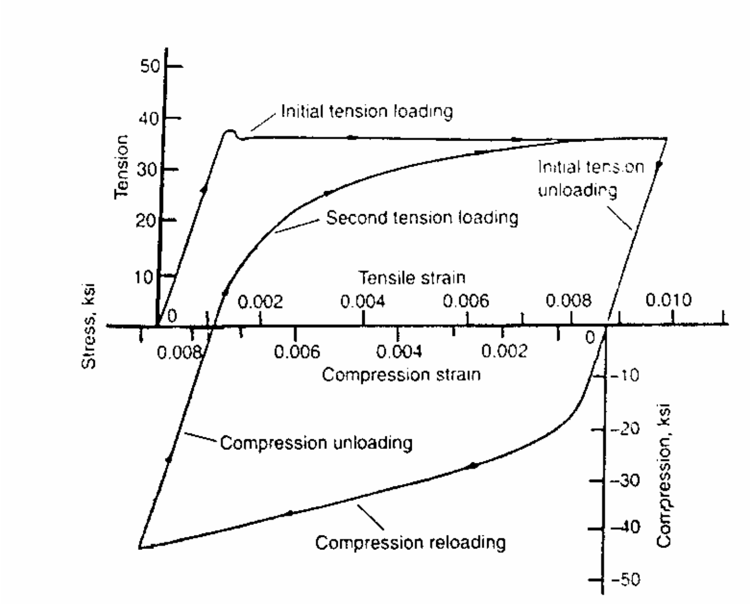

Figure 18 - Example of the Bauschinger Effect and Hysteresis Loop in Tension-Compression-Tension Loading (from ASM Handbook)

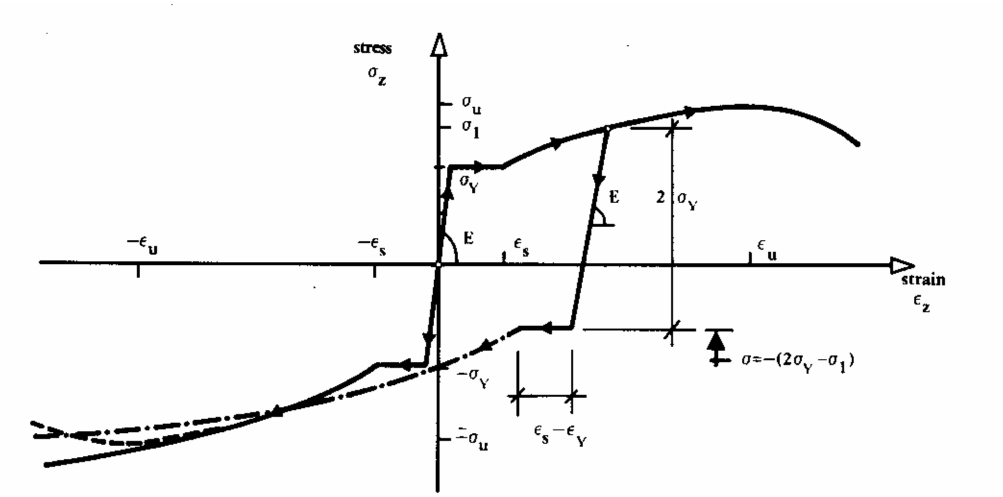

Figure 19 - Complete Stress Strain Curve at Constant Temperature (from Lay)

Figure 19 shows the complete (Tension and Compression) stress strain curve [31] at a uniform temperature. Figure 20 is the effect of elevated temperatures [31] on steel properties.

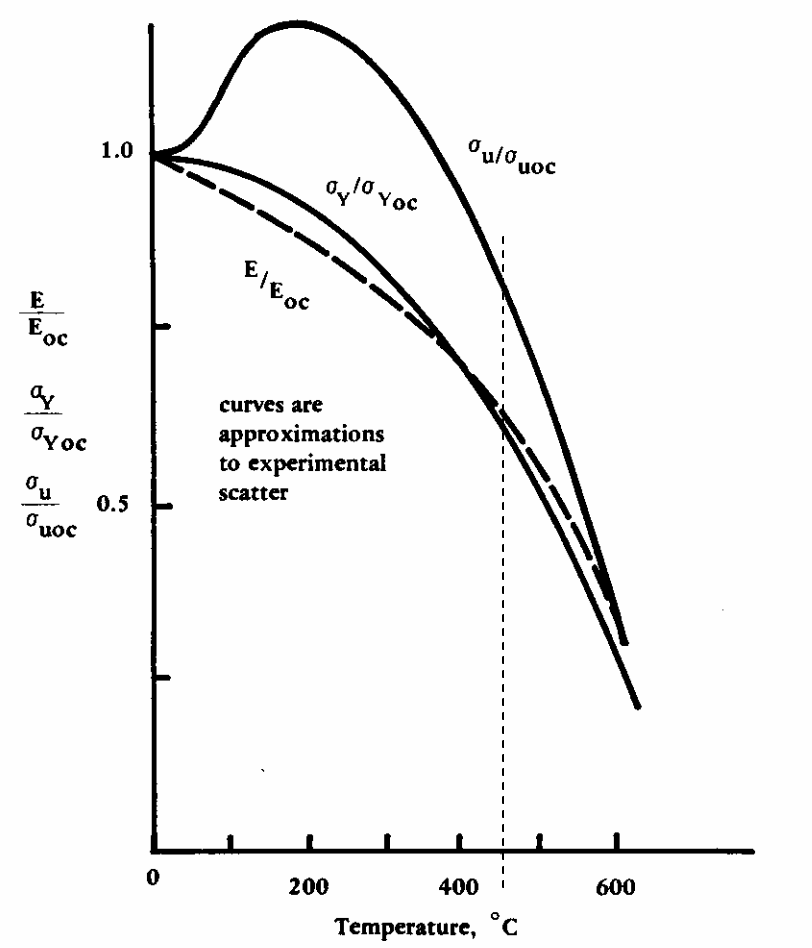

Figure 20 - Effect of Above Ambient Temperatures on Steel Properties (from Lay)
The added dashed line represents the nominal galvanizing temperature

In an experimental program possibly relevant to the galvanizing of fabricated (as cut, punched, cold formed, and/or welded) steel, Hancock and Ives[37], using copper – 8% aluminum specimen, with mercury as the embrittling liquid, explored the question of:

> "is it sufficient for the liquid metal environment to be introduced *subsequent* to the deformation or must the deformation occur in the presence of the liquid metal?"

(Note that exposure to liquid metal after mechanical and/or thermal processing is analogous to fabricating and galvanizing steel in commercial practice)

Previous work had shown that when copper-aluminum samples were deformed in a mercury environment, rapid intergranular fracture occured after tensile strains on the order of 3 – 5% percent. The question of how prestraining of such materials in air before reloading in mercury would effect the strain-to-fracture characteristics was explored. A schematic of their experimental conditions is shown in Figure 21. Specimen were prestrained in air to various levels, and subsequently reloaded in the presence of mercury until fracture.

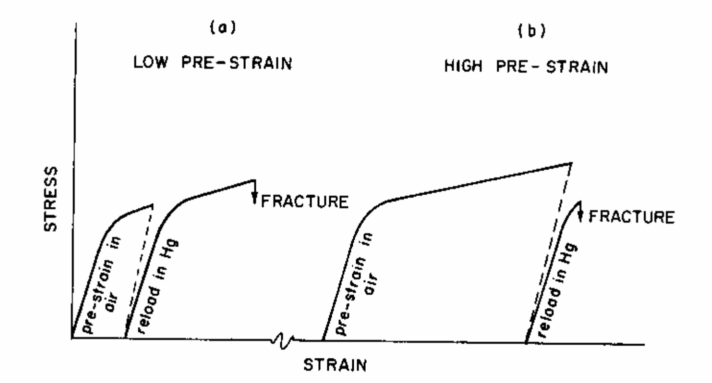

Figure 21 - Schematic Description of Prestrain Experiments (from Hancock and Ives)

The results of those experiments are shown in Figure 22 where (quoting from Hancock and Ives):

> "it is evident … that the necessary amount of additional strain in the presence of mercury decreases with prestrain and becomes very small at prestrains greater than 0.2." "Both the total strain and the fracture stress were found to vary with prestrain in these experiments"

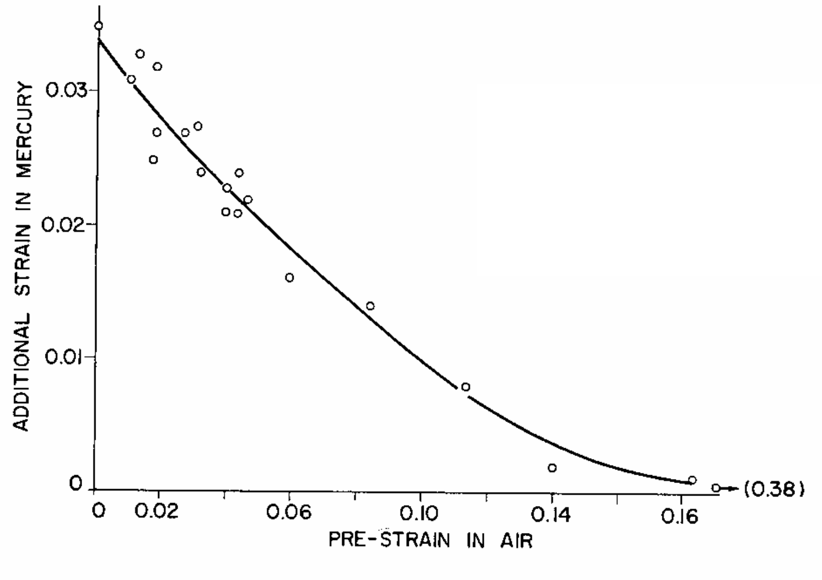

Figure 22 - Additional Strain to Fracture in Mercury After prestrain in Air (from Hancock and Ives)

Japanese researchers have done a significant amount of work related to the matter of stress/strain generation in hot dip galvanizing practice, however the amount of work translated into English is insufficient to fully understand the results and value of their work. For example, Figure 23[38] is a collection of diagrams outlining the stress and strain values while the plate girder in the upper left, is dipped in molten zinc. The curve marked

(a) is the temperature differential at a point (point B where the horizontal stiffener terminates) on the surface as a function of time in seconds. Curve (b) is the stresses and strains generated as a result of the differences in temperature due to dipping speed. Full immersion was reached (point 3) in about 40 seconds. The compressive strains are shown on curve (b), reaching a maximum at point 3, whereupon a stress and strain reversal occurred, going into tension. The value of the resulting tensile strain is marked by a range comprising the length of the arrow. In other related work, there has been a notation "ε_{ZC}" which refers to a critical strain in zinc, which is a threshold value, and has been related to steel composition through the CEZ or $S_{lm\text{-}400}$ equations. However the lack of adequate English translations of some of the work leaves much of this specific work unavailable.

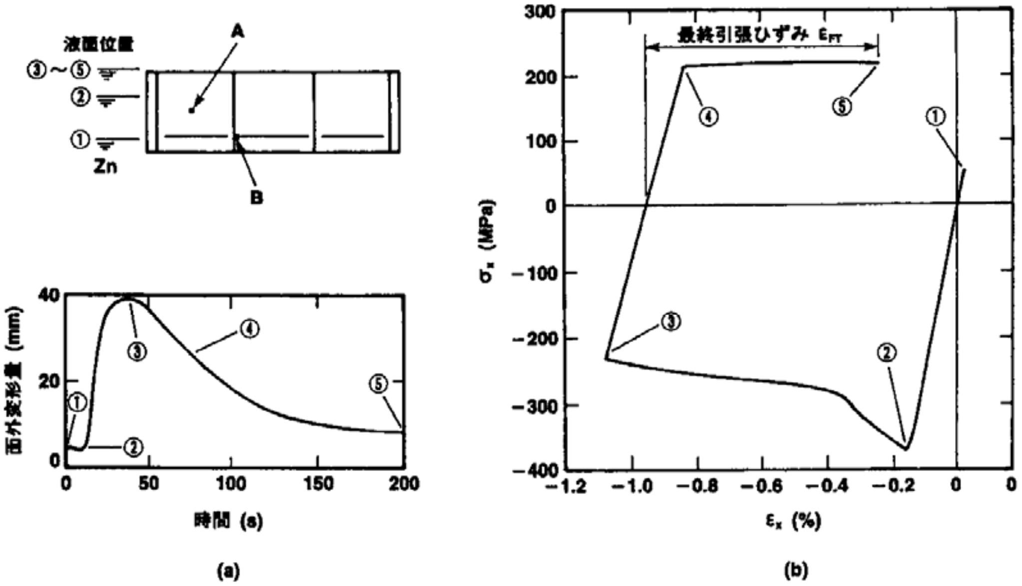

図 3. 35　めっき時の鈑桁橋梁部材の熱弾塑性解析結果（No. 1 モデル）

Figure 23 - Stress/Strain Reversal on Plate Girder during Dipping (private communication)

The question of stresses/strains induced in the galvanizing thermal transient has been studied by many, including field measurements as well as Finite Element methods. A general finding of these studies is that with the exception of unique combinations of thin-shelled, heavy baseplate monopoles, rapid immersion in the galvanizing bath minimizes the distribution of stress due to uneven heating of complex fabrications, or sections of varying thicknesses.

As shown in the galvanizing process schematic previous, the steel is normally immersed in an aqueous flux solution of $ZnCl_2$ and NH_4Cl. The necessary flux is usually heated, and the steel temperature rises to some degree during residence in the flux solution. The fluxed steel is then dried by evaporation in most cases, or in some cases by delay in a heated chamber which may be as much as 130°C or more. The completeness of this evaporation is a function of time, temperature and surrounding air humidity, but is also a function of chemistry of the flux, or more specifically, the ratio of $ZnCl_2$ and NH_4Cl.

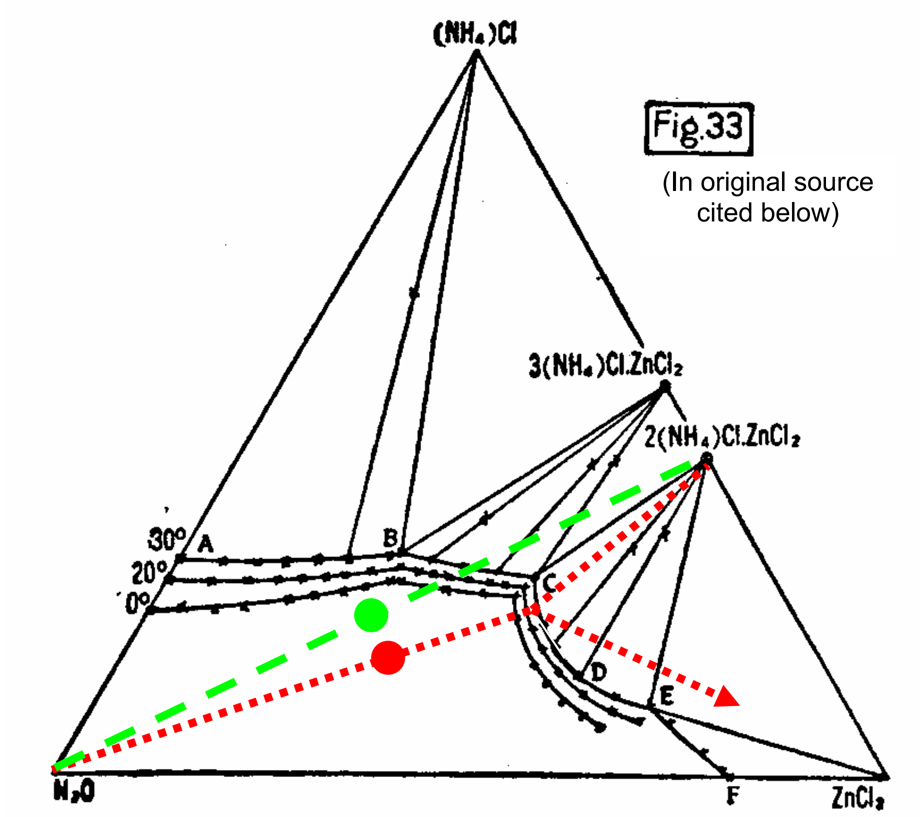

Figure 24 - Ternary Solubility Diagram for NH_4Cl,-$ZnCl_2$-H_2O (from International Critical Tables)

The ternary solubility diagram shows that the water solubility of $ZnCl_2$ (point F) is much higher than that of NH_4Cl (point A), indeed, $ZnCl_2$ is perhaps the most soluble of all common Chloride salts. Related to water solubility is hygroscopicity, thus $ZnCl_2$ has a high affinity for water and therefore is difficult to dry. The dot on the dashed line represents a typical flux composition, in which the NH_4Cl, $ZnCl_2$ ratio is “balanced” with a known solid double salt composition as indicated by the end of the dashed line. If that aqueous flux were to dry, the double salt would begin to precipitate on the steel, and given enough heat to drive evaporation, the drying would be complete along the right side of the triangular diagram. If the salt ratio in the aqueous flux were to become unbalanced, as shown by the dot on the dotted line, evaporation reached the solubility limit, the double salt would begin to precipitate, but the remaining solution (actually aqueous film) would begin to become richer in $ZnCl_2$ along the solubility line, and the composition of the remaining flux film would drift towards the $ZnCl_2$ corner of the diagram (as shown by the arrowhead) which is a more hygroscopic aqueous concentration – harder to dry.

If water is retained in the flux film because of incomplete dryness due to inadequate heat in the steel or its surroundings, or because of imbalance of the flux ratio, the result is “flash evaporation” when the moist flux film enters the molten zinc which is nominally at ~450°C. These percussions can create dangerous molten zinc “spatter” in the vicinity of the galvanizing bath, and a common and understandable practice is to slow the immersion, or delay entry until the heat conducted by the already-immersed part of the steel completes the drying of the flux film. This slow or intermittent immersion is contrary to good practice from a differential expansion viewpoint, and can lead to exacerbation of the strains possible in entry into the galvanizing bath. If the steel being immersed is susceptible to molten metal cracking, the potential for such cracking increases. Thus flux maintenance and galvanizing practice (as in flux drying and rapid immersion) are worthy of continued scrutiny.

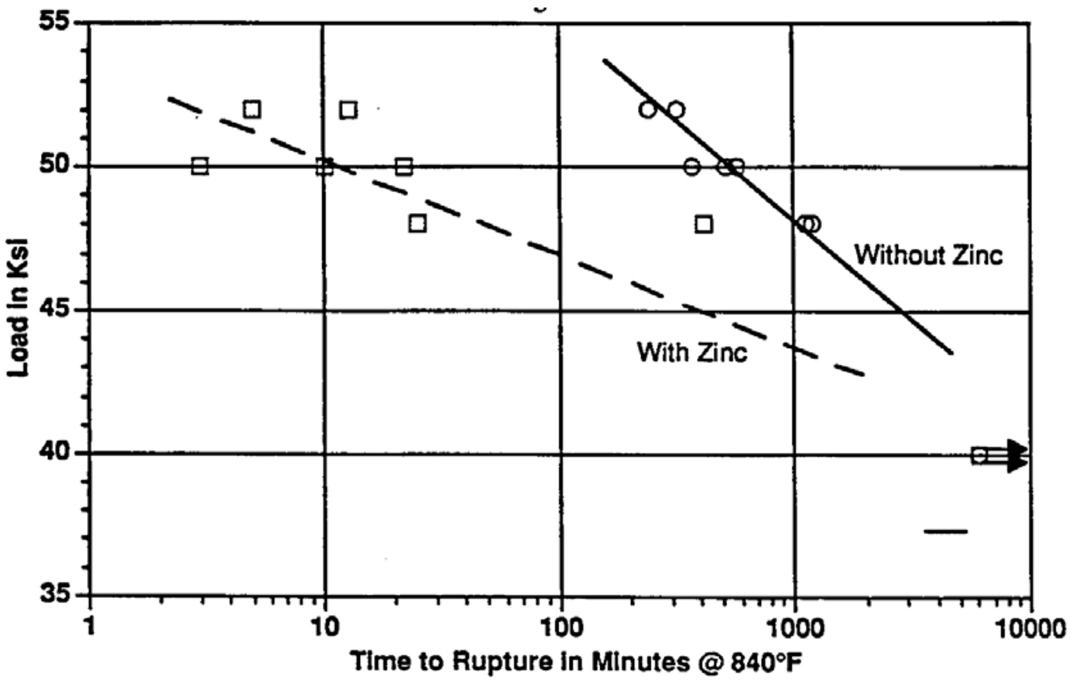

Figure 25 - Time-to-Rupture at 840 Degrees F as a Function of Load and in the Presence or Absence of Liquid Metal (from Kinstler)

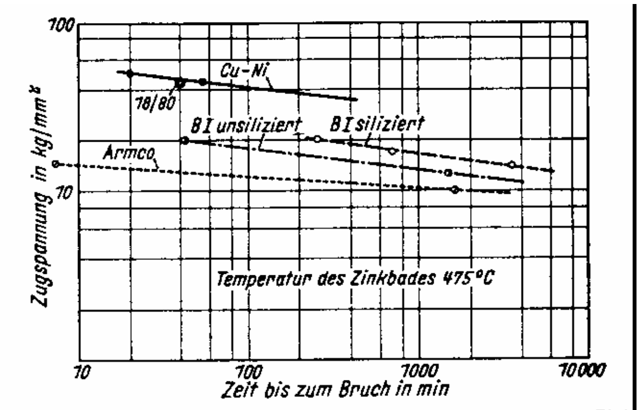

Bild 13. Lebensdauer verschieden legierter Stähle in flüssigem Zink in Abhängigkeit von der Zugspannung

Figure 26 – Endurance (Time-to-Crack in Minutes) of Different Steel Alloys in Molten Zinc as a Function of Load (from Radeker)

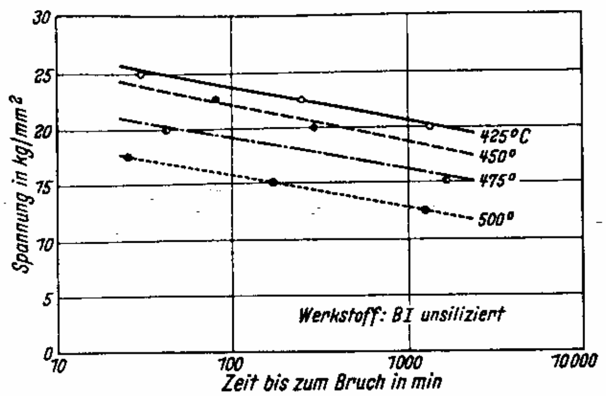

Bild 12. Lebensdauer von Dauerzugproben in flüssigem Zink in Abhängigkeit von Spannung und Temperatur

Figure 27 - Endurance (Time-to-Crack in Minutes) as a Function of Load and Molten Zinc Temperature (from Radeker)

The matter of time is also important as a number experiments have shown that an "incubation" time is usually seen with LMAC phenomena. Kinstler,[39] and Radeker[40] have shown that the time-to-crack of a given steel is a function of test load, and also zinc bath temperature. nOte that Kinstler has shown that the test steel, which was a commercially available A36 composition failed at similar loads at the nominal galvanizing temperature of 840°F, but at much shorter times in the presence of molten zinc. The steel tested ruptured under sustained load when the load approximated the UTS, while loads of approximately the Yield Strength increased the endurance in molten zinc by three orders of magnitude. Figure 26, from Radeker, supports the above finding. Time at galvanizing temperature is related to many factors including design as it affects difficulty in handling in the galvanizing bath, and individual piece weight. Thus it is clear that Figure 11 should be redrawn as below:

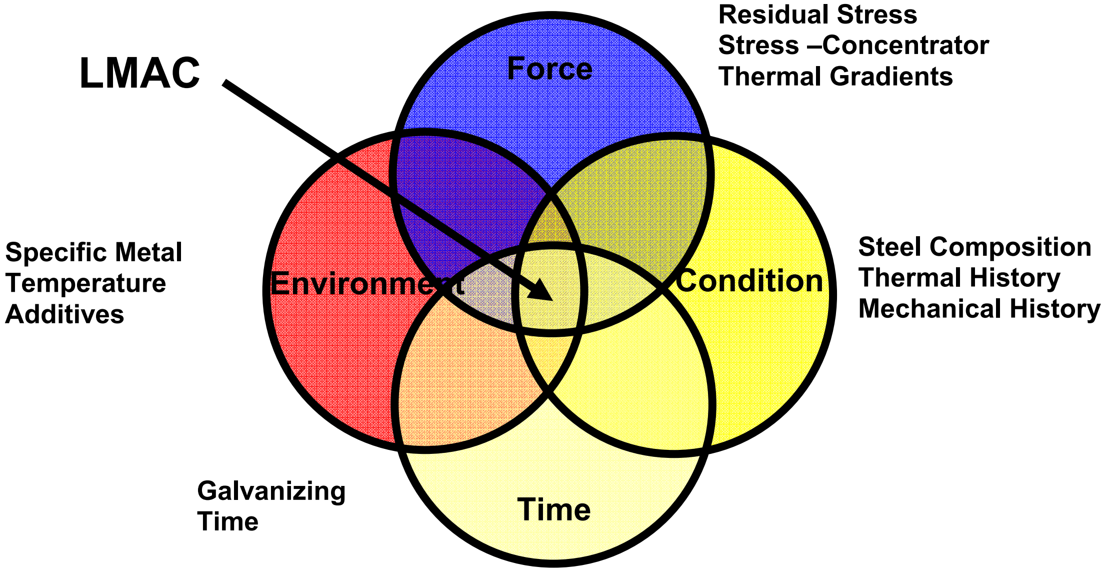

Figure 28 - Liquid Metal Assisted Cracking – Four Necessary Components

Environment – Liquid Metal

Figures 4 and 5 show the schematic of typical batch galvanizing practice, and the resulting coating morphology. The coating microstructure shown is typical, with an adherent zinc outer layer bonded to a series of largely coherent zinc-iron alloy layers, providing the galvanized coating with its unique combination of toughness and corrosion resistance. The outer zinc layer is often initially shiny in appearance, and sometimes with a "leafy" or "spangled" appearance as shown below

Figure 29 – Initial Surface Appearance of Typical Galvanized Coating (from International Lead Zinc Research Organization)

The coating microstructure affects the surface appearance, and from time to time, all or part of the steel being galvanized reacts very rapidly with the Zinc producing a coating which is dull grey in appearance, excessively thick, brittle, and poorly adherent. Thus measures to counteract the enhanced reactivity as a function of the steel composition are a central facet of galvanizing process development. Typical coating microstructures on "normal" and "reactive" steels, in approximately correct relative size are shown below:[41]

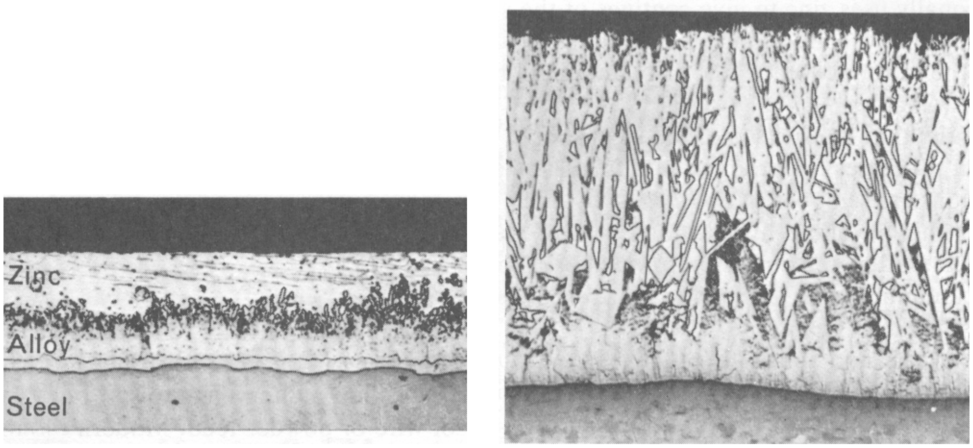

Figure 30 - Galvanized Coating Microstructures Produced from "normal" (left) and "high reactivity" (right) Steels (from Porter)

The "chaotic" growth of the intermetallics on high reactivity steels, relative to the more "ordered" growth on less reactive steels has in the past been related to Silicon content in certain ranges, and anecdotal experience suggests that through the 1980s to today, has been increasing as the use of continuous casting in steel making has grown. The seminal work which describes the effect is that of Sandelin, and the curve relating silicon content of the steel and the magnitude of zinc-iron intermetallics formed is often called the "Sandelin curve." A depiction of the general shape of the "Sandelin Curve" related to both silicon content of the steel, and galvanizing time at a constant temperature is shown below[42]:

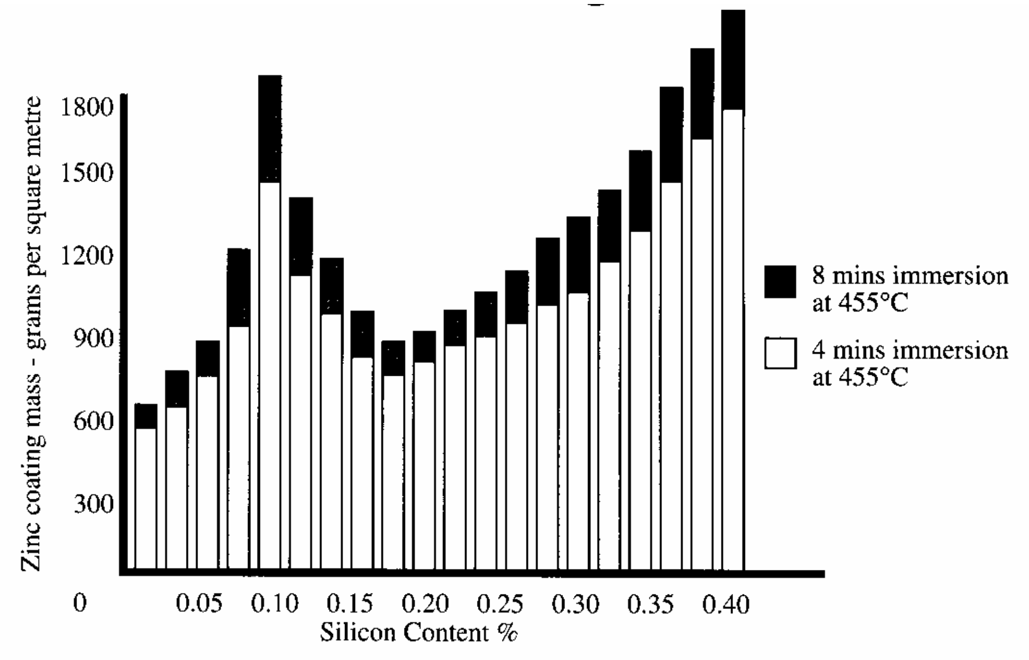

Figure 31 - Effect of Silicon of Steel on Galvanizing Coating Thickness (from Industrial Galvanizers Pty Ltd)

The work by Sandelin has been verified many times, and has been extended to include the significant unit effect of phosphorus. As a general rule, the "Silicon Content" on a typical "Sandelin Curve" should be calculated so as to include the effect of Phosphorus using the "Silicon Equivalent" equation:

$$Si(eqiv) = Si\% + 2.5(P\%)$$

As shown in Figure 5, the galvanized coating is composed of two basic structures, the intermetallics, the thickness of which is related to steel chemistry, zinc chemistry, reaction time, and temperature, and the outer zinc layer which is a function of the temperature (more correctly the cooling rate), drainage conditions, additional forces beyond gravity, such as wiping, centrifuging, or other mechanical effects, and zinc viscosity and surface tension. Reactivity is also affected to some degree by steel surface roughness and residual stresses. Drainage can be affected by geometric design and fabrication.

The practical range of galvanizing temperature is from approximately 430°C - 460°C, so while some control of reactivity can be realized by temperature variation, as a practical matter, solubility changes with temperature, as well as heat capacity of the galvanizing kettle limits temperature as a reactivity control strategy. Change in galvanizing time is of variable effect due to limited pre-galvanizing knowledge of steel article chemistry. zinc chemistry has been somewhat effective in reactivity control, as well as drainage control with developments over the past twenty years or so. The table below lists some of the elements which have been added to zinc for reactivity and drainage effects:

Additive	Zone Affected	Primary Effect
Al	Outer Zinc Layer	Adds "brightness" to initial coating appearance
Pb	Outer Zinc Layer	Historically found in some grades of zinc, significantly affects drainage by lowering surface tension
Ni	Intermetallics	Inhibits Silicon effect within certain ranges
Bi	Outer Zinc Layer	Has similar effect as Pb, reportedly also has reactivity effect when used with Sn
Sn	Both Zones	Inhibits silicon reaction within certain ranges, improves drainage of excess zinc as the outer layer forms, and can also enhance "spangled" and "brightness" appearance of outer layer

While there are many "recipes" for the zinc spelter used in batch hot-dip galvanizing, the most common nominal compositions[43] in addition to unalloyed Zn (typically Special High Grade) (not in any specific order) are:

- Zn - ~1% Pb (Prime Western Grade)
- Zn - ~0.05% Ni - (Pb)
- Zn - ~0.05% Ni - ~0.1% Bi - (Pb)
- Galveco© Alloy (Zn - Sn - Bi - Ni)

The zinc – nickel baths have been found to suppress the first "peak" in the Sandelin reaction curve, but is less effect on the second rise of coating thickness at higher Si(equiv) values. The use of tin is reported to both surrpress the first "peak" and significantly lower the second reaction range.[44] Gilles and Solokowski, and Beguin et al[45] have proposed that the mechanism by which The Zn-Sn-Bi-Ni alloy works to inhibit the otherwise chaotic reaction with reactive steels is twofold:

> "If elements such as tin or bismuth, which are not soluble in the intermetallics, are introduced into the zinc melt, these elements are rejected during the growth of the intermetallics and form a film around the intermetallic phase. The diffusion of zinc and iron through this film is by this means hindered. If the concentration of these elements are too low, the

film thickness decreases and becomes less effective. The second effect is the reduction of Iron diffusion across the intermetallic layers.”

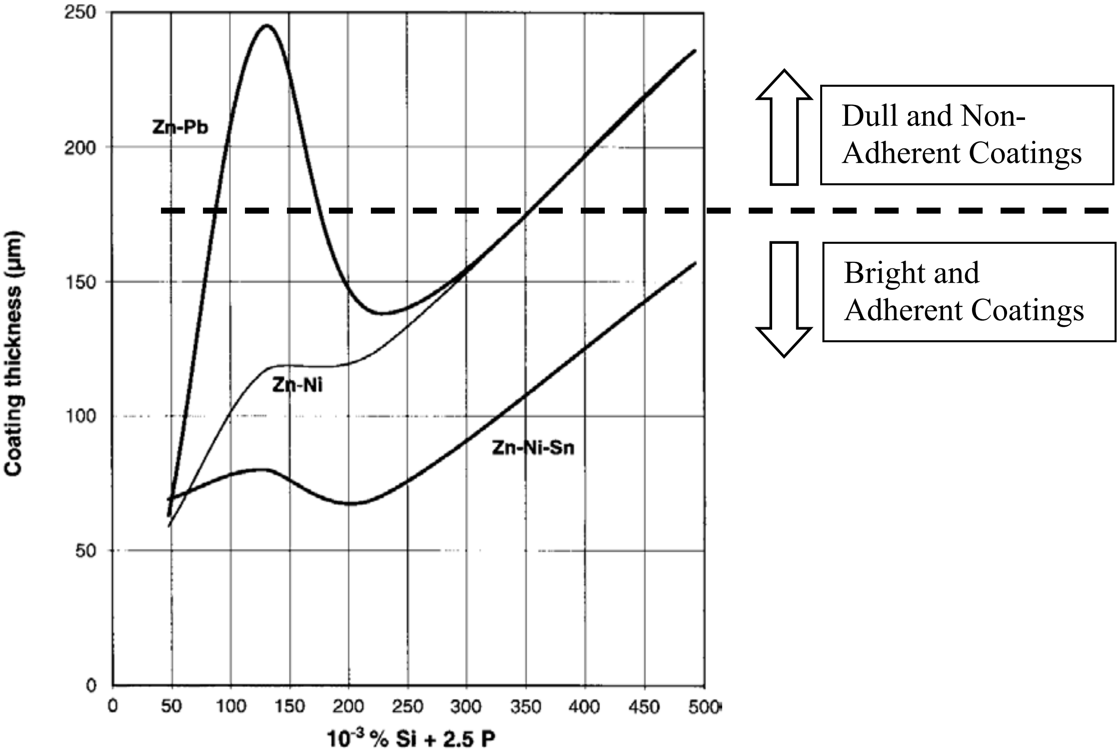

Figure 32 - Coating Thickness Achieved on Different Steel Grades with Various Zinc Alloys (from Gilles and Sokolowski) (modified)

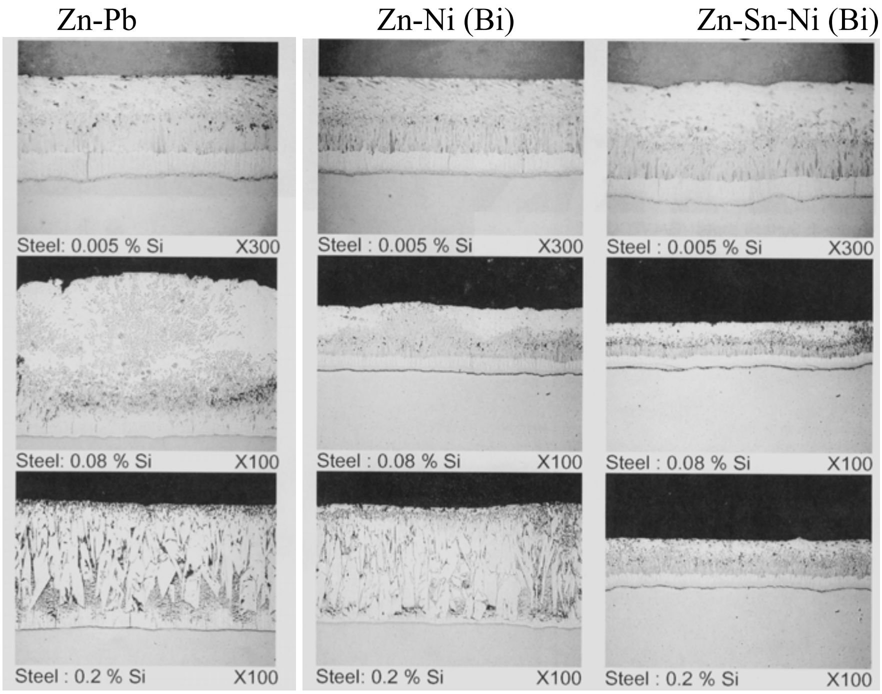

Figure 33 - Cross Sections of Coatings ((from Pankert et al)

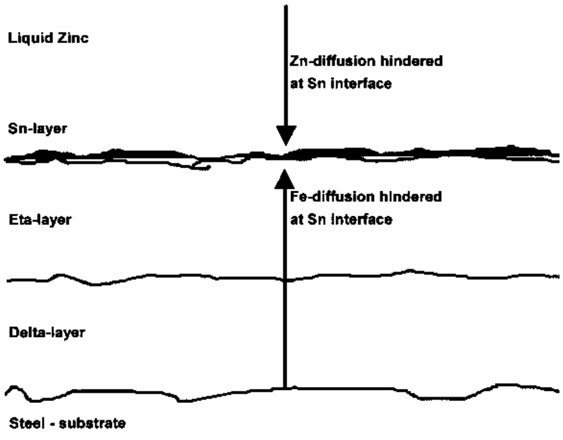

Figure 34 – Mechanism of the Galveco© Alloy (Zn-Sn-Bi-Ni) (from Beguin, et al)

Pankert et al have demonstrated the effect as shown below:

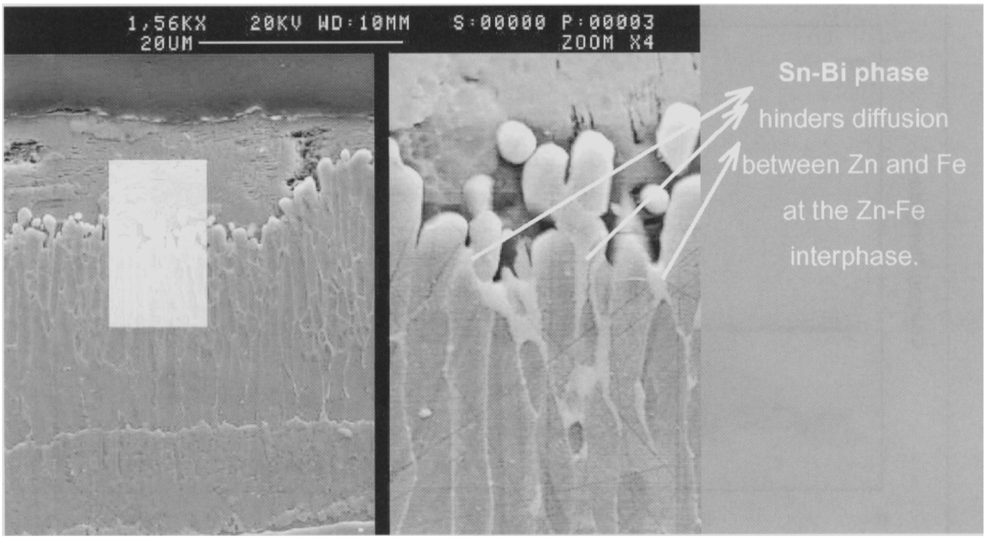

Figure 35 - Mechanism of the Galveco© Alloy (Zn-Sn-Bi-Ni) (from Pankert et al)

The phase diagram below shows the melting point of zinc at about 420°C, and tin melts at about 232°C, with a binary eutectic at about 198°C. The solubility of tin in zinc is about 0.1%. It has often been reported that tin creates a "spangled" or "flowery" crystal appearance on solidifying zinc. Krepski[46] has reviewed the effects of bath alloy additions in hot dip galvanizing. He reports that:

> "Tin exerts its influence on spangle formation by altering the manner in which the coating solidifies. The solubility of tin in solid zinc is less than 0.1%, so rejection of tin to the liquid phase will accompany the growth of dendrites of zinc solid solution. Under equilibrium conditions, this tin-rich liquid will not solidify until the eutectic temperature of 198°C is reached."

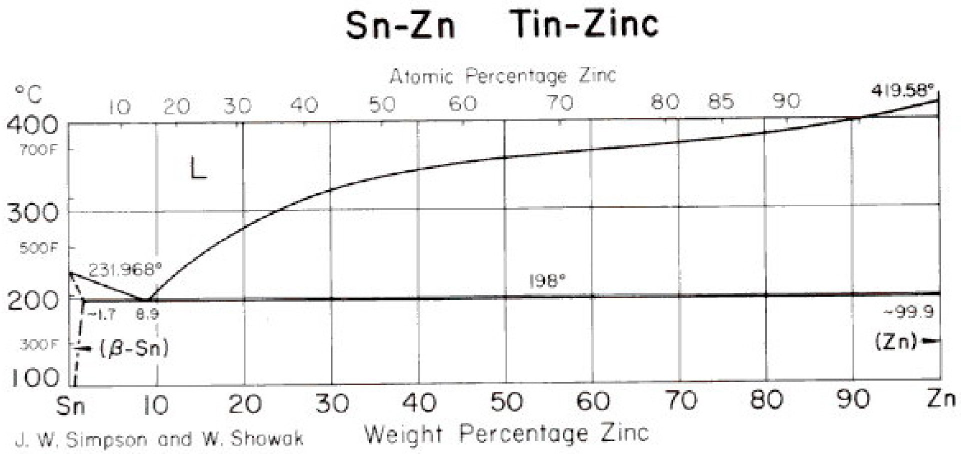

Figure 36 - Tin - Zinc Phase Diagram

However, the alloy additions to zinc in general galvanizing is unlikely to be a simple binary. For example, the Galveco® alloy described above is at least a ternary of zinc, tin and bismuth, for which the Freezing Pint Diagram is shown below:

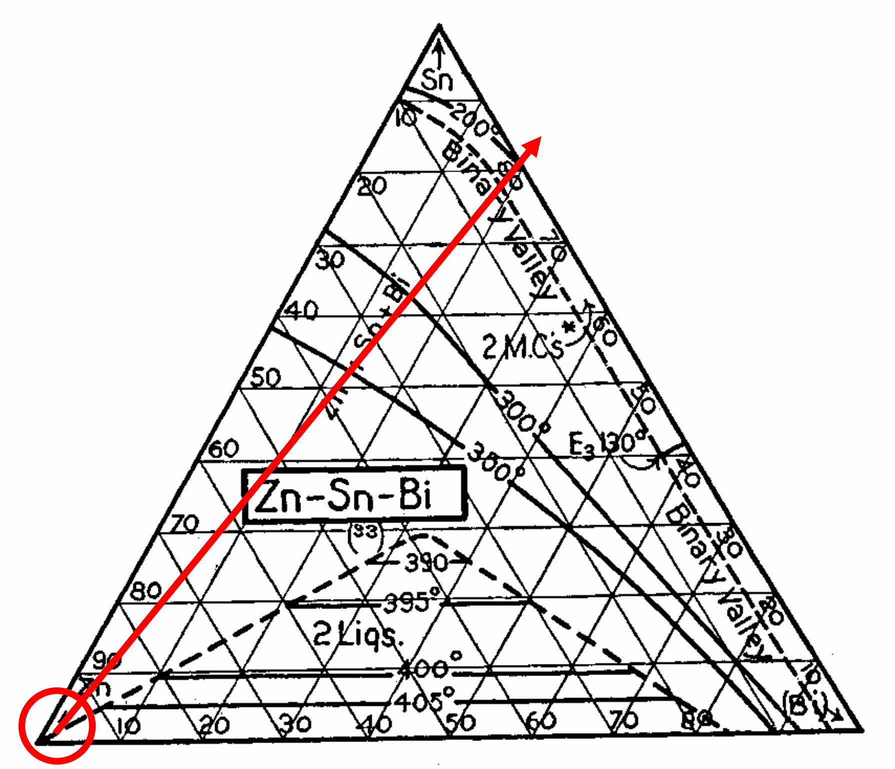

Figure 37 - Zinc - Tin - Bismuth Freezing Point Diagram (from International Critical Tables)

For the typical ternary galvanizing alloy, the composition is almost all zinc and therefore, the composition can be found very near the lower left hand corner of the diagram (designated by the red circle), and the freezing point will be nominally around 400°C. As prepared steel (iron) is introduced to the melt, such as in common galvanizing practice, the zinc and iron will react to form the solid, high-melting, intermetallic layers as shown in Figure 5. Thus, zinc is “consumed,” and the rejected tin and bismuth go into the melt.

However, if for any reason, the zinc has entered a surface crack, void, defect, or grain boundary of the steel, dilution of the rejected tin and bismuth into the bulk zinc melt will be inhibited by the distance and likely tortuous path, and the liquid composition within the crack will quickly reach a tin and bismuth-rich, zinc-poor composition approaching the right hand side of the ternary diagram as shown by the red arrow – the angle of the arrow, assuming no interaction or other compound formation, will be according to the tin – bismuth ratio in the original melt composition.

Note that the freezing points along the right hand side of the triangle are much below the ~400°C range of the original bulk znc alloy melt. For example, the symbol E_3 denotes the ternary eutectic composition for the metals, and the freezing point is only 130°C, although there is no evidence that the E_3 would be reached in practice. Thus, if a crack in steel being galvanized is initiated by whatever reason in the ternary melt, the “consumption” of the zinc by the galvanizing alloying reaction, results in a local composition which will remain liquid much longer in the galvanizing and cooling (and therefore contraction) cycle, possibly adding in the propagation of the original crack, or melt intrusion. The composition of that liquid metal pool will be nominally, the composition of the alloying additions without the zinc.

This mechanism is consistent with detailed findings of investigations of cracks found after galvanizing. For example, the earlier-cited paper by Sedlacek et al, reporting on an examination of cracks found in a European structure after galvanizing in a Zn-Sn-Pb-Bi Bath. SEM-EDX analysis found tin and lead-rich phases (Figure 33) consistent with the intermetallic insolubility and pooling of rejected, low-melting elements mechanism outlined above.

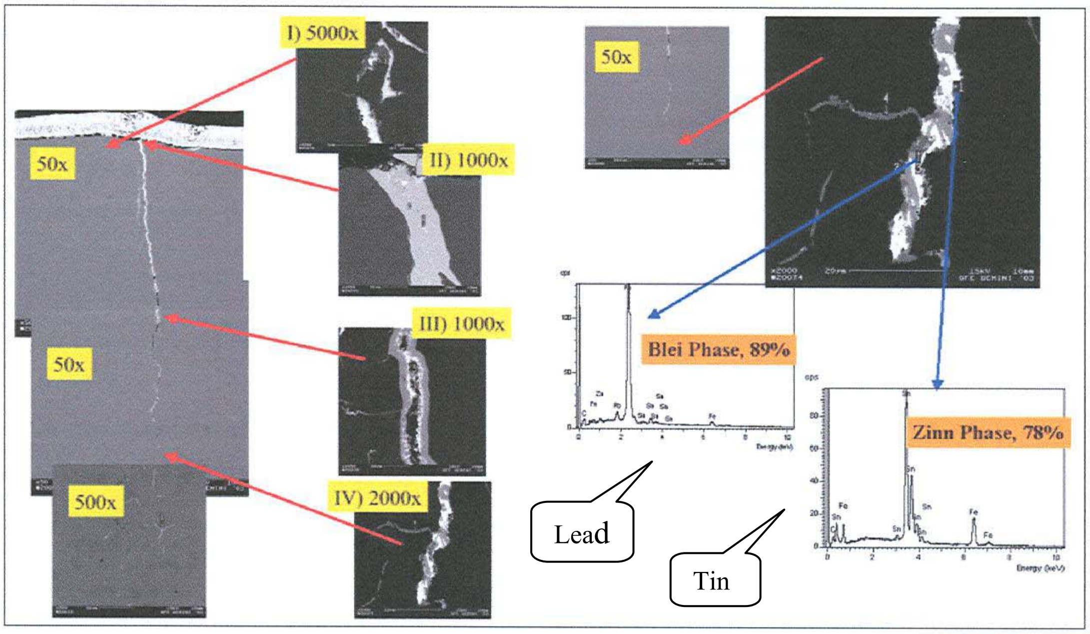

Figure 38 - Increased Lead and Tin Concentration (Bright Areas) at the Edges of a Crack filled with Solidified Bath Metal: View of the crack (left) and Chemical Analysis of the Crack Tip (right) (from Sedlacek et al))

Similarly, cracks in a highway bridge truss were examined after they were found after galvanizing in a Zn-Sn-Pb+ by visual and magnetic particle inspection[47].

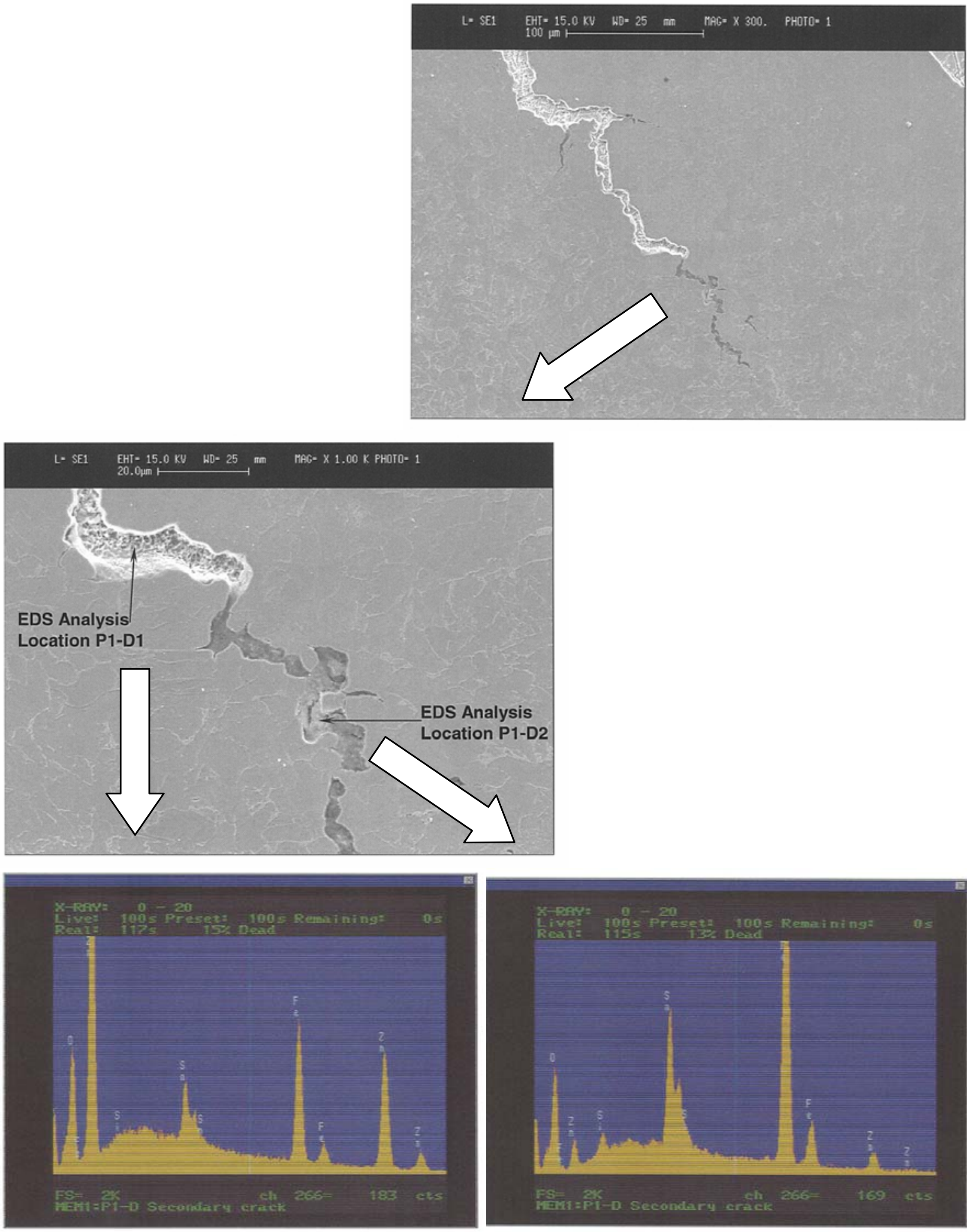

Figure 39 - Secondary Crack (at Two magnifications) Found in Bridge Structure Connection Plate after Galvanizing, with EDS Analysis of Two Locations Approaching Crack Tip (from Private Communication)

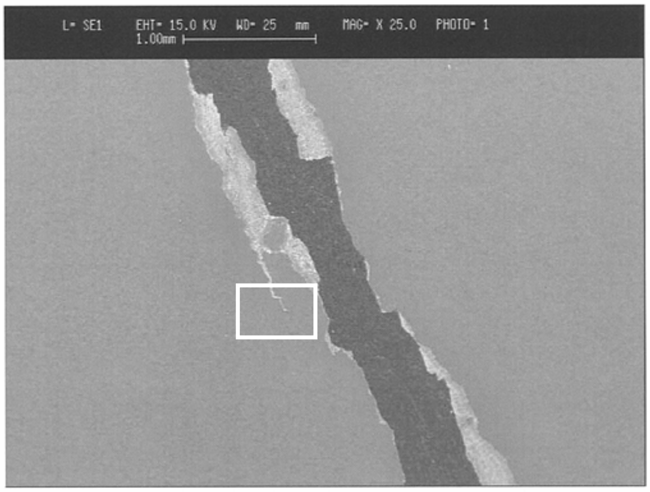

Figure 40 - Location of Secondary Crack Detailed in Figure 34

The EDS image on the left, within the "body" of the secondary crack, indicates zinc and iron as the predominant elements, which is normal for the cross section of a galvanized surface. The right image, nearer to the tip of the crack indicates a predominance of tin, with only small indications for zinc.

The Images and EDS indications from another crack is shown below:

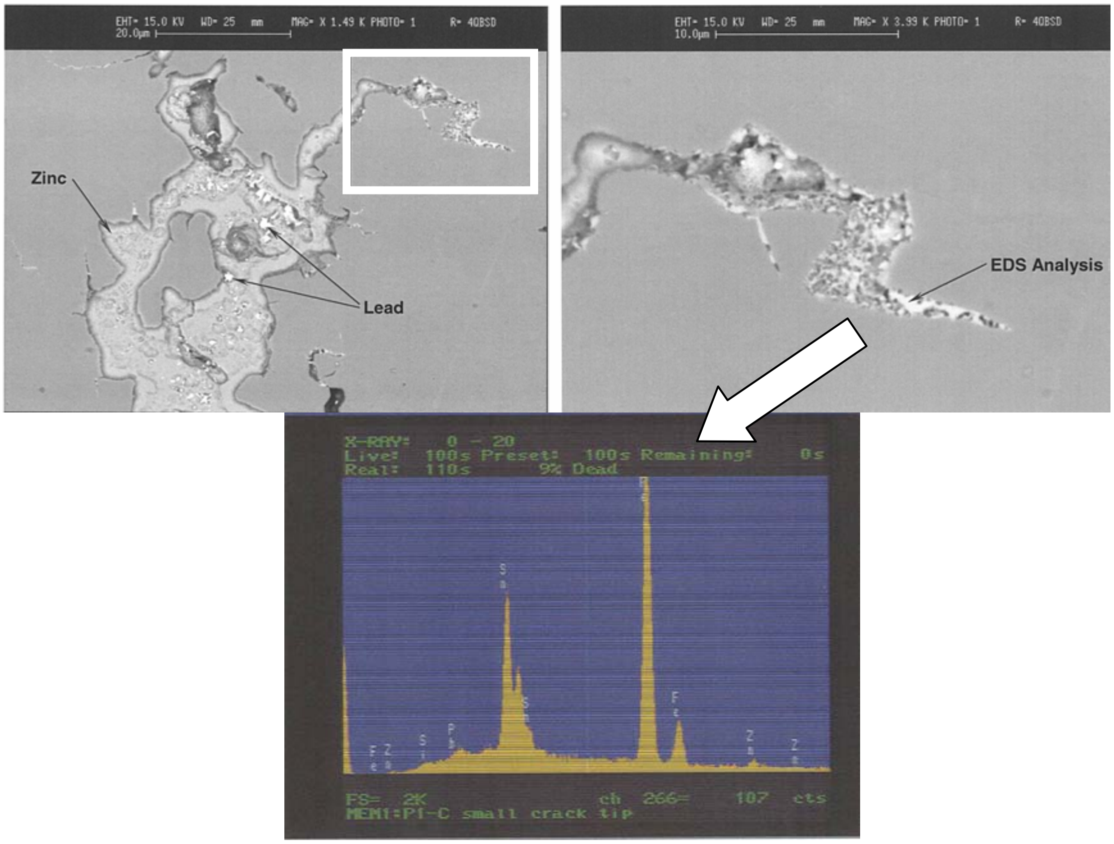

Figure 41 – Back-Scattered Electron Image of Secondary Crack (from Private Communication)

In the back-scattered electron mode, the higher an elements atomic weight, the brighter it will appear. Of the elements present, iron is the lowest atomic weight, followed by zinc, tin and finally lead. Consequentially, lead and tin will appear bright, whereas iron and zinc will have a less prominent appearance.[48] Other crack images from the same sample are shown below. Note the predominance of elements heavier than zinc at crack tips.

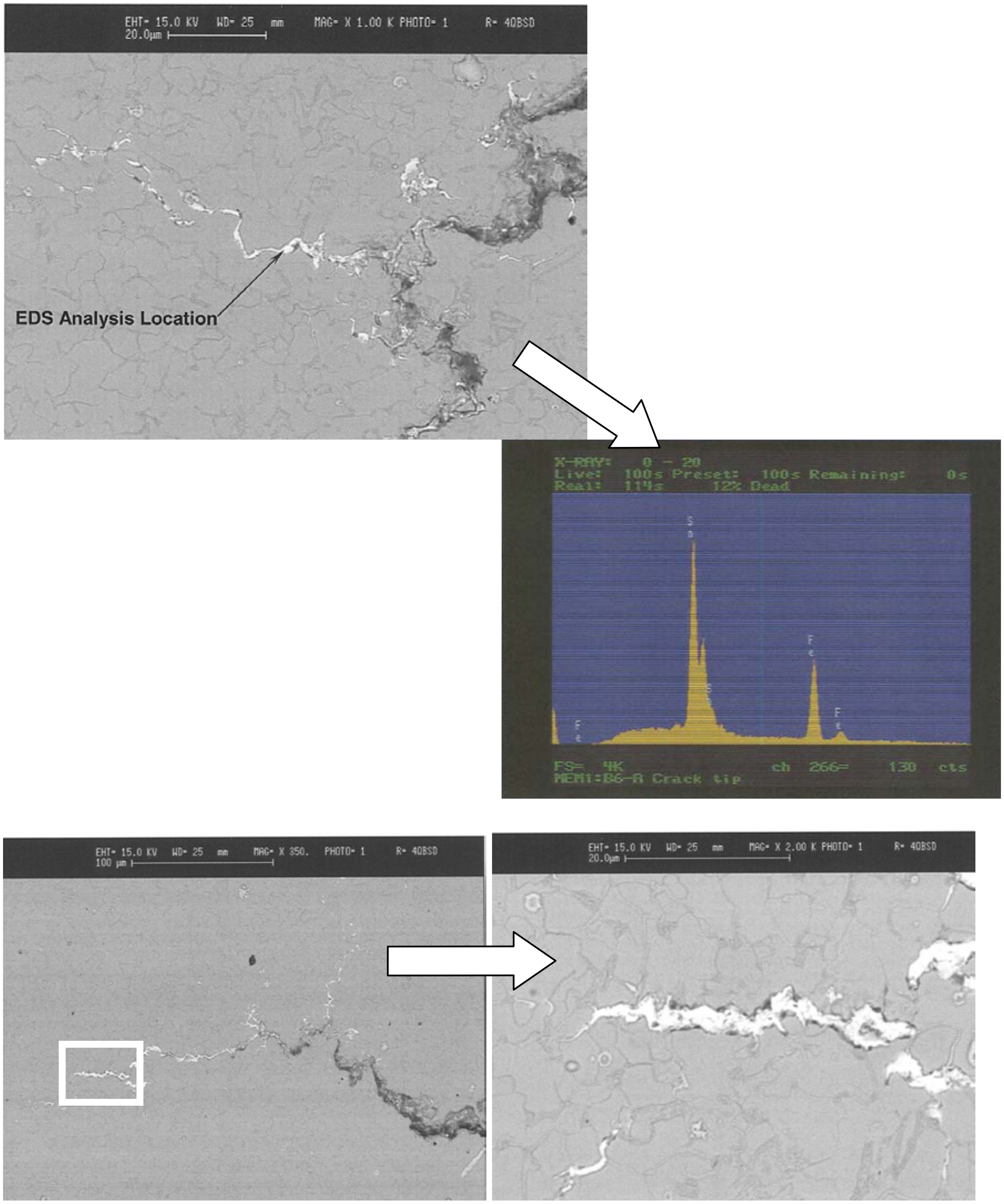

Figure 42 - Back-Scattered Electron Image of Two Different Secondary Cracks, One with EDS Analysis (from Private Communication)

The bright images at the crack tips, and the EDS analysis for one image showing little zinc, and predominantly higher atomic weight elements known to be in the zinc melt, is consistent with the mechanism discussed above. With the zinc bound by reaction to form the well-known solid, intermetallic layers while still at the galvanizing temperature of over ~420°C, the resulting pool of rejected elements, such as tin, bismuth, and lead, all of which have lower freezing points and are known to "wet" iron (steel), is still liquid, perhaps well into the cooling cycle after removal from the galvanizing bath. Any cracks which may have formed, or which had been present before galvanizing would undergo tensile forces as the cooling steel contracts as allowed by the geometry of the fabrication. The presence of increasing tensile stains, in the presence of an "internal" liquid pool suggests "liquation" cracking as a mechanism subsequent to galvanizing.

The freezing points on the subject galvanizing bath components and known eutectics are listed below[49]:

Element or Components	Low Freezing Temperature °C
Zn	419°
Pb	328°
Zn-Pb	314°
Bi	272°
Zn-Bi	250°
Sn	232°
Zn-Sn	198° ?
Pb-Sn	181°
Zn-Sn-Bi	130°
Bi-Pb	125°
Pb-Sn-Bi	124° ?
Bi-Sn	124°

It should be clearly noted that the matter of cracking on thermal cut edges and welds was a very rare, but not unknown occurrence, well preceding the introduction of zinc alloy additions such an nickel, bismuth., and tin, developed to counteract the perceived increase of "Sandelin"-type reactivity in steels. During that period, and the preceding decades, lead was a common component of typical batch galvanizing baths. As recently as 2000, a survey of batch galvanizing baths in North America reported only about one quarter had lead contents less than 0.2%.[50] In addition, much of the research reported throughout this paper used "Prime Western" or equivalent grades of zinc, which implies lead contents nominally at about 1%, theoretically up to the saturation value at galvanizing temperature, or about 1,4%. Thus lead has been historically present during the period when such cracking was extremely rare, essentially unreported and thus unknown, suggesting that the presence of lead alone is not the causative agent in more recent cracking phenomena. Steel embrittlement as a result of severe cold work and then subsequent exposure to the galvanizing thermal transient has been known for decades as a form of strain age embrittlement[51]

A property of the zinc alloy additions which has been investigated is the property of "wettability." The facility to "wet" a surface is a necessary precondition for surface reaction, and Pankert et al discusses a possible increase in propensity to distort or crack steel using the tin, bismuth, nickel type alloy as related to increased thermal gradients, and associated asymmetry of stresses/strains caused by the increased "wettability" of these alloys relative to historical zinc spelter compositions.[52] Measurements of heat transfer rates as a function of variation of alloy composition, as well as galvanizing process variables are shown below:

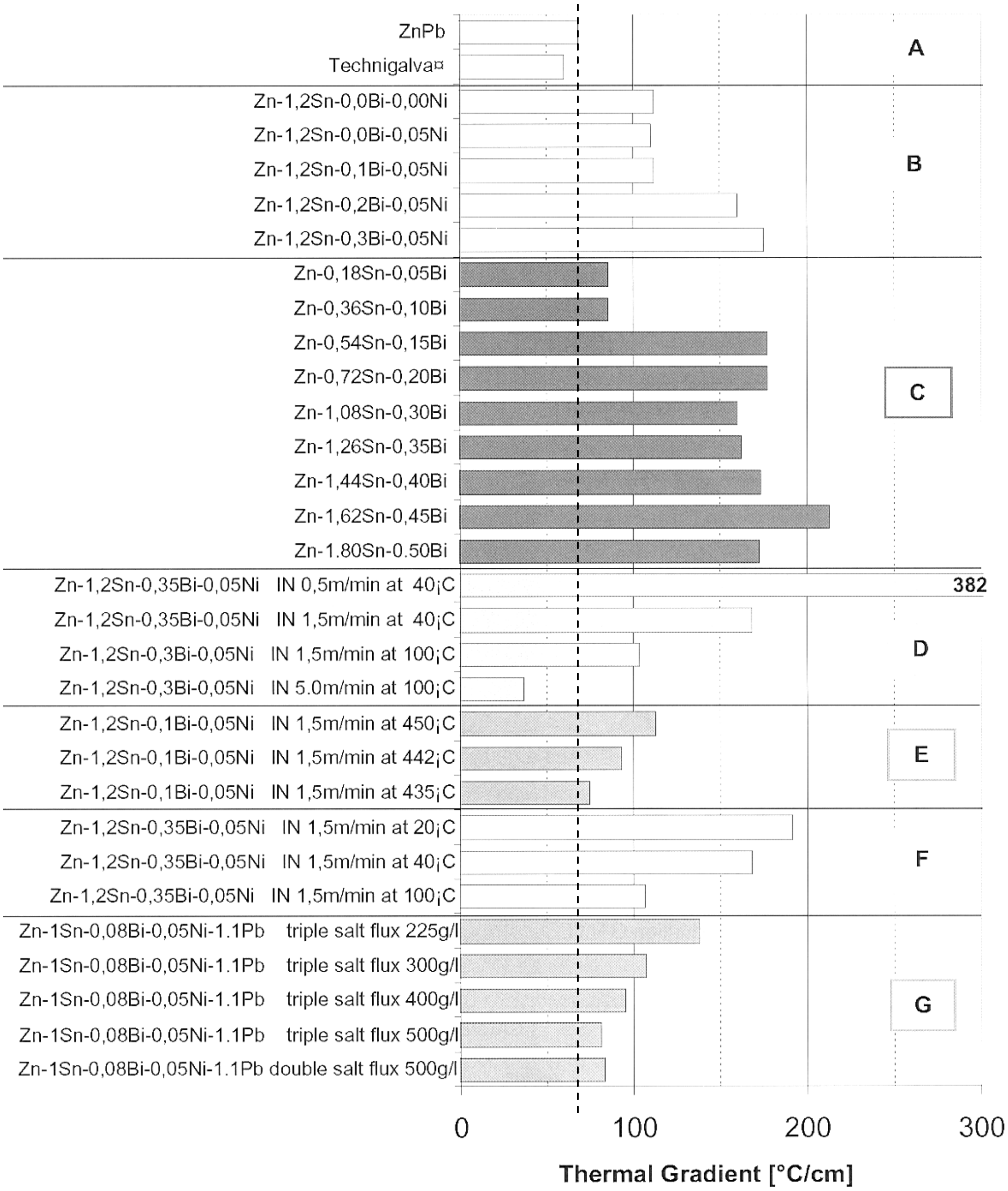

Figure 43 - Increase of Galvanizing Parameters and Alloy Composition on Thermal Gradient During Dipping (from Pankert et al)

The dashed line in the figure is the level of gradient resulting from Zinc spelter compositions historically associated with hot dip galvanizing, and thus give a baseline from which assessment of the newer alloy effects can be judged.

- Note in group B, the increase in gradient as bismuth is increased at constant tin and nickel contents.

- Group C varies both tin and bismuth composition, with resulting increases in measured thermal gradient.

- Group D relates dipping speed and steel preheat before dipping to thermal gradients. The value of rapid immersion had been known from other work including the previously mentioned studies from Japan. It is clear that rapid immersion and preheat can reverse any adverse effect from tin and bismuth additions. Note the high thermal gradient at very low immersion speed.

- Group E show the result of changes in zinc bath temperature

- Group F adds a lower steel temperature to the values in Group D

- Group G varies the flux concentration applied before dipping

The data show the increased thermal gradients resulting from various alloys and processing conditions, but also show that gradients similar to those found in historical practice can be achieved by other means beyond reversion to the historical zinc alloy compositions. The data are generally consistent with the findings of Poag and Zervoudis.

Condition

The effect of hot-dip galvanizing on steels has been well studied. Weigand and Nieth[53] reported basic mechanical properties of structural steels before and after galvanizing. Using 12mm (1/2 inch) test bars of DIN St37 steel, they reported negligible changes in yield point, tensile strength, elongation, and reduction in area as a result of the hot dip process.

Among the most comprehensive test programs reporting on the effect of the galvanizing process (pickling and thermal cycle of exposure to zinc with ~1.0% lead) on the mechanical properties of steels and weldments, is that published by the International Lead Zinc Research Organization (ILZRO) [6] in 1975. In this test program, steels from the UK, USA, Canada, Australia, Japan, and France were studied. At the time, most of the subject steels were produced from the Oxygen or Open Hearth method, presumably using the ingot process for reduction to shape. The selection of steels in the study covered a wide range of commercially available strength levels. Hershman and Browne[54] studied the effect of galvanizing on the mechanical properties of US, Canadian, and Japanese steels. Their results showed that, as expected, cold working somewhat increased the proof stress and tensile strength, and decreased the elongation, and that galvanizing had little untoward effect.

The mechanical properties of welded steels and the effect of welding was reported in the aforementioned ILZRO research, as well as others including Kinstler,[55] whose results showed no detrimental effect on the reported properties as a result of normal commercial galvanizing plant procedures, using Prime Western Zinc.

Both the comprehensive research in Japan (only a small fraction of which is cited here), and the ILZRO sponsored research[24] have made a clear correlation with hardness of a Heat Affected Zone (HAZ) from either welding or oxy-fuel cutting, and propensity to crack in the presence of a tensile force field, and coincident exposure to liquid zinc. In turn, the collective Japanese work has shown a correlation and cracks found after galvanizing with steel chemistry, and HAZ hardness.

McDonald[56] studied galvanizing effects on welds and base metal samples purposely treated to induce high strength levels by quenching form 870°C (1,600°F) and tempering to simulate microstructures that might be anticipated in heat affected zones (HAZ) of low energy welds. These specimen were then Hydrogen charged electrolytically, or by acid pickling. He found that although hydrogen damage could be operative in ungalvanized specimen, the time and temperature cycle normal to commercial galvanizing practice was sufficient to eliminate the potential for delayed cracking due to Hydrogen at hardnesses below R_C 36. Further, in other tests, he found a softening of the high hardness in the HAZ of the welds after galvanizing. This reduction in weld area hardness caused by the tempering effects of typical galvanizing thermal cycles was contrasted to ungalvanized samples where stresses remained at the original high levels after galvanizing. Typical results of this hardness reduction after galvanizing are shown below:

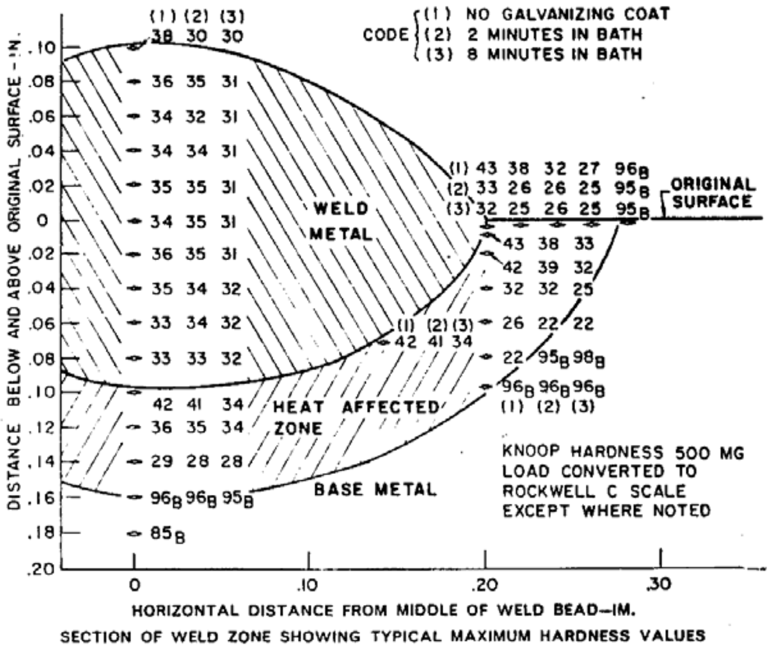

Figure 44 - Representative Hardness Values of Weld Zones after Galvanizing (from McDonald)

Note the lowering of hardness values in the three columns, representing increased galvanizing time. Similar weld hardness reductions were reported by McDonald[57] using thermal cycling (similar to typical galvanizing transients) of hard weld areas in lead rather than zinc, demonstrating the thermal cycle rather than reaction, coating formation, or spelter factors were causing the effect. Aoyama, studying full-scale effects in highway bridges, similarly found a lessening of the residual welding stress after galvanizing[58]

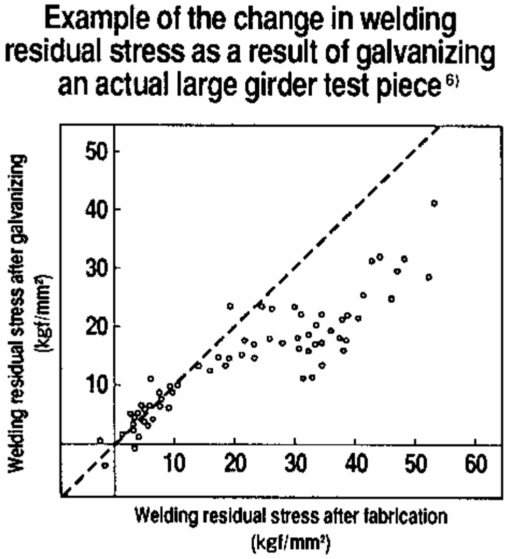

Figure 45 - Reduction in Residual Welding Stresses after Galvanizing (from Aoyama)

Similar effects on Y-groove welding tests were shown by Kikuta et al.[59]

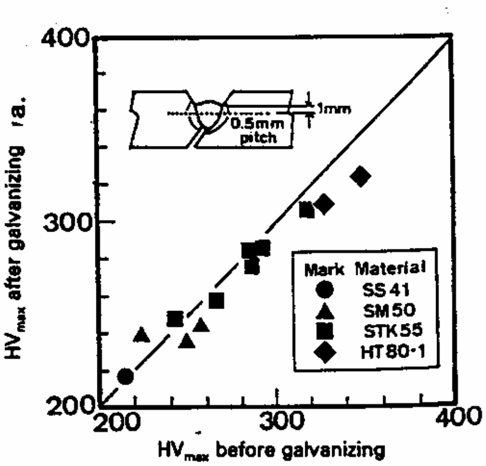

Figure 46 - Hardness before and After Galvanizing (from Kikuta et al)

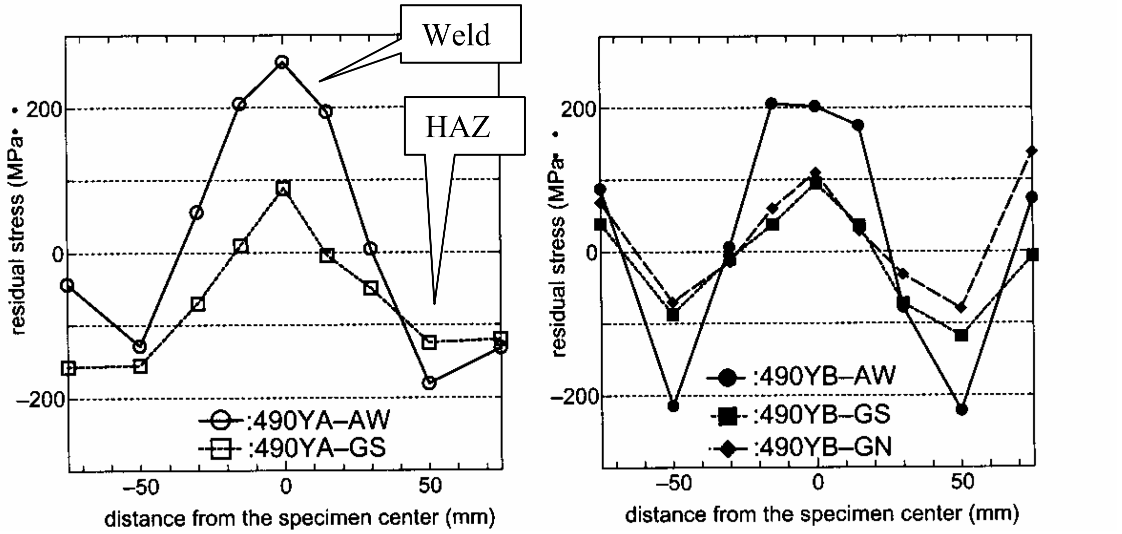

Figure 47 - Residual Stress Distributions in Specimen As-Welded and After Galvanizing for 480 sec, and Subsequently Quenched (from IIW Doc. XIII-1926-02) (Mori et al)

Mori et al[60] have shown the stress distributions at welded gusset joints as welded and after galvanizing and quenching. As shown above, the residual stress maximum drops roughly in half after galvanizing in typical commercial practice.

The previously cited ILZRO program also studied susceptibility of steels from the UK, USA, France, and Japan to hydrogen embrittlement as a result of galvanizing procedures. The steels were studied in the "as manufactured," and well as "40% cold rolled" conditions, as well as specimen quenched from 1200°C (2192°F) to simulate the extreme case of a hardened HAZ resulting from poor welding practices. Various mechanical tests were carried out on untreated, pickled, and pickled and galvanized specimen. The results showed that in the absence of cold work, none of the tested steels were susceptible to hydrogen cracking after pickling. Cold rolling to 40% reduction increased the strength levels and therefore the susceptibility to hydrogen embrittlement. After pickling, the three steels with tensile strengths greater than 810 N/mm^2 (117,500 psi) exhibited hydrogen embrittlement behavior. However these same steels, when galvanized after pickling, exhibited normal non-brittle behavior, indicating the efficacy of the thermal cycle of galvanizing in eliminating any hydrogen charging as a result of acid pickling.

Quenching from 1200°C (2192°F) increased the strength to a much greater extent. For example, ASTM A572 Grade 60 type 4 had its "as manufactured" tensile strength of 617 N/mm^2 (89,650 psi) raised to 1,585 N/mm^2 (230,300 psi) – roughly the equivalent to a hardness of R_C 47. At that strength level, susceptibility to hydrogen embrittlement was evident under the test conditions. Except in zone of extremely high induced hardness, hydrogen embrittlement can be eliminated as a major source of cracking problems under normal galvanizing practices.

Severe cold work has been known to produce cracks or embrittlement of normal construction steels and steel codes often contain minimum bending radii for cold bending of plates as a function of steel type and thickness. While these code radii are intended to eliminate immediate crack formation during fabrication, it is possible foe a severely cold worked, but visibly crack free area, to exhibit embrittled behavior after a period of time or "aging." This phenomenon is termed "strain aging," and it has been found that steel composition, specifically "mobile" components such as uncombined nitrogen and carbon are relevant factors. Increasing steel temperature after straining can vastly decrease the time required for embrittled behavior to become evident. For example, the time required at 150°C (~300°F) to produce approximately equal aging effect shown at 21°C (~70°F) drops from six months to ten minutes.[61]

Sandelin[62, 63] studied the phenomenon extensively and concluded that the amount of cold work, as measured by the bending radius, is the most important single factor to consider when there is concern for brittle-type failure of steel galvanized after cold working. He further concluded that ***for the steels avalable at the time,*** that a bending radius of three time the section thickness will ordinarily not induce sufficient strain to result in the accelerated embrittled condition after the galvanizing cycle. A more complete discussion of the steel mechanical effects from galvanizing can be found in McDonald.[64]

The strain-age embrittlement phenomenon related to structures can be found possibly in two areas, a conflict in Standards and Codes or lack of following the codes, and the rolling and straightening of structural shapes.

There are a number of cases where Standards or accepted guidelines are conflict. In the case of rectangular structural tube (also termed "Rigid Hollow section or "RHS" in some locations), the degree of cold work at the corner bend is a function of the radius of the bend as shown in Figure 39.

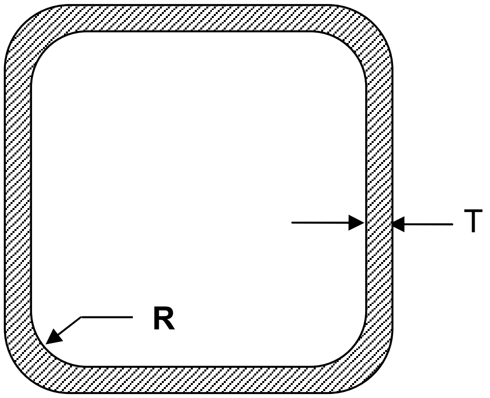

Figure 48 - Typical Structural Tube (RHS)

The US Standard for structural tube is ASTM A500, wherein section 10.6 of the -98 edition of the Standard states

> "For square and rectangular structural tubing. The radius of each *outside* corner of the section shall not exceed three times the section thickness." (*Emphasis added*)

If the tube is to be galvanized to Standard ASTM A123, the typical galvanizing Standard in the United States for structural components, then Standard A143 applies, which in section 5.1 of the -94 edition states:

> " …cold bending radii should not be less that that which is proven satisfactory by practice or by the recommendations of the steel manufacturer. These criteria generally depend on the direction of grain, strength and type of steel. A cold bending radius of three times (3X) the section thickness, or as recommended in the AISC Manual of Steel Construction[65] will ordinarily ensure satisfactory properties..."

The AISC manual, called out in A143, states on page 4-174:

> "The following table gives the generally accepted *inside* minimum bending radii of bends in terms of thickness "T" for the various steels listed. Values are for bend lines transverse to the direction of final rolling. When bend lines are parallel to the direction of final rolling, the values may have to be approximately doubled. When bend lines are longer than 36 inches, all radii may have to be increased if problems in bending are encountered." (*Emphasis added*)

A500 requires that the maximum *outside* bending radius be 3 X T, therefore the *inside* maximum radius = 3T – T = 2T.

A143 requires the minimum bending radius be 3 X T, it does not specify *inside* or *outside,* however it has ususally been interpreted as being *inside*. Further, the statement calls out The AISC manual which specifies for application of its radii table, the *inside* radius. In structural tube the bend lines are clearly *parallel* to the direction of final rolling. Therefore, application of the AISC guidelines could require that the minimum *inside* radius be doubled, or 2 X 2.5 X T = 5T for Grade 50, ⅜ inch material under A143, while A500 would require a maximum *inside* radius of 2T.

Another example of Standards or Codes conflict can be seen in the work of Ride[66] related to fracture mechanics analysis of low toughness areas in W shapes as a result of contemporary rotary straightening practice. Using a fracture mechanics analysis approach, he calculated in a subject case, that the critical crack size for the determined notch toughness, and an assumed stress of 550 MPa, was 0.3 mm. In contrast, to the nominal flame roughness of 5 mm permitted by AISC in section M2.2 of the Manual of Steel Construction,[67] as pictured below:

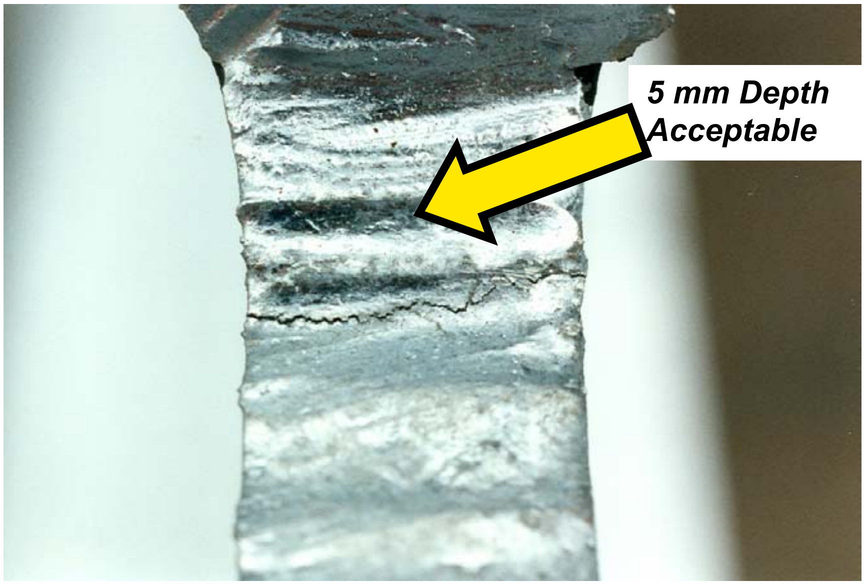

Figure 49 - Grooves from Flame Cutting (from Kinstler)

Sections M2.2 and J1.8 include the statements that

> “Thermally cut free edges which will be subject to substantial tensile stress shall be free of gouges greater than 3/16 inch. Gouges greater then 3/16 inch deep and sharp notches shall be removed by grinding or repaired by welding.…Beam Copes and weld access holes shall meet the requirements of Sect. J1.8.” “In hot rolled shapes and built up shapes, all beam copes and weld access holes shall be free of notches or sharp re-entrant corners …”

The effect of stress concentration as a result of notch radius at a 2.0 mm constant notch depth was studied by Kominami et al[68] Using a sample configuration, cut after welding as shown following as Figure 43, and with tip radii of 0.2, 0.5, and 2.0 mm, the stress concentration factors were calculated as K_t = 4.3, 3.2, and 1.95 respectively. The sample s were then subjected to 400 second immersion (timing began after 60 seconds temperature equilibration) in a 450°C zinc bath containing zinc with about 1.2% lead. In cases where the sample fractured before the full 400 second immersion, the time in seconds is listed on the plot in Figure 44. As expected, as K_t increased, the critical stress for fracture decreased. These results are consistent with earlier work by Kikuchi[69, 70]

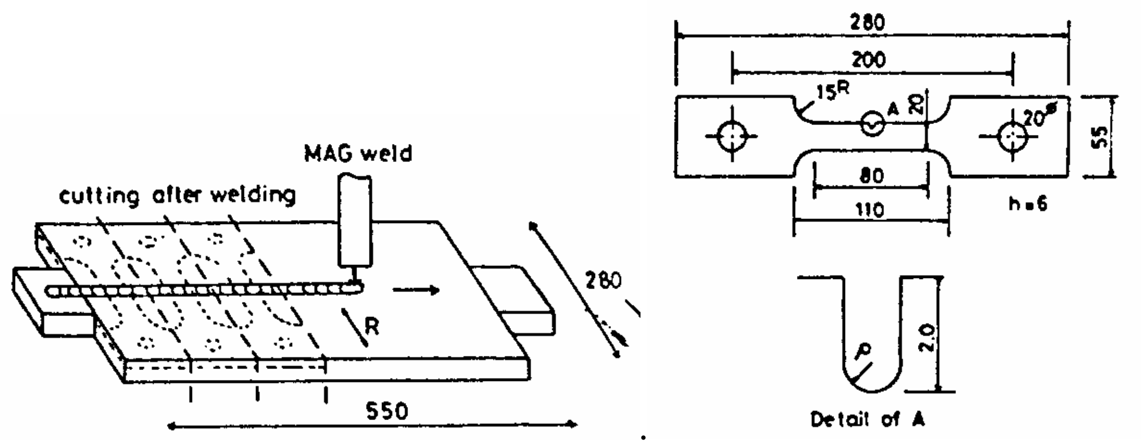

Figure 50 - Welding Method and Sample Configuration (from Kominami, et al)

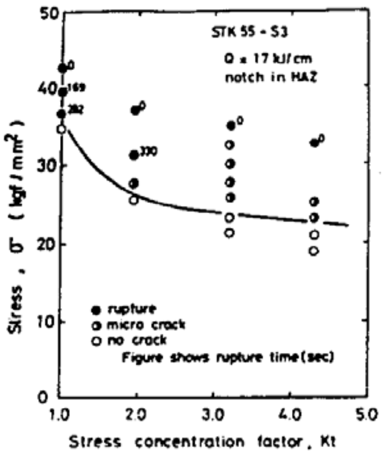

Figure 51 - Effect of Stress Concentration Factor for Critical Cracking Stress (from Kominami et al)

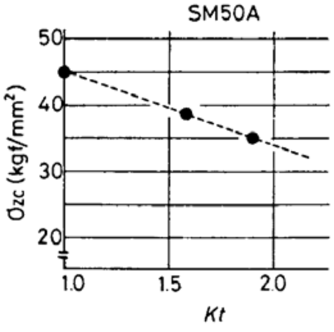

Figure 52 - The Relation Between K_t and σ_{zc} for SM50A Steel (from Kikuchi)

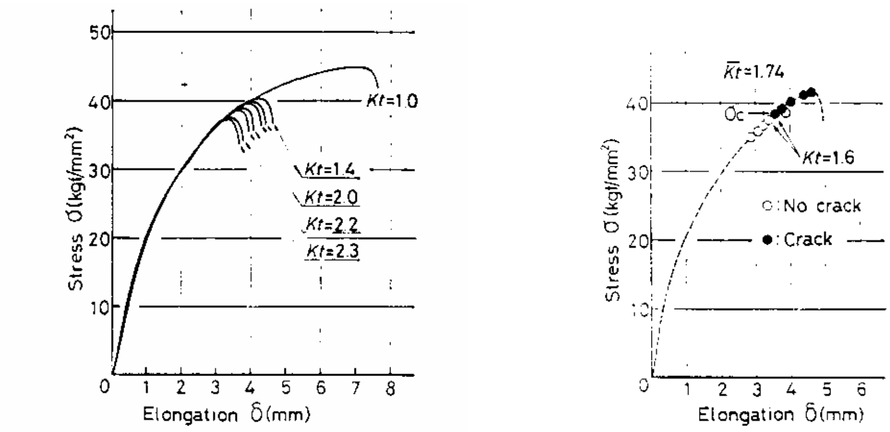

Figure 53 - Effect of Stress-Concentration Factor (left) and Results of Tensile Tests of Specimen Unloaded at Various Stress Levels in Molten Zinc (Right) (from Kikuchi and Iezawa)

For many years, the Manual of Steel Construction[71] has illustrated a recommended practice for cutting copes as shown below:

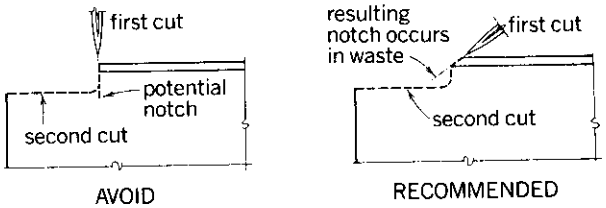

Figure 54 - Recommended Practice for Thermally Cutting Copes (from AISC)

It is clear from the notation on the sketch, that the "double cut" raises the potential for microstructural, mechanical, and/or compositional change, however, the flange angle-cutting method is seldom used in practice. An alternate method is suggested below:

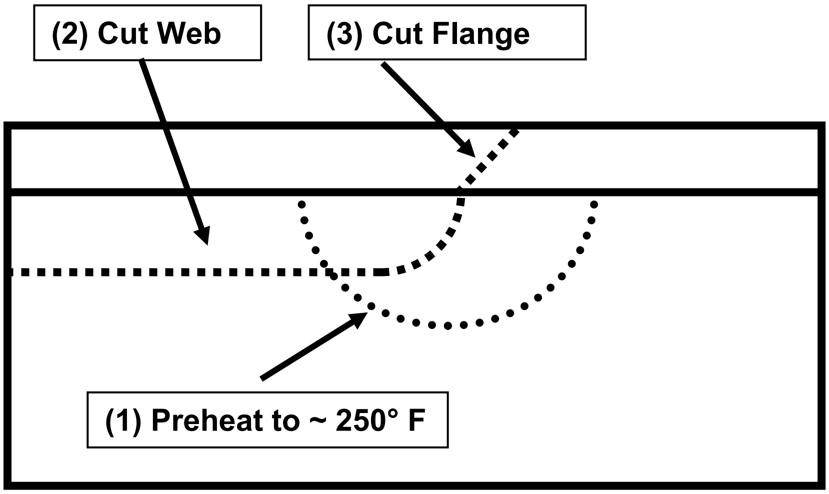

Figure 55 - Alternate Cope Cutting Sequence

An indication of such changes within the cope radius has been clearly shown in an investigation of cracks found after galvanizing.[72]

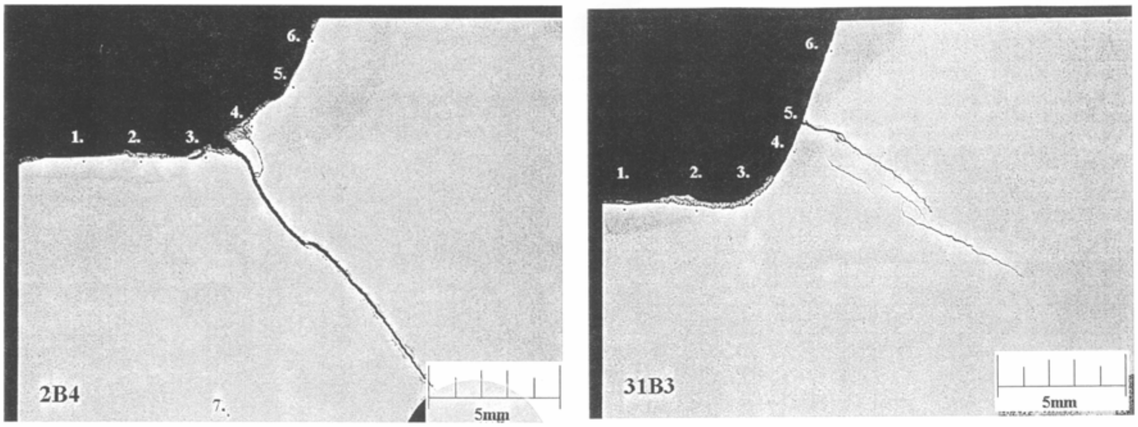

Figure 56 - Micrographs and Hardness Measurements of Cracked Copes (Private Communication)

	Vickers Harness Number	
Location	Sample 2B4	Sample 31B3
1	243	212
2	205	253
3	222	247
4	233	257
5	180	256
6	228	237
7	192	202

All of the cracked beams in the investigation (only two shown here) shared a commonality, in that each crack seemed to be have some type of notch, stress concentration, or surface irregularity as an initiation site. No investigation was made for either toughness, or chemical changes at the thermally cut sites. Note that thermal cutting increases the hardness of the cut surface relative to the base material, location 7 in each case. However it appears that the “radius” of the cope has a significantly greater increase in hardness than the “straight” surface. In the case of 31B3, the hardness is just within the range found by numerous researchers to be susceptible to cracking in molten Zinc. The increase in hardness around the “radius” may be an artifact of the perpendicular flange cutting procedure, as discussed above, or it could possibly be a result of constrained heating and cooling due to the “geometry” of the cope, and the surrounding “heat-sink” of the web area surrounding the radius cut. The copes were cut with a standard procedure of cutting the web first, followed by cutting of the flange. The fabricator had used the same procedure in the past with beams for galvanizing with no previous occurrences of the cope cracks after galvanizing.

As related to surface smoothness, as well as hardness as a factor in galvanizing and cracking, Poag and Zervoudis,[73] showed that even susceptible steels, formed as hollow structural steel (HSS) tubing, could be prevented from cracking during galvanizing, at the test conditions, if the rough inner bend corner were polished smooth. Their research examined the effect of various zinc bath compositions additions such as lead, nickel, bismuth, and tin on steel cracking, as well as various galvanizing practice variables such as dipping speed, galvanizing bath temperature, preheating before galvanizing, flux composition, as well as steel treatment variable such as stress relieving before galvanizing, and inside corner smoothness.

Microhardness numbers were taken at the corners 25μm in from the inner corner surface and 150 μm in from the surface. Additional readings were taken at the middle and outer radii. Tube B was found to be the softest, with the two inner values bracketing 200 VHN, while Tube A was the hardest at innermost value at about 300 VHN.

Tube A (without heat treatment) cracked under almost all test conditions, while Tube B did not crack. A subset of Tube A samples was stress relieved according to the recommendations of ASTM A 143 at 595°C (1100°F) for 45 minutes and furnace cooled. The treatment substantially reduced the inner hardness value to about 225 VHN. Cracking under the same conditions was reduced from 100% (all four corners) to 0%, similar to the results from smoothing the inner corners.

An example of the cracking phenomenon on HSS from a different experimental program[74] is shown below. Note the absence of cracking in the weld.

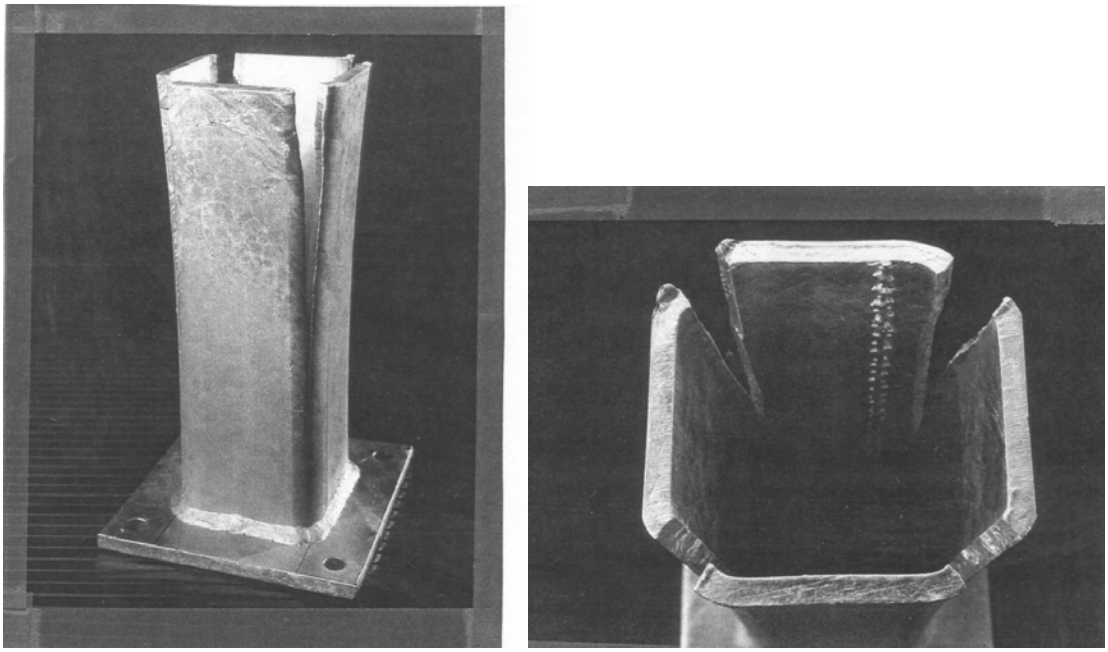

Figure 57 - Hollow Steel Structural Tube (HSS) Cracked in Galvanizing (from CANMET)

The corner microstructures of the four (5 X 3 X ⅜ inch) test specimen used in the Poag and Zervoudis experiments are shown below:

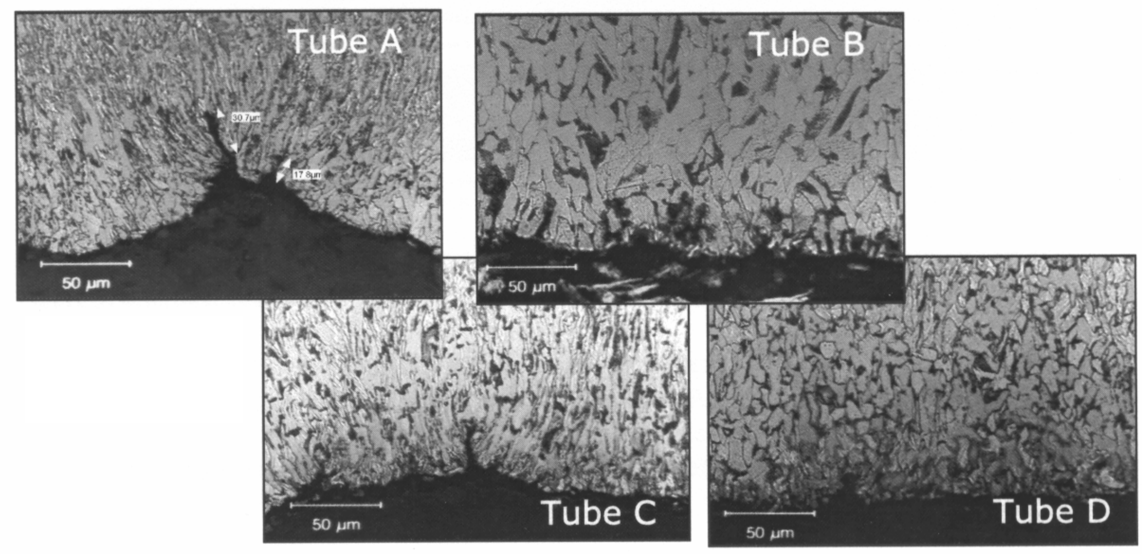

Figure 58 - Microstructures of Inside Corners of Four Commercially Available Hollow Structural Steel Tubes (from Poag and Zervoudis)

The findings of the study beyond those related to the smoothness of the inner corner surface and the heat treatment to reduce cracking incident are that alloy additions to the SHG Zinc bath did have an effect on the occurrence and severity of cracking, but only on susceptible tubes:

- Lead in the galvanizing bath increased both the incidence and severity of cracking

- nickel additions to Prime Western (PW) baths (~1.0% lead) did not adversely influence cracking, and there was some evidence that nickel was helpful in reducing cracking in PW baths

- The occurrence and extent of cracking in baths containing tin and bismuth levels below approximately 0.2% were the same as that of a conventional PW bath.

- When levels of tin or bismuth exceeded approximately 0.2%, the size of cracks became greater than those obtained in samples from a PW bath. As tin levels increased above 0.3%, crack size continued to increase, whereas the extent of cracking did not seem to increase further as bismuth levels increased above 0.2%.

The results of the study related to galvanizing process variables (physical variables as opposed to chemical variation of the bath metal as above) were intriguing, however the "scale-up" of those limited findings to galvanizing of larger and complex-shaped sections has not been established.

The central value of the study is to identify that galvanizing bath chemistry is only one of the factors influencing cracking of galvanized structural steels. The predominant variable has been found to be in the steel. For example, the presence of any alloy addition including tin up to 1.0% could not cause Tube B to crack. On the other hand, Tube A (in the absence of stress relieving) cracked under all bath chemistry variable conditions, including Special High Grade Zinc with no alloy additions.

All of the many research programs which have studied hardness of flame-cut edges and their associated heat affected zones (HAZ), and cracking in molten zinc are in agreement that:

- There is a threshold hardness value above which the steel is susceptible to cracking in molten zinc
- The threshold value is between about 250 and 300 H_V (VHN) depending on the thickness of the steel, and possibly other steel-related variables
- Re-attainment of a hardness below the threshold value, in previously harder steel reduces susceptibility of the steel to molten zinc cracking

It has been firmly established, that the thermal cutting of a steel surface results in a multi-layered heat affected zone (HAZ) with a series of microstructure, hardness, compositional and residual stress changes. The hardness profile of a typical thermal-cut HAZ is shown[75] following. It has been further established that the outer layer residual stress tends to be compressive, as a result of the approximately 5% expansion with the transformation from austenite on cooling below the transformation temperature.[76] These compressive stresses are balanced by a tensile force field just below the surface. The variation residual stresses coincide with the variations in microstructure and microhardness,[77] with a hard Carbon-rich layer on the surface, and a series of step-wise microstructures below.

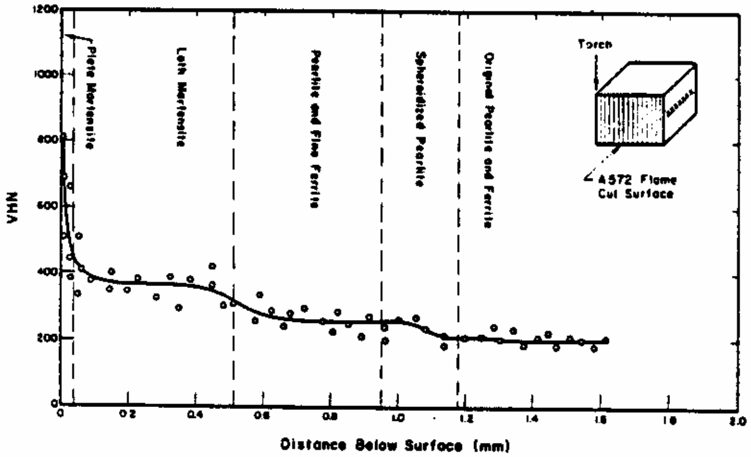

Figure 59 - Microhardness Profile at the Mid-thickness of A572 Flame-cut Steel (from Ho et al)

Harris notes that the ANSI/ASHTO/AWS D1.5-88 (since superseded) specifies a maximum surface roughness for oxygen cutting of 1,000 microinches for material thicknesses up to 4 inches. The commentary on the code mentions that thermal cut edges can frequently have surface hardnesses in excess of the equivalent of HR_C 50 to HR_C 60.

Some States specify a maximum surface hardness of HR_C 30 for plasma-cut edges. Harris further states that the British Bridge Welding Code, BS 5400 Part 6 gives a number of alternative requirements (one of which must be met) for such cut edges, one of which is that the surface hardness is not to exceed 350 VHN.

The cut surface is generally crack-free by optical inspection, but Wilson,[78] using electron microscopy was able to detect very small characteristic intergranular fissures on the as-cut edge on all thermally-cut specimen, a typical example showing extension of surface microcracks into the martensite HAZ region (left-light optical, mirror image right-SEM, both at 500X) is shown below:

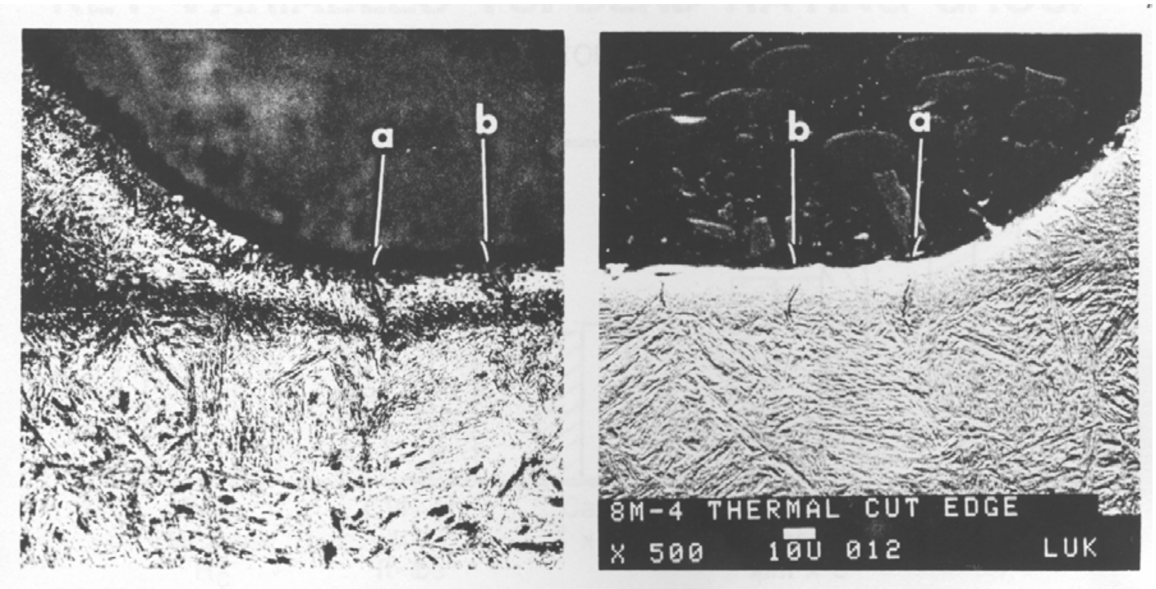

Figure 60 - Surface Microcracks Extending into Martensite Structure (from Wilson)

The fact of surface hardness as affecting the susceptibility for molten metal cracking has been studied and confirmed by many research projects, and it is almost universally confirmed that above a threshold of about 250-290 VHN (depending on thickness and other criteria) the susceptibility to such cracking accelerates. Rather than cite the findings of the many such independent research programs, a partial synopsis of the ILZRO program has recently been published by Elboujdaini et al, which contains some of the central and widely confirmed findings.[79]

Among the findings, is the fact that the susceptibility of a steel made susceptible by thermal cutting can be reversed by heat "softening" of the sensitive region by localized flame heating, or furnace treatment. Among the many steels studied in the ILZRO/CANMET project, two were specifically reported in the above cited paper:

Table 2 - Steels Reported by Elboujdiani et al (table numbering from their paper)

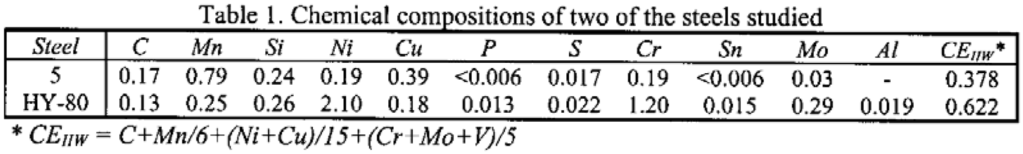

Table 1. Chemical compositions of two of the steels studied

Steel	C	Mn	Si	Ni	Cu	P	S	Cr	Sn	Mo	Al	CE_{IIW}*
5	0.17	0.79	0.24	0.19	0.39	<0.006	0.017	0.19	<0.006	0.03	-	0.378
HY-80	0.13	0.25	0.26	2.10	0.18	0.013	0.022	1.20	0.015	0.29	0.019	0.622

* $CE_{IIW} = C+Mn/6+(Ni+Cu)/15+(Cr+Mo+V)/5$

The steels were tested as-received, flame-cut, plasma water-cut, furnace softened (after cutting) (650°C for one hour), torch softened (after cutting) (heated to "cherry-red (650-900°C with an acetylene torch and air cooling). Galvanizing was by conventional practice in a PW (~1% Lead) bath. The microhardness at 100 μm depth, and notations as to whether they cracked in galvanizing, for the various treatments is shown below:

Table 3 - Results from Elboujdiani et al (table numbering from their paper)

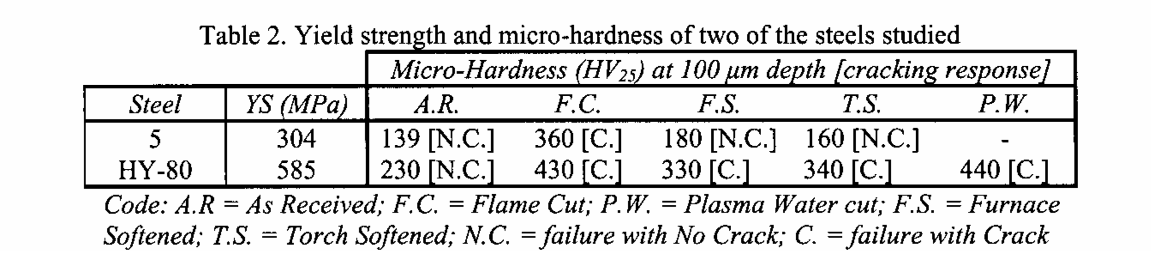

Table 2. Yield strength and micro-hardness of two of the steels studied

		Micro-Hardness (HV_{25}) at 100 μm depth [cracking response]				
Steel	*YS (MPa)*	*A.R.*	*F.C.*	*F.S.*	*T.S.*	*P.W.*
5	304	139 [N.C.]	360 [C.]	180 [N.C.]	160 [N.C.]	-
HY-80	585	230 [N.C.]	430 [C.]	330 [C.]	340 [C.]	440 [C.]

Code: A.R = As Received; F.C. = Flame Cut; P.W. = Plasma Water cut; F.S. = Furnace Softened; T.S. = Torch Softened; N.C. = failure with No Crack; C. = failure with Crack

Note steel 5 did not crack as-received, was hardened (at 100 μm) to above the 270 VHN threshold by flame cutting and subsequently cracked, a similar sample either flame softened or furnace softened had the below-surface hardness reduced to below the stipulated threshold, and subsequently did not crack in galvanizing.

When similar data from 15 steels from their previous work is plotted, similar trends regarding the microhardness threshold, and the field-reversibility are shown:

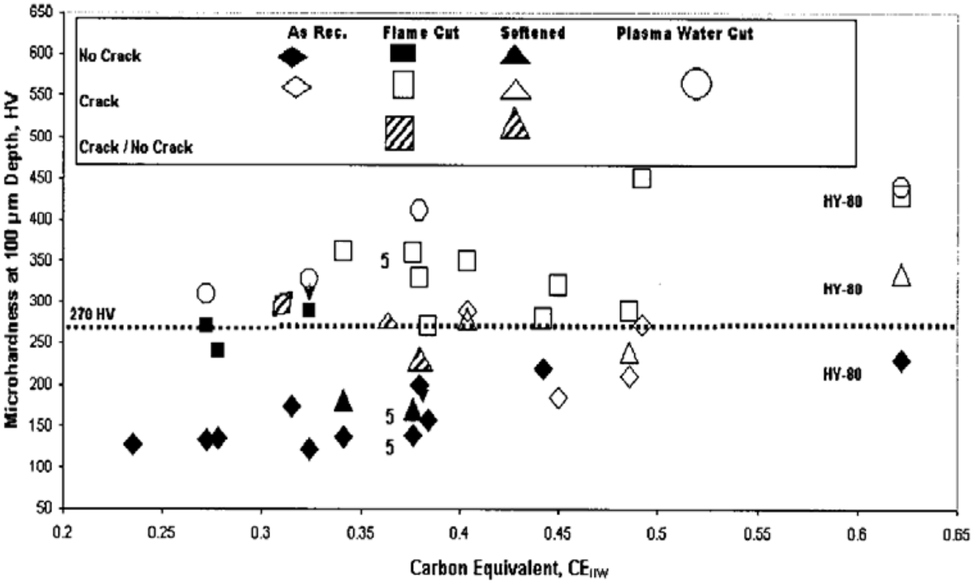

Figure 61 - Cracking Susceptibility as a Function of Microhardness (from Elboujdianai et al)

The sensitivity of steel compositions to cracking in molten zinc has been studied extensively, in Japan particularly. Researchers have developed a method using a Notched Bar Tensile specimen (NBT) as shown below:

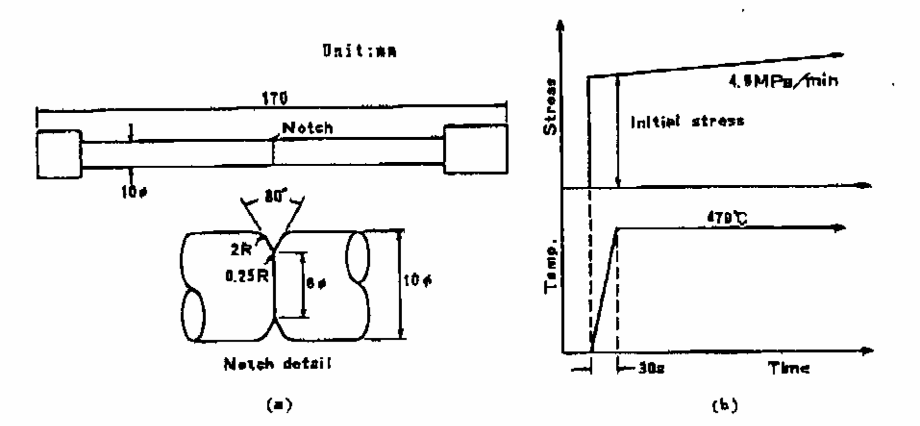

Figure 62 - Notched Bar Tensile Specimen for Determination of Steel Sensitivity to Liquid Metal (from Abe et al)

The specimen are subjected to a prior thermal treatment to simulate welding, with a heating temperature of 1400°C, and a subsequent cooling time from 800° to 500°C in 8 seconds. The multiple tensile tests are then carried out in Zinc at 470°C (actually higher than commercial galvanizing temperature) and in Air also at 470°C. The specimen are loaded to the 0.2% proof load (yield point), and load and time to fracture is recorded. The resulting data set is then applied to the equation:

$$S_{LM} = \frac{\text{NBT Stress in zinc}}{\text{NBT Stress in Air}} \times 100$$

The sensitivity to liquid metal is expressed as a percentage. If the stress in zinc is the same as the stress without zinc, (in air), the percentage is calculated as 100%, which may be misleading, as the "sensitivity" as in a susceptibility to crack because of the presence of the liquid metal is actually "zero." The equation, at least conceptually, determines the "insensitivity," as the same failure values with and without liquid metal would describe a "100% insensitivity" or a "zero % sensitivity."

A large number of steel compositions were studied and from that data set, a target value was determined, and by regression analysis, S_{LM} composition equations were developed for specific steel types, a commonly applied one being:

$$S_{LM} = 201 - 370C - 22Si - 51Mn - 35P + 33S - 28Cu - 22Ni - 87Cr - 123Mo - 275V - 182Nb - 82Ti - 24Al + 1700N - 155{,}000B$$

By setting the equation to $S_{LM} \geq 42\%$ and converting to CEZ formula, the equation becomes:

$$CEZ = C + Si/17 + Mn/7.5 + Cu/13 + Ni/17 + Cr/4.5 + Mo/3 + V/1.5 + Nb/2 + Ti/4.5 + 420B \quad \leq 0.44$$

The use of these equations must be investigated as to the range of individual element with which they are valid. For example, the above operates with Carbon levels below 0.12, Boron less than 10ppm (if the boron level is between 4 and 10 ppm, a value of 4 ppm is used in the calculation), and Nitrogen levels near 30 ppm. Nitrogen levels in US EAF steels are in the range of 85 ppm, and in general, boron is not reported. However, the P_{CM} calculation performed at some mills uses boron in the equation, so the information may be available.

The Japanese Industrial Standard JIS G 3129 (1995),[80] includes two carbon equivalent equations. For general specification use carbon equivalent is calculated by the equation below:

$$CE(\%) = C + \frac{Mn}{6} + \frac{Si}{24} + \frac{Ni}{40} + \frac{Cr}{5} + \frac{Mo}{4} + \frac{V}{14}$$

And for class SH 590P, and 590S steels, the CE% values shall be 0.40 max., and 0.45 max., respectively. For SH 590P, boron shall be 0.0002% max., while for SH 590S, boron is not specified.

The following paragraph in the Standard calls out an "Equivalent on sensitivity of crack by hot-dipped zinc-coating," which shall be 0.44% or less calculated by the following equation with the further stipulation that boron shall remain at or below 2 ppm:

$$Equivalent(\%) = C + \frac{Si}{17} + \frac{Mn}{7.5} + \frac{Cu}{13} + \frac{Ni}{17} + \frac{Cr}{4.5} + \frac{Mo}{3} + \frac{V}{1.5} + \frac{Nb}{2} + \frac{Ti}{4.5} + 420B$$

The "$Equivalent(\%)$" above is the same concept as the "*CEZ*" discussed elsewhere.

The thermal cycle used to create the HAZ in the work in Japan from which the S_{LM} and thus the CEZ equations were derived, used a cooling rate between 800°C and 500°C of 8 seconds. The cooling rate in the Gleeble device in the CANMET study was 6.5 seconds. Malik and McGoey[81] estimate the actual cooling rate of oxy-fuel cutting as less than 2.4 seconds. They discuss the matter as follows:

> "The peak temperature reached in the immediate vicinity of the cut edge is about 1370°C, the melting point of the slag (FeO), and does not seem to depend on the thickness of the plate being cut. There is an exponential decline in the peak temperature reached with distance from the cut edge. (see Figure 2). The visible heat affected zone (HAZ) in his [Ruge] studies was approximately 1.5 mm, the distance from the cut edge over which the peak temperature exceeds the A_{c1} temperature.
>
> The heating rate at the cut edges is approximately 2000° to 6000°C/s depending on the cutting speed. More importantly, the cooling rates measured over the temperature range 1200° to 850°C were also extremely high. Thus, as shown in Figure 3, the cooling rate at the cut edge can be from 600° to 1750°C/s depending on the cutting speed. Even at a distance of 0.5 mm from the cut edge the cooling rates are about 250° to 850°C/ Assuming that the cooling rates over the temperature range 800° to 500°C

> are half those in the temperature range 1200° to 850°C will be less than 2.4 seconds. In comparison, for shielded metal arc welding process, such cooling rates are associated with arc strikes, and for typical stringer weld beads, the 800° to 500°C cooling times are at least 5s, and more typically 10 to 20s."

The cooling rate, or specifically the time between 800° to 500°C is significant when considered within the Schematic CCT curve shown below:

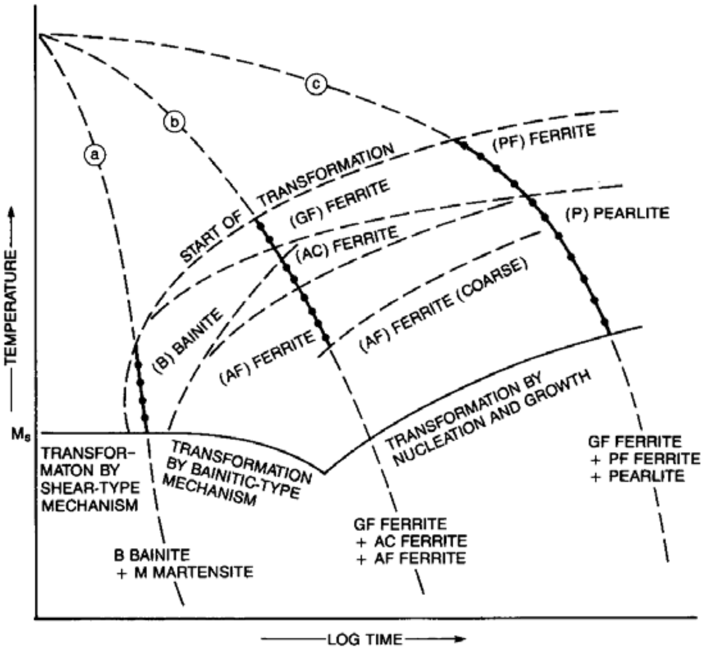

Figure 63 - Schematic CCT Diagram for a Low-Carbon, Plain Steel Weld metal (from Welding Metallurgy, Vol. 1 AWS)

Curves a, b, and c represent cooling at ("very fast," "intermediate," and "very slow," rates. While the diagram relates to weld metal, the general effect of increasing cooling rate on transformation in steel base metals is much the same as for weld metals. As cooling rate is increased, the occurrence of pearlite decreases and the amount of polygonal ferrite is diminished until it is limited to grain-boundary (GF) ferrite. The term "allotriomorphic" ferrite sometimes is applied to GF ferrite when present in veins or as thin rims because of the ragged and imperfect form of the ferrite grains along the prior austenite grain boundaries (PAGB)[82]

In weld metal, manganese and nickel are known to be quite effective in promoting acicular ferrite, and reducing the amount of polygonal ferrite (PF) and side pale ferrite (SP). In the following figure, regimes of three typical forms of microstructure, namely martensite, acicular ferrite and pearlite, have been positioned across a scale of cooling rates. As cooling rates become slower, the amount of manganese required to obtain acicular ferrite are indicated by the sloping lines on the left and right. The connecting lines predict approximate percentages of acicular ferrite to be expected at different levels of manganese. The predictions of the diagram have been found to be in good agreement with the work of other investigators.[83] From the diagram and the estimated cooling rate from oxy-fuel cutting, by Malik and McGoey, suggest that increased manganese content would be detrimental to ferrite formation. As the cooling rate increases, the upper limit of manganese to minimize the formation of martensite goes down.

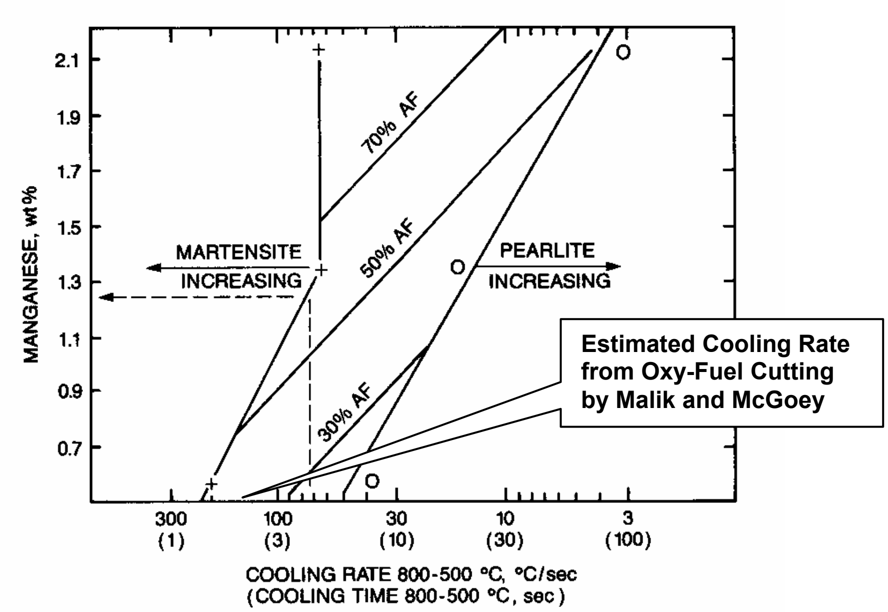

Figure 64 - Influence of Manganese Content in C-Mn Steel Weld Metal Over a Range of Weld Cooling Rates in Producing _Particular Weld Zone Microstructures (from Welding Metallurgy, Vol. 1 AWS)

Kou,[84] in discussing weld metal, illustrates schematically the transformation effects of cooling rate and shifting of the CCT curves as a result of alloy content, and other measures:

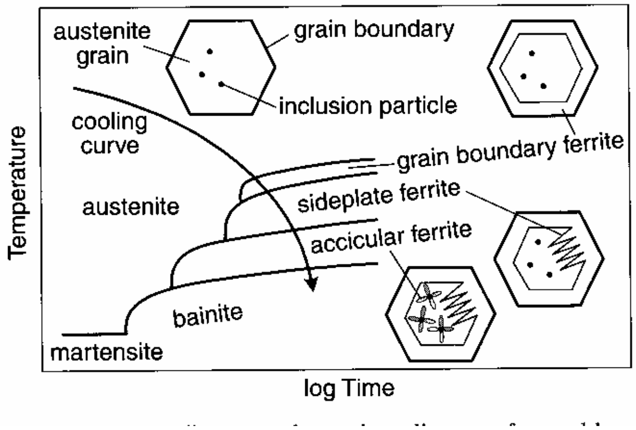

Figure 65 - Continuous-cooling Transformation Diagram for Weld Metal of Low Carbon Steel (from Kou)

The schematic diagram above illustrates the development of microstructures in weld metal, and by extension, in the melted and partially-melted zone of flame cuts during cooling. The hexagons represent the transverse cross sections of columnar austenite grains in the weld metal. As austenite (γ) is cooled down from high temperature, ferrite (α) nucleates at the grain boundary and grows inward adopting or transforming into various structures such as side plate ferrite, acicular (needle-like) ferrite, etc, depending upon a number of factors including the presence of inclusions which can act as further nucleation sites. Borrowing from Bhadeshia and Svensson,[85] and using the same representations of microstructure shown earlier, Kou showed the effect of several factors on microstructure development.

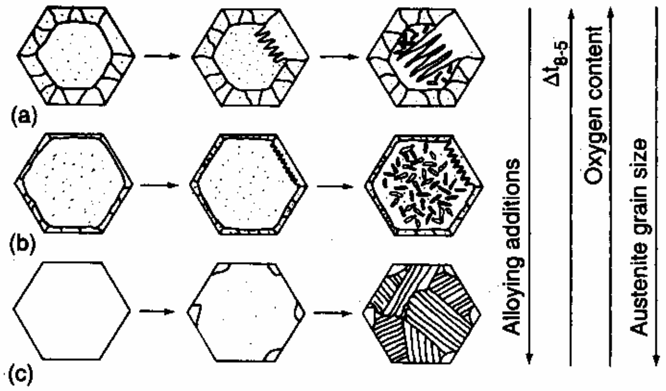

Figure 66 - Schematic showing the Effects of Alloy Additions, Cooling Time from 800 to 500° C, Weld Oxygen Content, and Austenite Grain Size (from Kou, original source: Bhadeshia and Svensson)

The vertical arrows indicate the directions in which these factors increase in strength, for example, as cooling time through the range 800 to 500°C increases, the microstructire development tend to follow the pattern in (a) rather than (b) or (c). Note the absence (schematically) of grain boundary ferrite in (c) relative to (b) and (a). The effects of cooling rate and alloy composition is further illustrated schematically below:

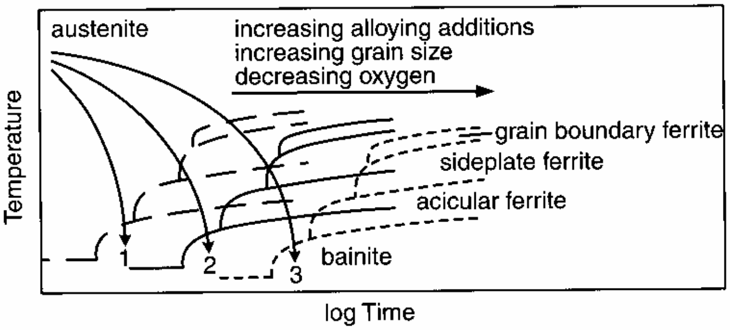

Figure 67 - The Effect of Alloying Elements, Grain Size, and Oxygen Content, Together with Various Cooling Curves, on CCT Diagrams for Weld Metal of Low-Carbon Steel (from Kou)

As cooling slows down ($\Delta\ t_{8\text{-}5}$ increases) from curve 1 to curve 2 to curve 3, the transformation product changes from predominately bainite to predominately acicular ferrite to primarily grain boundary ferrite, and Widmanstatten ferrite. Note that higher cooling rates were shown for flame cutting by the Fleet laboratories/CANMET studies cited previously. An increase in alloy additions (higher hardenability) will shift the CCT curves (to the right) toward longer times and lower temperatures. Combining the rapid cooling of cooling curve 1, and the rightward shift of alloy additions, as shown in the dashed-line structure family, a "worst case" for grain boundary presence and low hardness can be seen.

The ferrite in the prior-austenite grain boundary (PAGB) is often called "allotriomorphic" meaning that it is ferrite which grows without a regular faceted shape. An example of the relevant microstructures is shown below for weld metals on low-carbon steel:

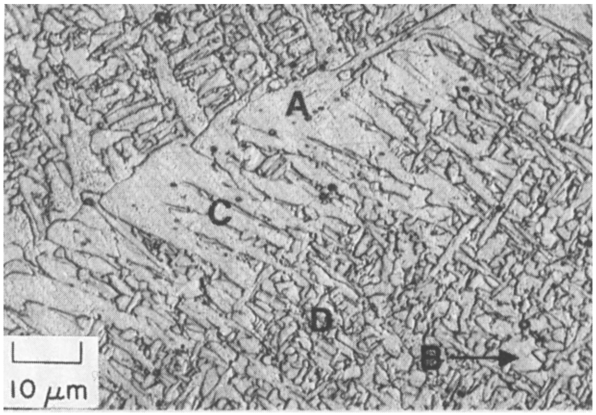

Figure 68 - Micrograph Showing Typical Weld Metal Microstructures: A, Grain Boundary Ferrite; B, Polygonal Ferrite; c, Widmanstatten Ferrite; D, Acicular Ferrite. (from Kou)

The ratio of the amount of allotriomorphic ferrite (or "grain boundary ferrite") to grain boundary length has been (inversely) correlated to susceptibility to cracking as shown further in this section

Fatigue characteristics of steel after galvanizing has been studied in Japan and elsewhere. Mori et al[86] describe a "modified steel to prevent embrittlement due to galvanizing" as being included in the test matrix. It is further described as "SM490YB and SM400 used here have comparatively low content of Silicon and Manganese, and they are correspondent to ones with high ductility against galvanizing crack." Their finding include: "The fatigue strength of 490YB-GS and 400-GS specimens made of SM490YB and SM400 corresponding to the steel with high resistance to galvanizing crack is equivalent or higher than that of the as-welded specimens. However the fatigue strength of 490YA-GS specimens made from SM490YA, which involve comparatively much content of silicon and manganese, is low in comparison with that of as-welded specimens by about 20%."

Interestingly, the results of the after galvanized fatigue tests are influenced by the silicon and manganese contents of the steels. The mechanical properties and chemical compositions of the steels used in the tests are shown following:

	Y.S. MPa	T.S. MPa	Elong %	% C	% Si	% Mn	% P	% S	% Cu	% Ni	% Cr	% Ti
SM490YA	440	559	26	0.14	0.48	1.51	0.02	-	-	-	-	-
SM490YB	466	542	20	0.16	0.22	1.04	0.01	0.01	0.01	0.01	0.02	0.01
SM400	226	421	33	0.17	0.09	0.55	0.02	0.01	0.02	0.01	0.02	-
Weld Metal	500	560	31	0.05	0.60	1.50	0.02	0.01	-	-	-	-

Other research in Japan has studied the grain boundary microstructure on welds and cracking experienced after subsequent galvanizing.

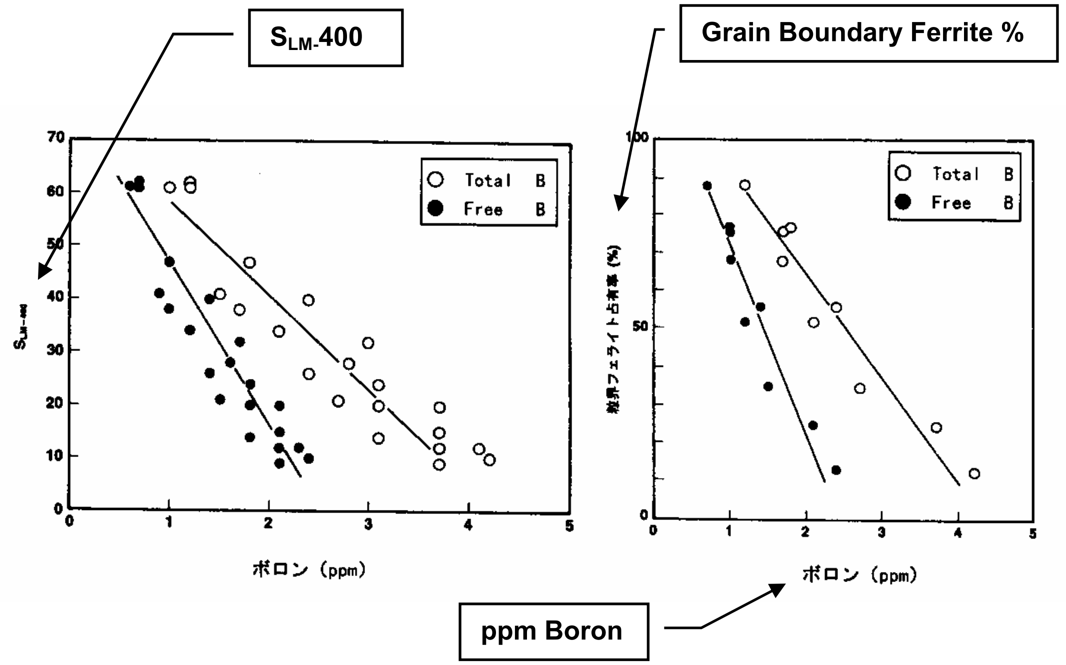

Figure 69 - S_{LM}, and Grain Boundary Ferrite Percentage as a Function of Boron Content of Steel (Private communication)

Abe et al[87] have described the inter-relationship between to appearance of the PAGB, and the ferrite fraction, and Zinc infiltration.

> "The typical microstructure in HAZ consists of primary ferrite (FP), upper bainite (UB), lower bainite (BL) and martensite (M), and the prior austenite boundary becomes extremely blurred in FP or BU structure transformed at high temperatures. It can be predicted that the grain boundary diffusion of Zinc is restricted at the blurred boundary such as this and the liquid Zinc embrittlement as also surpressed. On the contrary the prior austenite boundary can clearly be observed in the case of BU, BL, or M transformed at relatively low temperatures and it can be thought that zinc segregation at the boundary is facilitated to cause liquid zinc

> embrittlement. By taking the fraction of blurred boundaries share as boundaries ferrite percentage, its relation with S_{LM} has been studied.
>
> The increase in ferrite fraction percentage results in decreasing the crack susceptibility. As already described, this cracking is caused by diffusion into the grain boundaries under stress. According to the above prediction, the ferrite precipitation at the prior austenite boundaries at HAZ retards the segregation of diffusing zinc.
>
> It is absolutely important to decrease the quenching hardenability at the boundaries in order to increase the boundary ferrite fraction percentage. In other words, the chemical compositions of the steel shall be changed to C-low, Mn-low alloy, and more preferably, the boron content shall be 0.0002% or less."

Test samples where ferrite was not present were studied by analytical transmission electron microscope (TEM) It was observed that along the grain boundary, 1 to 2μm deposits were generated. The crystal structure of these deposits was cubic, and their lattice constant was a = 0.381 nm. Its chemical composition was mainly Fe and Zn in a 3:1 ratio, with a few % on Mn. All phases expected to be resulting from the Zn-Fe intermetallic reaction which is the foundation of the batch galvanizing process have a higher ratio of Zn to Fe. Thus the deposit formed was not an artifact of the galvanizing reaction. With investigation, the deposit was identified as $Fe_3(Zn, Mn)C_{0.5}$ The formation of this deposit assumes that zinc infiltrates into the grain boundary while bonding with cementite in the boundary, because a similar structure is formed when zinc is substituted as part of Fe_3C.[88] It should be noted that the effect of boron is pronounced at the range of 0 - ~5 ppm, above that level, the effect may diminish.

Steelmaking practices have changed substantially over the past twenty years - modern economical and efficient methods are utilized, and continue in development, including electric arc furnaces (EAF), continuous casting, and controlled rolling. In past steel making history (for example, "Ingot Practice"), the conventional concern of hot rolling was simply to reduce the cross section of the steel. However, with the use of microalloying elements, such as niobium, vanadium, and/or titanium, hot rolling at controlled temperatures is also used to condition the austenite so that fine ferrite grain size is produced during cooling. This method of hot rolling, known as controlled rolling, relies on the precipitation of carbonitrides of the various microalloying elements (if any) to control austenite grain growth and recrystallization. The various types of controlled rolling include conventional controlled rolling, recrystallization controlled rolling, and dynamic recrystallization controlled rolling, and together with other elements now found in the scrap feed, has led to the production of steels with nearly twice the yield strength of commodity grades produced by conventional rolling methods.[89] The increased strengths are developed by variations in both composition and processing, but compositions can not be viewed alone, as products with the same nominal "compositions," are produced by different producers in different ways. The trend, however, seems to be towards higher alloy content, higher manganese content, and more aggressive, lower temperature reduction and rolling practices

The key to the use of controlled rolling is the formation of fine austenite grains that transform on cooling to very fine ferrite grains. Deformation of austenite induces strains which at higher temperatures are rapidly eliminated by recrystallization, followed by grain growth in the austenite. However at low deformation temperatures, grain growth is considerably retarded. If the temperature is low enough, even recrystallization is suppressed, especially in steels to which small amounts of alloying elements such as niobium have been added. The niobium, which is soluble at high temperatures, precipitates out as fine niobium carbides at low austenizing temperatures. These fine precipitate particles stabilize the deformation substructure of the deformed austenite and prevent recrystallization. Upon cooling, ferrite grains nucleate on the closely spaced grain boundaries of the unrecrystallized austenite and form very fine grain structure.[90]

It has been shown earlier, that the presence of stress concentrators such as notches might make an otherwise unsusceptible steel fabrication, susceptible to cracking. Working with a martinsitic steel and liquid lead, such an effect has been shown by Legris et al[91] wherein a certain steel composition appeared to be immune from embrittlement by liquid lead, however, when a notch was introduced into the specimen, failure by LME was observed. Thus, reduction of hardness below the stipulated threshold range cannot be considered as complete immunity from liquid metal interaction.

The mechanical properties of as-rolled sections are recorded in Certified Mill Test Reports (CMTR), and are use to demonstrate adherence to relevant Standards, Specifications, and Codes. The locations and other parameters of those tests are usually stipulated so as to represent the mechanical behavior of the section in service. Recent incidents (mostly not-galvanized) of brittle crack initiation in the "k" area of wide flange beam and column sections suggest some material or manufacturing change resulting in a non-uniform, or unforeseen mechanical behavior. For example, some mechanical tests require that samples be takes at 1/6 the width of the flange as shown below:

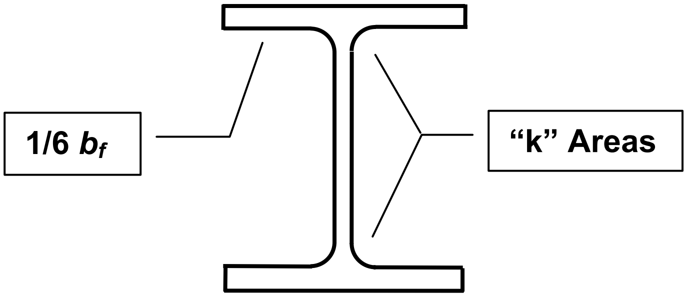

Figure 70 - Schematic of Wide Flange Shape

A research program focusing on mechanical tests at other than stipulated sites was completed. Tensile Strength, hardness, and CVN toughness were obtained to quantify the distribution of properties and their relation to the cracking incidents. Among the findings of investigations was that the mechanical properties in the “k” area were materially altered from those properties expected in the remainder of the web and flange areas.[92]

The CVN toughness distribution for a W920 X 233 (the flange in nominally 25 mm thick) measured from the outer flange area down into the web is shown below:

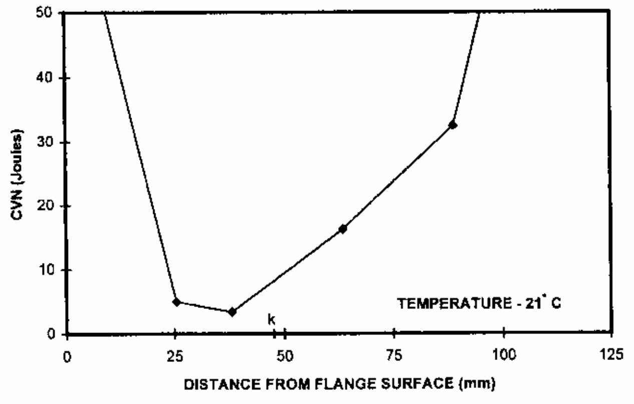

Figure 71 - CVN Toughness Distribution (W920 X 233) (from Ride)

There was a suspicion that roller straightening had cause the problem due to the cold work postulated to occur in the web area.

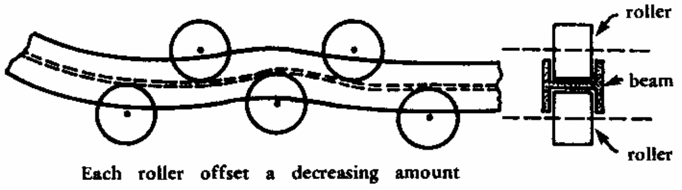

Figure 72 - Exaggerated Schematic of Roller Straightening (from Lay)

It is important to note at this point, the phenomenon of Strain-Age Embrittlement. Strain aging occur in low carbon steels deformed certain amounts, and the n aged, producing an increase in strength and hardness, but a loss in ductility. The resulting brittleness varies with aging temperature and time. Aging at room temperature is very slow, however as the aging temperature is increased, the time for maximum embrittlement decreases, often dramatically. In low carbon steels, strain aging is caused chiefly by the presence of interstitial solutes carbon and nitrogen. These interstitial solutes have high diffusion coefficients in iron, and high interaction energies with dislocations. Strain aging that is due to carbon is generally considered to be low relative to nitrogen, particularly at low temperatures. Strain aging attributable to nitrogen is caused by nitrogen that is not tied up with strong nitride formers, for example aluminum, titanium, zirconium, vanadium, or boron[93]. Thus it should be noted that the amount of nitrogen in the steel, which is generally considered to be higher with EAF practice, than earlier open hearth, or current oxygen practice, should be balanced stoichiometrically with nitride forming elements to control the amount of free nitrogen available for migration and diffusion. In addition, the formation of nitrides and carbonitrides introduce other particles and constitutents, which themselves could contribute to changed mechanical properties. For example, the precipitation of aluminum nitrides has been shown to cause embrittlement in aluminum-killed steels, however the problem was manifest in earlier ingot practice processes, and the application to current continuously cast steels is unknown. Nevertheless, the question of segregation, desegregation, and/or precipitation in grain boundaries, of uncontrolled, residual, or reaction products remains an area for fruitful exploration. It is known that the segregation of alloying and impurity elements to prior austenite grain boundaries (PAGBs) controls temper-embrittlement, although the precise microchemical and microstructural interactions are , as yet, unclear because of the complexity, and many variables involved.[94]

Dynamic strain aging is also a possibility, particularly in light of the expected low temperatures for final rolling and rotary straightening. In this case, the effective strain rate, that is, the dislocation velocity, controls the extent of aging of a particular steel. For normal tensile strain rates, dynamic strain aging occurs in the temperature range of 100 - 300°C, which includes the temperatures at which blue brittleness occurs. If the interstitial solute content is substantial, dynamic strain aging can be observed at room temperature. As above carbon and nitrogen are the most important elements in dynamic strain aging, however it is thought that nitrogen is more important than carbon because of the lower solubility of carbon.[95]

An investigation with a W14 X 176 (ASTM A992/A572 Gr. 50) section to compare the mechanical properties of similar sections as a function of the straightening, and the manner in which the straightening was accomplished.[96] Part of the results are shown below, together with the stress strain curves of specimen taken from the k – area of three differently processed sections, As-rolled, gag (three point) straightened, and rotary straightened. The k-area hardness and CVN values for the three differently processed sections follow:

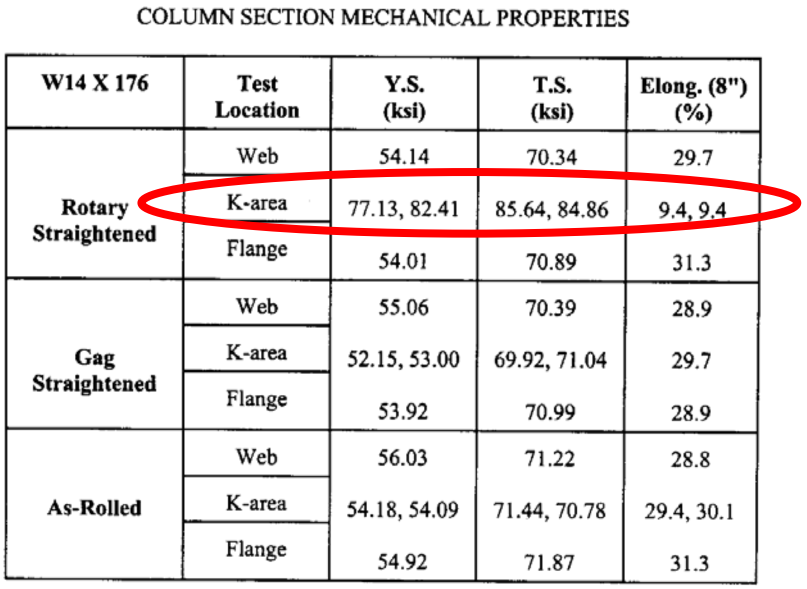

COLUMN SECTION MECHANICAL PROPERTIES

W14 X 176	Test Location	Y.S. (ksi)	T.S. (ksi)	Elong. (8") (%)
Rotary Straightened	Web	54.14	70.34	29.7
	K-area	77.13, 82.41	85.64, 84.86	9.4, 9.4
	Flange	54.01	70.89	31.3
Gag Straightened	Web	55.06	70.39	28.9
	K-area	52.15, 53.00	69.92, 71.04	29.7
	Flange	53.92	70.99	28.9
As-Rolled	Web	56.03	71.22	28.8
	K-area	54.18, 54.09	71.44, 70.78	29.4, 30.1
	Flange	54.92	71.87	31.3

Figure 73 - Mechanical Properties of W14X176 Section as a Function of Straightening Method (from Kaufman and Fisher)

Note the difference in K-area properties highlighted above for the rotary-straightened specimen. Similar changes CVN and hardness values are shown following:

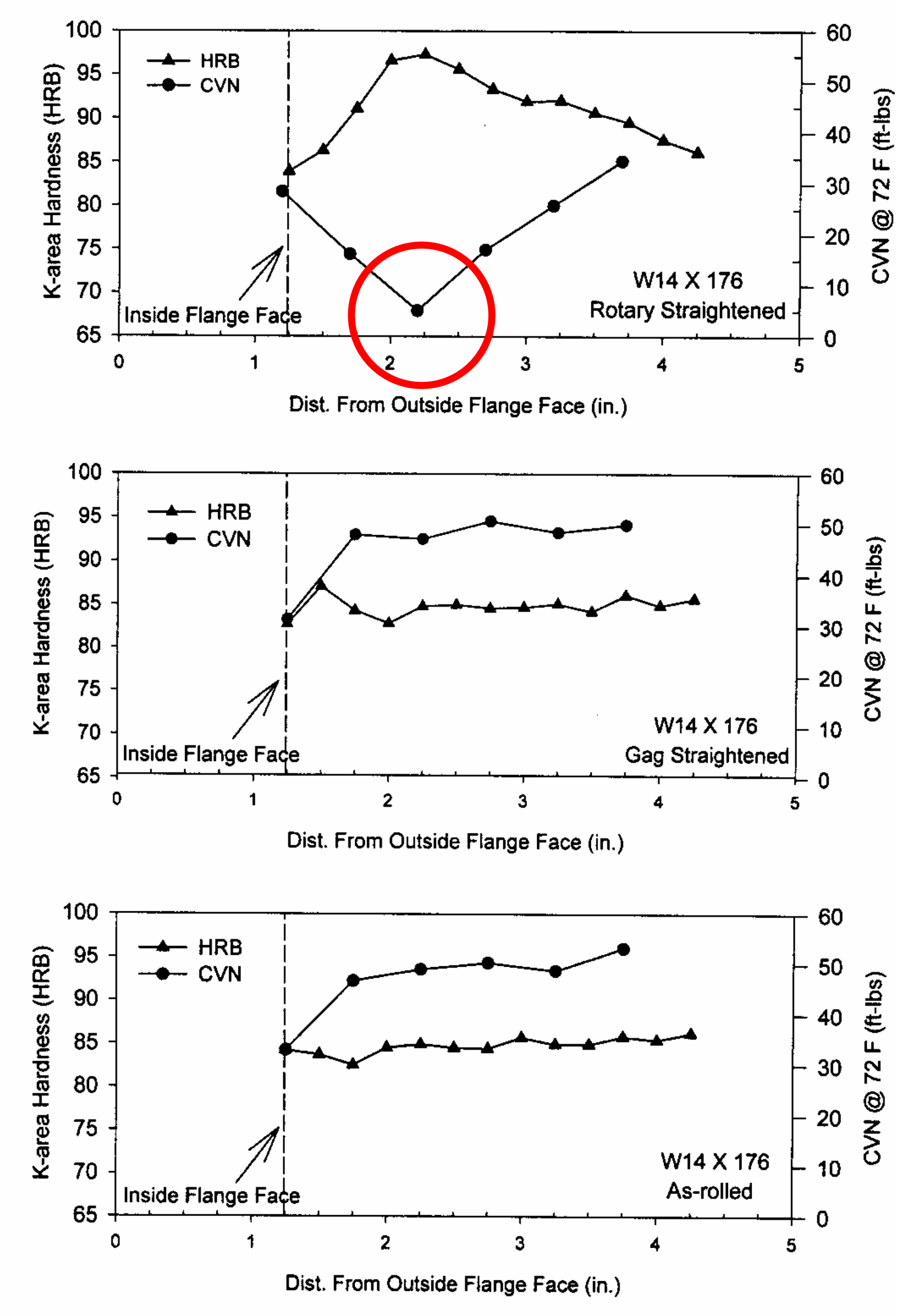

Figure 74 - K-Area Hardness and CVN for Three Differently Processed Sections

(from Kaufman and Fisher)

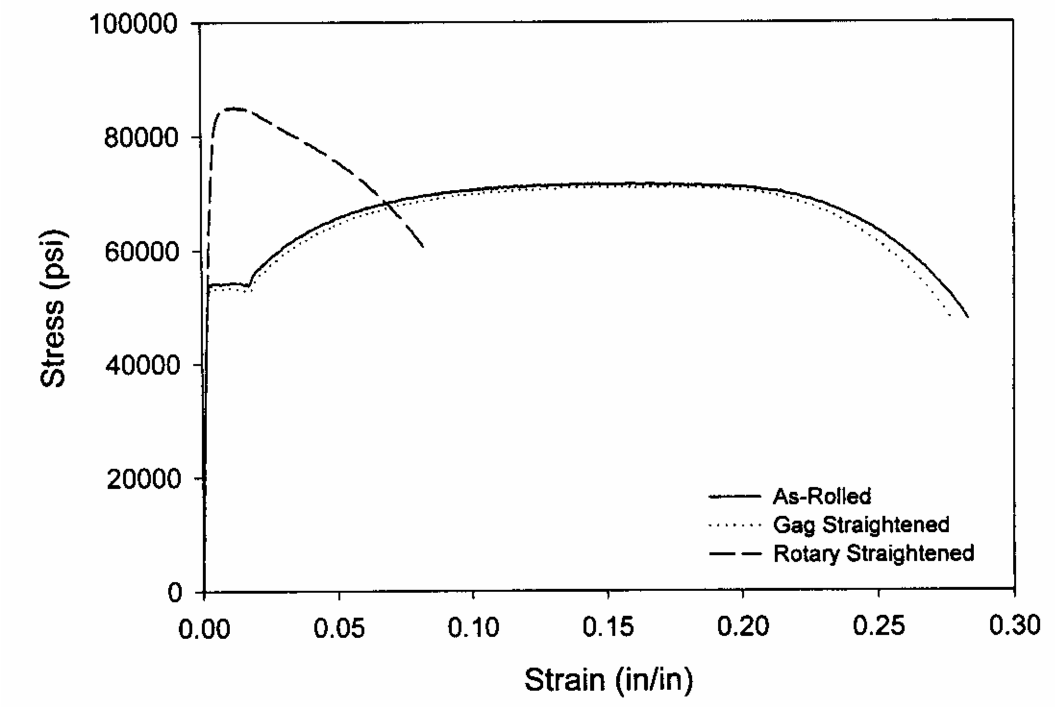

Figure 75 - K-Area stress strain behavior for the Three Differently Processed Sections (from Kaufman and Fisher)

The results from the two test programs are almost identical. The ATLSS Report clearly states that “ Rolled sections manufactured from the same heat of steel and straightened by rotary straightening process exhibit marked change in mechanical properties in the k-area compared to the as-rolled condition.”

These matters relate to galvanizing in a number of ways:

- A “cope” will almost always intersect the k-area of a beam
- Rolled beams have a residual tensile stress field within the k-area, and a flame-cut edge is likely to have small otherwise-tolerable intergranular microfissures which may act a initiators for crack growth
- The ability of a material to arrest the growth of a crack will be a function of the material toughness, and the stress field in that area.
- The cold work in the k-area, in the presence of free Nitrogen, and prior to the thermal cycle incident to the galvanizing process, constitute the conditions consistent with strain-age embrittlement

The matter of k-area loss of toughness may be shown by photos of a coped beam which was delivered for galvanizing, but fell from the truck while being unloaded. Note the flange was able to plastically deform, however, the cope in the k-area fractured.

Figure 76 - Cracks in Cope Area of a Beam Before Galvanizing

Discussion and Synthesis

The problem of cracking coincident with galvanizing is particularly difficult to research for a number of reasons. The phenomenon is:

- Invisible – The occurrence of the problem is apparent only after processing. In the galvanizing plant environment, there is no physical precursor or signal which can be used to predict which beams will crack There is no way yet to determine exactly when (and therefore under what process conditions) the cracks occur.

- Transitory – In the very few cases in which the cracking occurs, beams which are processed nominally the same throughout the production, fabrication, and galvanizing sequence show sporadic cracking with no processing variable clearly seen to accentuate or retard the phenomenon

- Extremely Rare – The incidences of cracks occurring is very rare. As a result, no investigative protocol is in place to preserve samples, and parameters of occurrence

- Exceedingly Complex – All general precautions (such as smoothness of the cope surface, or radius of cut) which might be expected to impact the problem do not seem to have any effect in either causing or solving the problem.

- Undocumented – As noted above not only is the frequency of occurrence quite rare, but also the galvanizing process effectively destroys any micro evidence which might be on the fracture surface such as concentrations of precipitates or elements on the zinc-reacted grain boundaries. In addition, in the commercial manufacturing-fabricating-galvanizing environment, acceptable trade documentation such as mill test reports would be inadequate in a forensic probe of the effect of steel composition, for example, as a factor in a phenomenon because the prescribed reported elements may not include a relevant element, and/or the database of potential critical elements may not be sufficient to positively identify which elements are critical. In addition, elemental composition may be insufficient when a phenomenon results from further interplay of prior thermal and mechanical history.

However, this review of the available technical literature, combined with substantial knowledge of current and historical galvanizing practice, and anecdotal field observations has lead to a working theory about the cause of the problem, and from that theory, and to the extent that some portions of the theory are correct, potential mitigation or avoidance strategies.

The cause(s) of the problem must lie within the factors described in the Venn diagram of Figure 28. Further, it must be recognized that for the most part, the problem is a relatively "new" one, as millions of tons of steel have been successfully galvanized in the almost century-long tenure of commercial hot dip galvanizing (HDG) practice without reports of significant cracking problems. Evaluation of the four variable sets in Figure 28 from a temporal perspective leads to recognition that some of the factors have not changed quantitatively (notwithstanding efficiency upgrades), while some of the factors have changed significantly, particularly in the past twenty years or so, which is generally contemporaneous with the manifestation of the LMAC problem. For example, the table below describes current status of development of the various factors:

Factor	Status of current practices	Examples
Forces	Legacy	Temperature, rates, angles, dimensions, fabrication methods
Time	Legacy	Exposure to liquid zinc
Environment	Developing	Additions to zinc
Condition (Susceptibility)	Developing	Scrap feed, TMCP

The first factor, Force is composed of induced forces, due to loading during galvanizing, differential thermal expansion and contraction, are plausibly the same as when the LMAC problem was unreported and therefore arguably non-existent. For example, the ratio of flange-to-web thicknesses of wide flange sections has changed little over the tenure of HDG, and given that the rates of entry and exit from the galvanizing bath, in other words the potential for differential thermal expansion and contraction, are virtually the same as the past, the induced thermal stresses/strains are the same now as when the LMAC problem was unreported and thus reasonably considered insignificant.

Fabrications have grown in size and complexity over the years, but the sizes of galvanizing baths have been in reasonable balance with the sizes of the fabrications, and the crane dimensions and operating characteristics have also evolved in reasonable balance with such processing needs. Immersion speeds and angles are governed by crane characteristics and building dimensions, which are balanced to the size of the galvanizing bath. Indeed, it has been shown that faster immersion speed reduces the potential for differential thermal effects, and in the development of more efficient galvanizing practices, it is reasonable to expect that as commercial practice developed, entry/exit speeds did not decrease (given adequate drying before immersion) but probably increased if any change.

The effective weight of steel immersed in molten zinc is lowered as a result of buoyant forces related to the density difference between the steel and zinc, and the volume of zinc displaced by the steel. This load reduction is roughly 90%, and at any rate, has not changed with the evolution and development of commercial galvanizing practice.

The residual stresses resultant from fabricating techniques such as welding and flame cutting are difficult to quantify, and are related to steel “response” characteristics. It is reasonable to posit that those structural steel fabricating techniques which would relate to stress development have not changed, or at least did not take a significant short-term slope change during the period during which the LMAC problem started to be reported.

Galvanizing bath temperature has remained reasonably constant during the century of practice, bounded below by the freezing point of zinc, and above by the sharply enhanced attack of the iron galvanizing vessels at higher than conventional spelter temperatures. If any change could be expected, it would be towards slightly lower temperatures as a result of unit energy costs, and the search for coating control and moderation of more newer, higher reactivity steels (Sandelin effect).

Galvanizing Time is a function of steel weight, steel configuration and dimensions, and primarily galvanizing bath temperature. As galvanizing bath temperature has not risen, galvanizing times have remained reasonably constant, perhaps even decreasing some in the drive for productivity, although slightly lower bath temperatures, if any, would be counterbalanced by slightly increasing time.

Thus the first two factors in the Venn diagram, Forces and Galvanizing Time, have generally followed legacy practices which were essentially identical when LMAC was unknown in commercial practice.

The third factor, Environment (molten zinc) has seen some developments in zinc additions in the quest for reactivity control and excess zinc reduction, but it is important to recognize that the LMAC problem surfaced well before the purposeful addition of Sn, Bi, Ni to zinc, and further experiments have shown conclusively that these additions by themselves, in the absence of some thermal transient such as welding and/or flame cutting, do not cause steels to crack. In addition, almost universal legacy practice was to use zinc with nominally 1% Pb, a lower melting element similarly rejected from the zinc-iron intermetallic layers, all during the long period up to about 20 years ago, during which the LMAC effect was not a recognized commercial problem.

That being said, there is evidence that the process-control element additions mentioned can cause increase in LMAC activity above defined zinc composition thresholds, and with steels made “susceptible” through some interaction between newer steel compositions and steel making practices, when subjected to legacy fabricating practices. When viewed with the knowledge that the LMAC manifestation is (almost always) intergranular, and always after a thermal and/or cold work process, it becomes apparent that steel grain boundary integrity and reactivity is an essential ingredient to the LMAC problem. Zinc additions can accelerate the problem, but they are not the root cause of the problem.

Thus, the fourth and remaining factor in the Venn diagram, Steel Condition becomes the fertile area for investigation. Steel condition is a result of the interaction of Steel Composition, Thermal History, and Mechanical History. There is a building body of evidence, some admittedly circumstantial, that the LMAC problem is a closely related to steel condition.

That molten zinc affects the ductility characteristics of steel strained beyond the yield point, as shown in Figures 6 and 7, has been well known for over half a century, during which the LMAC problem was unheard of in commercial practice. So the fundamental effect above is not the cause of the now-manifest LMAC problem. It may well be the *mechanism*, but that mechanism has not been operative at the stress/strain levels, and steel conditions and characteristics heretofore seen in commercial practice, as LMAC was not evident. Note that the strain applied in the referenced experiments were pure tensile, while it appears that in "cope cracking," the strain may well be in the "shear" plane, which would be compatible with the nominal 45° orientation seen in commercial practice.

Further, the phenomenon of strain age embrittlement due to prior straining and a subsequent, accelerating thermal cycle including cycles such as the thermal transient of HDG has been similarly well known for over half a century, and effective guidelines to avoid the unique strain level followed by rapid aging, have been successfully used for similar periods. The straining anticipated by such well-promulgated guidelines was usually seen as severe cold working fabricating practices, and with subsequent galvanizing, the steel could be fractured by shock loading at some time after galvanizing. Note that many investigations, including by this author, have shown high hardness levels in the steel region where the subsequent embrittlement occurs. Note further that the sensitization effect can be reversed prior to galvanizing by thermal treatment at higher temperatures and times than incident with the galvanizing thermal cycle, implying a diffusion or mobility effect as an ingredient in the root cause. It has been well shown that this effect is related to the mobility of carbon (minor) and nitrogen (major), and thus the free nitrogen level in the steel is an important factor.

There is independent, corroborating evidence that hardened sections of the flame cut, welded, or cold worked steel are susceptible to LMAC in molten zinc. The threshold of microhardness is in the range of 250-300 H_V depending on certain unspecified variables. The work cited in Japan related susceptibility to LMAC to composition and rolling processes, such as Thermo-Mechanical Controlled Processing (TMCP).

The TMCP practice relates to processing (rolling) at temperatures lower than earlier practice in order to control the recrystallization of austenite, which then results in a smaller ferrite grain size on subsequent cooling, with strengthening effects on the finished product. The ability to perform controlled thermomechanical processing successfully depends on the total composition of the steel and the solubility of nitride- and carbide-forming elements in the hot working temperature range and below. For example, vanadium nitrides (along with columbium and titanium carbides and nitrogen-rich vanadium carbonitrides) can precipitate during hot deformation and therefore help control austenite recrystallization - the basis for controlled rolling[97] The interaction between nitrogen scavengers and interstitial nitrogen, and diffusion parameters, determines the effect and amount of free nitrogen available, and thus the potential for strain aging. This overall balance and amount, even if in stoichiometric balance results in nitride precipitates, which can migrate and redistribute or even segregate through subsequent thermal and processing cycles, and affect subsequent mechanical properties. For example, aluminum nitride is known to be related to cracking phenomena in earlier ingot practice.

Manganese very strongly retards the transformation of austenite and therefore promotes deep hardening in heat treatable steels. Manganese also lowers the transformation temperature and the eutectoid carbon content. These properties - especially the first two - account for the wide use of manganese in steels in which transformation must be controlled. Manganese does enhance susceptibility to temper embrittlement when present in excess of 0.30% and care should be taken to avoid the critical temperature range (375-575 C, 700-1070 F) during tempering.[98] Note that the galvanizing temperature is within the stated range. Note further that low manganese levels have been associated with low cracking propensity after galvanizing in earlier cited fatigue work.

The investigations in Japan have resulted in control of boron in Japanese structural steel standards, as the presence of very small amounts of boron were correlated to sharp increases in LMAC susceptibility. Boron is known to be an effective nitrogen scavenger, easily forming boron nitride. It is also known that boron inhibits, or at least retards the formation of grain boundary primary ferrite, which is correlated with LMAC.

It is clear from the citations above, that steel composition alone has an important role in LMAC susceptibility, however the work in Japan relating to primary ferrite in the PAGB shows that grain boundary microstructure and microchemistry are important and inter-related. Note that the controlled rolling, or TMCP process affects the grain size of austenite, and the structure and propensity for nucleation sites in the PAGB. Note that TMCP process variables are closely held.

The effect of roller straightening on the mechanical properties of wide flange beams (columns in the reported work) not related to galvanizing. In the author's limited experience, such roller straightening is done a very low temperatures relative to rolling temperatures, which are already low relative to earlier practices where LMAC was not evident. The cold working evident in the reported work could well be the necessary prior "straining" for the later thermal cycle (”aging”)of galvanizing. Note that the loss of mechanical properties is adjacent or contained in the area where the post-galvanizing cope cracks are found. Note further that the double "heating" affect shown in Figure 54 mayy well be the "aging" necessary to cause the prior-strained area to harden as a result of diffusion of some level and composition of "hardening" agent incident with newer alloy steel compositions. Figure 76 is supportive of such a hypothesis. Such a pre-sensitized steel could well crack under simple entry into the zinc spelter at previously well-tolerated rates and conditions.

The hardenability of steels as a result of high cooling rates and alloying elements causing right-shifted CCT curves and subsequent susceptibility to zinc LMAC is supported by unpublished work, and when coupled with the known and widely determined relation between threshold hardness values and susceptibility to LMAC, a strong working hypothesis begins to appear:

As listed in one of the earliest paragraphs of this work, some degree of certitude can be applied to disparate observations or findings based on the *convergence of probabilities.*

The works, anecdotal experiences, and published conclusions cited here are at least compatible, often complementary and confirmatory, and align with a general explanation and mechanism for the hypothesis that the root cause of the recent occurrences of zinc LMAC are related to the composition and microstructure of steels thermally and/or mechanically processed by heretofore tolerable methods. The higher strength steels, produced from higher proportions of scrap, and processed at temperatures and pressures higher than prior practice result in high properties, but at the expense of reduced tolerance for conventional fabricating practice. The presence of diffusible constituents, precipitates and segregants create a sensitivity to molten zinc, which combined with heretofore acceptable levels of induced stress from conventional dipping practices causes a propensity for cracks in the steel. The cracks, once initiated, propagate by LMAC or conventional mechanisms until the stress field is relieved, exhausted, outrun, or until the supply of liquid metal is reduced. Under post-galvanizing cooling, thermal strains are introduced by contraction, which may be additive to the problem. In addition, activity of the molten zinc can be enhanced by low-melting elements added for processing efficiency, however there is experimental support that a non-susceptible steel can not be made to crack by element additions in the ranges recently seen in practice. Further anecdotal evidence suggests that a susceptible, thermally or mechanically processed steel may have a higher incidence of cracking in the presence of the low-melting zinc additives

Given the above supported, but unproven hypothesis, two main avenues of mediation appear: change in steel sensitivity, or change in fabricating practice. It has been shown that some of the effects of fabrication as increasing LMAC susceptibility are reversible by post-flame cut heating, and or welding adjacent to the flame cut edge. Such anecdotes are compatible with the hypothesis that diffusion/precipitation/segregation/desegregation of steel constituents, and control of sensitive microstructures as correlated with hardness are part of the fundamental answer to this problem. Most reasonable controls of force development in galvanizing dipping practice are well known and probably universally practiced currently, but vigilance should be kept high, and zinc additives should be carefully examined as to threshold levels for accelerating LMAC.

This work was completed with support from the American Institute of Steel Construction, and the author gratefully acknowledges that support and that of Thomas Schlafly, Director of Research

Cited material:

---

[1] ASTM Standard A 123, Currently listed as Standard Specification for Zinc (Hot-Dip Galvanized) Coatings on Iron and Steel

[2] ASTM 143, Currently listed as for Safeguarding Against Embrittlement of Hot-Dip Galvanized Structural Steel Products and Procedure for Detecting Embrittlement

[3] ASTM A385, Currently listed as Standard Practice for Providing High-Quality Zinc Coatings (Hot-Dip)

[4] Kinstler, Thomas J., "Galvanized Steel in the Pulp and paper Industry- Research and Survey" Proceedings of the 1993 TAPPI Engineering Conference, TAPPI Press, 1993

[5] Kinstler, Thomas J., "Structural Steel Coating – Economic Analysis for Pulp and Paper Mills," TAPPI Journal, Vol 62, No. 6, June 1979, Pgs 41-44

[6] "Galvanizing Characteristics of Structural Steel and their Weldments," prepared by the BNF Metals Technology Centre, Wantage, Oxfordshire, England, Published by the International Lead Zinc Research Organization, 1975

[7] Poag, G., and Zervoudis, J., "Influence of Various Parameters on Steel Cracking During Galvanizing." Presented at the AGA Tech Forum 2003, Kansas City, Oct 2003

[8] Private communications, unpublished

[9] Metals Handbook, Tenth Edition, Volume 1, "Properties and Selection: Irons, Steels and High Performance Alloys," ASM International, Metals Park OH, page 717.

[10] Joseph, B., Picat, M., and Barbier, F., "Liquid Metal Embrittlement: A state-of-the-art appraisal, The European Physical Journal, Applied Physics, Volume 5, 1999, Pages 19-31

[11] Report AIH-7H, American Iron and Steel Institute, Washington, DC

[12] World Steel in Figures, International Iron and Steel Institute, 2004 Edition, Brussels, 2004, page 13

[13] "Galvanizing for Corrosion Protection, A Specifiers Guide," American Galvanizers Association, 1995, Page 8

[14] "Galvanizing Reactive Steels, a guide for galvanizers and specifiers," International Lead Zinc Research Organization, Research Triangle Park, NC

[15] Beguin, Ph., Bosschaerts, M., Dhaussey, D., Pankert, R., and Gilles, M., "Galveco©, A Solution for Galvanizing Reactive Steel," Intergalva 2000, Proceedings of the Nineteenth International Galvanizing Conference, Berlin, EGGA, 2000

---

[16] Adams, G., and Zervoudis, J., “A New Alloy for Galvanizing Reactive Steels,” Intergalva 97, Proceedings of the Eighteenth International Galvanizing Conference, Birmingham UK, EGGA, 1997

[17] “B6 -Specification for Slab Zinc,” Annual Book of ASTM Standards, Volume 02.04, ASTM, Philadelphia

[18] Langill, T., “North American Galvanizers Process Survey,” Intergalva 2000, Proceedings of the Nineteenth International Galvanizing Conference, Berlin, EGGA, 2000

[19] Langill, T., “Technological Changes by North American Galvanizers,” Intergalva 2003, Proceedings of the Twentieth International Galvanizing Conference, Amsterdam, EGGA, 2003

[20] McDonald, R.D, “Steel Embrittlement Problems Associated with Hot Dip Galvanizing – Causes, Mechanisms, Controls, and Selected References,” Materials Performance, January 1975, Pages 31-37

[21] Weigand, H., “The Effects of Hot Dip Galvanizing on the Mechanical Properties of Steel Sections,” Proceedings of the sixth Hot Dip Galvanizing Conference, Interlaken, 1961, Pages 69-77

[22] Zervoudis, J., and Anderson, G., “Galvanized Steel Cracking, Literature Review,” Teck Cominco, Unpublished, 2003

[23] Kinstler, T.J., “The Mechanical Properties of Galvanized Structural Steels and their Weldments.” 1986 Fifth International Symposium on Corrosion in the Pulp and Paper Industry, Vancouver, Canada, Volume 3, Pages 251-259

[24] Project ZM-396, “Control of Cracking in Galvanized Structurals,” Serial Reports produced by CANMET, Metals Technology Laboratories, Ottawa, Canada, under sponsorship of the International Lead Zinc Research Organization, 1993-1997

[25] Kinstler, T., “Status Report on the Cracking of Copes in Galvanized Structural Beams,” Metalplate Galvanizing, Inc., Limited and internal circulation

[26] Kinstler, T., “Cope Cracking Progress Report, 2/1/92 (rev 1),” Metalplate Galvanizing, Inc., Limited and internal circulation

[27] Kinstler, T., “Cope Cracking Report 5/3/194,” Metalplate Galvanizing, Inc., Limited and internal circukation

[28] Kikuchi, M., “Liquid Metal Embrittlement of Steels during Hot Dip galvanizing,” Tetsu to Hagane, (Iron and Steel), Volume 68, Number 14, 1982, Pages 1870-1879

---

[29] Kikuchi, M., and Iezawa, T., "Effect of Stress-Concentration Factor on Liquid Metal Embrittlement Cracking of Steel in Molten Zinc," Journal of the Society of Materials Science, Japan, Vol. 31, No. 352, March 1982, Pgs. 271-276

[30] Kinstler, T., "Presentation to the Technical Committee on Structural Shapes," Charleston, SC, October 2004

[31] Lay, M.G. Structural Steel Fundamentals – an engineering and metallurgical primer, Australian Road Research board, 1982, Page 186

[32] Cresdee, W., Edwards, W.J., Thomas, P.J. and Voss, G.F., "Analysis on Beam Distortion during Hot Dip Galvanizing." Materials Science and Technology, Vol 9, February 1993, Pages 161-167

[33] Sedlacek, G., Dahl, W., Hoffmeister, B., Kühn, B., Feldman, M., Pinger, T., langenberg, P., Eichenmüller, H., Grotmann, D., and Blum, M., "Zur sichern Anwendung feuerverzinkter Strahlträger," (On the Reliable Application of Hot Dip Zinc-coated Steel Beams), Stahlbau, 73, (2004) Heft 6, pages 427-437

[34] Beyer, St., Dünkel,, V., Hasselmann, U., Landgrebe, R., and Speckhardt, H., "Dehnungsinduzierte Spannungsrißkorrosion in der Flüssigzinkphase bei der Hochtemperaturverzinkung vo HV-Schrahben der Festigkeitklasse 10.9 mit großen Abmessungen," Mat,-wiss, u. Werlstofftech. 25, 1994, Pages 459-470

[35] "Glossary of Terms," ASM Handbook, Volume 8, Mechanical testing and Evaluation

[36] "Tension Compression, Bending, and Shear Testing," ASM Handbook, Volume 8, page 128

[37] Hancock, P.C. and Ives, M.B., "The Role of Plastic Deformation in Liquid metal Embrittlement," Canadian Metallurgical Quarterly, Volume 10, Number 3, (1971) Pages 207-211

[38] Private Communication

[39] Kinstler, T., "Cope Cracking Progress Report, 2/1/92 (rev 1)," Metalplate Galvanizing, Inc., Limited and internal circulation

[40] Radeker, W., "Die Erzuegung von Spannugsrissen in Stahl durch flüssiges Zink," "The Generation of Stress Cracks in Steel by Molten Zinc," Stahl und Eisen, 73 (1953) No. 10, 7 Mai

[41] Porter, F., Zinc Handbook, Properties, Processing and Use in Design, Marcel Dekker, New York, 1991, Figure 8.1, Page 144

---

[42] Industrial Galvanizers Corporation Galvanizing Design Manual, Fourth Edition, 2000, Page 12

[43] Pankert, R., Dhaussey, D., Beguin, P., and Gilles, M., "Three Years Experience with the Galveco© Alloy," Proceedings Twentieth International Galvanizing Conference, Amsterdam, 2003, European General Galvanizers Association

[44] Gilles, M., and Sokolowski, R., "The Zinc-Tin Galvanizing Alloy: A Unique Zinc Alloy for Galvanizing Any Reactive Steel Grade," Proceedings Eighteenth International Galvanizing Conference, Birmingham UK, 1997, European General Galvanizers Association

[45] Beguin, Ph,., Bosschaerts, M., Dhaussey, D., and Pankert, R., "Galveco®, A Solution for Galvanizing Reactive Steel," Proceedings Twentieth International Galvanizing Conference, Amsterdam, 2003, European General Galvanizers Association

[46] Krepski, R., The Influence of bath Alloy Additions in Hot Dip Galvanizing – A Review, St. Joe Minerals Corporation, 1980, Monaca, PA.

[47] Private Communication

[48] Private Communication

[49] International Critical Tables, and Lange's Handbook of Chemistry, Twelfth Edition

[50] Langill, T., "North American Galvanizers Process Survey," Proceedings Nineteenth International Galvanizing Conference, 2000, Berlin, European General Galvanizers Association

[51] ASTM Specification A143-01, "Standard Recommended Practices for Safeguarding Against Embrittlement of Hot-Dip Galvanized Structural Steel Products and Procedures of Detecting Embrittlement," ASTM Standards Vol. 01.06, 2003
.

[52] Pankert, R., Dhaussey, D., Beguin, P., and Gilles, M., "Three Years Experience with the Galveco© Alloy, *ibid*

[53] Wiegand, H., and Nieth, F., "Investigations into the Performance of Hot Dip Galvanized Steels and Structural members," Stahl und Eisen, Vol 84, #2, 1964, Pages 82-88

[54] Hershman, A, and Browne, R,. "Galvanizing Characteristics of Steels and their Weldments – Third progress Report," British Non-Ferrous Metals Research Association, August 1972

[55] Kinstler, T., "The Mechanical Properties of Galvanized Structural Steel and Their Weldments." Fifth International Symposium on Corrosion in the Pulp and Paper Industry,

---

Vancouver, B.C., Canada, Volume 5, Technical Association of the Pulp and Paper Industry, 1986, Pages 251-259

[56] McDonald, R., "The Hydrogen Embrittlement Susceptibility of Welded, Pickled, and Galvanzied Steel," Proceedings, Ninth International Galvanizing Conference, Dusseldorf, 1970, European General Galvanizers Association, pages 172-188

[57] McDonald, R., "Corrosion Tests in a Simulated Sea-Water Environment to Determine Susceptibility to Hydrogen Embrittlement Cracking at Welds in Galvanized Structural Steel," Canada Centre for Mineral and Energy Technology, Physical Metallurgy Research Laboratories, Report MRP/PMRL-75-10(J), Ottawa, 1975

[58] Minobu Aoyama, "Design and Construction of Hot-Dip Galvanized Bridges by the Japan Highway Public Corporation," Figure 11, The Second Asian-Pacific General Galvanizing Conference, 1994, Kobe, Japan Galvaniziers Association, 1994, Pages 20-38

[59] Kikuta, Y, Araki, T., and Yoneda, M, "Effect of Fabrication Procedure on Liquid Metal Embrittlement Cracking in Welded Steel Structures by Molten Zinc," Welding Journal, 1988, No. 2, Pages 146-151

[60] Mori, T., Minami, K., and Horikawa, H., "Fatigue Strength of Galvanized Web-Gusset Welded Joints, IIW Doc. XIII-1926-02, Figures 2a and b, Page 13

[61] Gannon, H, editor, The Making, Shaping, and Treating of Steel, Ninth Edition, US Steel, Pittsburgh, 1970, Table 41-IV, Page 1127.

[62] Sandelin, R., "Modern Trends in Steel as Affecting Hot Dip Galvanizing," Published by the American Hot Dip Galvanizers Association (AHDGA), Washington, DC

[63] Sandelin, R., "Embrittlement Characteristics of Different Types of Commercial Steels Resulting from the Hot Dip Galvanizing Process," presented at the AHDGA Annual Meeting, 1954

[64] McDonald, R., "Steel Embrittlement Problems Associated with Hot Dip Galvanizing – Causes, Mechanisms, Controls, and Selected References," Material Performance, NACE, Jan. 1975, pages 31-37

[65] Manual of Steel Construction, allowable stress design, Ninth Edition, American Institute of Steel Construction, Chicago, 1989, Page 4-174

[66] Tide, R.H.R., "Evaluation of Steel Properties and Cracking in "k"-area of W Shapes," Engineering Structures, Vol. 22, (2000), Pages 128-134

[67] Manual of Steel Construction, allowable stress design, Ninth Edition, American Institute of Steel Construction, Chicago, 1989, Page 5-87

---

[68] Kominami, Y., Yano, K., Ishimoto, K., Terasaki, T., and Murae, S., "Effect of Welding Factors on the Strength of Welded Joints in the Molten Zinc – Liquid Metal Embrittlement of Welded Joint of Steel during Hot Dip Galvanizing (Report 1). Quarterly Journal of the Japan Welding Society, Vol. 3, No. 2, May 1985, Pages 106-110

[69] Kikuchi, M., M., and Iezawa, T., "Effect of Stress-Concentration on the Liquid Metal Embrittlement Cracking of Steel by Molten Zinc," Journal of the Society of Materials Science of Japan, Voloume 31, No. 342 march 1982, pages 271-276

[70] Kikuchi, M., "Prevention of Distortion and of Crack Initiation," Proceedings Thirteenth International Galvanizing conference, London, 1982, European General Galvanizers Association, Paper 16

[71] Manual of Steel Construction, allowable stress design, Ninth Edition, American Institute of Steel Construction, Chicago, 1989, Page 4-175

[72] Private communication

[73] Poag, G., and Zervoudis, J., "Influence of Various Parameters on Steel Cracking During Galvanizing," *ibid,*

[74] Canada Centre for Mineral and Energy Technology, "ILZRO Project ZM-396, Phase IV Progress Report," October 1995

[75] Ho, N, lawrence, F., and Alstetter, C., " the Fatigue Resistance of Plasma and Oxygen Cut Steel," Welding Journal, November 1981, Pages s-231-236

[76] Harris, I., "Plasma Arc Cutting of Bridge Steels," NCHRP Report 384, Transportation Research Board, Washington, DC, 1997

[77] Goldberg, F., Ruge, J., Schimöller, H., and Sabelström, W., "The Relation Between the Residual Stress, Microstructure, Microhardness, of Gas- and Plasma-Cut Surfaces," IIW Do. No. !-537-74, International Institute of Welding

[78] Wilson, A., "Thermal Cutting of HSLA Bridge Steels," American Iron and Steel Institute, Washington, DC, 1987

[79] Elboujdaini, M., Tyson, W., and Goodwin, F., "Experiments on Delayed Failure During Galvanizing of Flame-Cut Structural Steels," 2004

[80] JIS G 3129 -1995, High Tensile Strength Steel for Tower Structural Purposes, Japan Standards Association, Tokyo, Japan, 1995

[81] Malik, L., and McGoey, L., "Investigation of Oxy-Acetyleme Cut Edges for Potential Susceptibility to Liquid Metal Embrittlement Assisted Cracking During Hot Dip

---

Galvanizing," Fleet Techniologies Limited, Report 4090CFR.LIT, Contained in Appendix to Final Report on Phase 2 of ZM-396, ILZRO, 1994

[82] Linnert, G., Welding Metallurgy, Carbon and Alloy Steels, Volume 1, Fundamentals, Fourth Edition American Welding Society, Miami, 1994, Page 870

[83] Linnert, G., *ibid,* Page 872

[84] Kou, Sindo, Welding Metallurgy, second edition, Wiley Interscience, 2003, Pages 232-238.

[85] Bhadeshia, H.K., and Svensson, L.E., Mathematical Modelling of Weld Phenomena, Eds. H. Cerjak, and K. Easterling, 1993 (as cited in Kou)

[86] Mori, T., Minami, K., and Horikawa, H., "Fatigue Strength of Galvanized Web-Gusset Welded Joints, IIW Doc. XIII-1926-02

[87] Abe, Hidehiko, Iezawa, T., Kanaya, K, Yamashita, T., Aihara, S., and Kanazawa, S., "Study of HAZ Cracking of Hot Dip Galvanized Steel Bridges," IIW Doc. IX-1795-95, International Institute of Welding

[88] Private Communication

[89] Metals Handbook,, Tenth Edition, Volume 1, ASM International, Metals Park, OH, 1990, page 115

[90] Metals Handbook, Tenth Edition, *ibid.* Page 131

[91] Legris, A., Nicaise, G., Vogt, J-B., and Foct, J., "Embrittlement of a Martensitic Steel by Liquid Lead," Scripta Materialia, 43 (2000), Pages 997-1001

[92] Tide, R.H.R., "Evaluation of Steel Properties and Cracking in "k"-area of W Shapes," Engineering Structures, Vol. 22, (2000), Pages 128-134

[93] Metals Handbook, Tenth Edition, *op cit.* Page 690

[94] Papworth. A., Knorr, D., and Williams, D., "The Evolution of the Segregation Behavior of Alloying Elements in a Low-alloy Steel," Scripta Materialia, 48, 2003, Pages 1301-1305

[95] Metals Handbook, Tenth Edition, *op cit.* Page 694

[96] Kaufman, E., and Fisher, J., "The Effect of Straightening Method on the k Area Loading Behavior of Rolled Column Sections," ATLSS Report No. 01-16, December 2001, Bethlehem, PA

---

[97] Ferroalloys & Alloying Additives Online Handbook,“Nitrogen,” http://www.shieldalloy.com/MVhandbook.html

[98] Ferroalloys & Alloying Additives Online Handbook,“Manganese,”*ibid*